Technological assessment of animal waste-based energy conversion systems

Thesis presented for the award of Doctor of Philosophy

Giannis Katsaros

Institute of Energy Futures

Brunel University London

Supervisors

Professor Savvas A. Tassou

Dr Yunting Ge

Submitted to Brunel University

January 2021

ACKNOWLEDGEMENTS

I would like to warmly thank all the people that helped me during my PhD journey.

Firstly, I would like to thank my principal supervisor, Professor Savvas Tassou, for his continuous support, guidance and interesting discussions we had during my stay at Brunel University London. I sincerely appreciate all his contribution to improving the structure and the content of the thesis.

Secondly, I would like to express my special gratitude to Dr. Daya Shankar Pandey for sharing his expertise during my research, but also for giving me the right directions, especially in periods of doubt and frustration.

During my research I had the opportunity to visit different research institutes in order to perform the experimental tests. Therefore, I would like to thank Dr. Lydia E. Fryda and all the personnel in ECN (part of TNO) research institute in Netherlands for providing knowledge and valuable data to me. Furthermore, I would like to thank Stefan Retschitzegger and Peter Sommersacher, from BEST research institute in Graz, for helping me in the performance of experiments and during my stay in Graz. I would also like to thank Dr Alen Horvat and Dr Guada Aranda Almansa for their valuable contribution both during the experimental tests and the writing of journal manuscripts.

I am also thankful to my friends and colleagues at Brunel University London, Matteo, Giuseppe, Hasan, Agnese, Kostas, Luga, Ashika, for all the funny moments we shared together. I will miss you guys!

Last but not least, special thanks to my family who supported me during this big and fascinating journey!

ABSTRACT

Environmental concerns associated with the excessive application of animal waste on cropland, demands the development of alternative methods pertaining to its sustainable disposal. This project focuses on bioenergy production from poultry litter (PL), by investigating two thermochemical conversion technologies, namely combustion and gasification. Until recently, limited research has been conducted on the chemical characteristics of PL and its potential suitability as a fuel for energy generation in farm installations. Thus, the present study aims to provide useful insights with regard to the parameters that need to be considered prior to design and installation of combustion and gasification systems onsite.

Firstly, experiments were conducted with a batch fixed bed lab-scale reactor to investigate the combustion behaviour of PL. Additionally, a blend of PL with wood chips (PL/WC) and softwood pellets (SP) on their own, were tested for comparison purposes. PL depicted the highest concentration in nitrogen (N) compared to the other fuels, and the performed evaluation tests suggested that it was mainly converted to ammonia (NH_3) in the cases of PL and PL/WC combustion. On the contrary, N present in SP composition was mostly converted into hydrogen cyanide (HCN) during SP combustion. Furthermore, the findings revealed that the highest aerosol emissions occurred during PL combustion, whereas the corrosion risk was greatest in PL and PL/WC combustion, compared to SP. Overall, high estimated aerosol emissions, increased risk of corrosion and potential conversion of N into NO_x emissions, reveal the main areas that need special attention before designing a combustion system based on PL.

Gasification of PL, blend of PL with beech wood (PL/BW) and beech wood (BW) on its own were investigated experimentally using a lab-scale bubbling fluidised bed reactor. Experiments were carried out at different temperatures (700-750 °C) and air equivalence ratios (ER) ranging between 0.18-0.28. The findings revealed that an increase in operating temperature had a positive effect on both the lower calorific value (LCV) and carbon conversion efficiency (CCE), whereas in higher ERs, LCV decreased and CCE increased. PL generated lower amounts of tar compared to woody biomass. However, presence of alkali metals in PL ash, led to agglomeration and shut-down of the gasifier at 750 °C. The findings suggest that PL can be a suitable fuel for gasification, with lower gas cleaning requirements compared to woody biomass, due to the lower presence of tar. However, mitigation of agglomeration is crucial during PL gasification, since this phenomenon has a detrimental effect on the process performance.

A modelling study of combined heat and power (CHP) production based on combustion of poultry litter, was also performed. Two different systems were investigated; i) a steam boiler coupled with a steam expander currently installed at an existing poultry farm and ii) a thermal oil boiler coupled with an Organic Rankine Cycle (ORC). The results suggested that for the same thermal input based on 0.1 kg/sec of PL, ORC outperformed the steam system by producing 157 kW of gross electrical power, compared to 110 kW. Moreover, heat generated in the condenser was ~1.25 MW for the steam system and ~1.15 MW for the ORC. Payback period (PBP) was found to be 4.4 years in the case of the steam expander system and 3.1 years in the case of the ORC system.

Contents

1. Introduction 1
1.1. Background 1
1.2. Meat production 3
1.3. Poultry litter management practices 4
1.4. Basis of the research 6
1.5. Research objectives 8
1.6. Thesis structure 9
2. Energy recovery from waste 12
2.1. Waste management hierarchy 12
2.2. Biochemical treatment technologies 13
2.2.1. Anaerobic digestion 13
2.3. Thermochemical treatment technologies 18
2.3.1. Combustion 18
2.3.2. Gasification 25
2.3.3. Pyrolysis 37
2.4. Summary of findings 44
3. Combustion of poultry litter in a lab-scale fixed bed reactor 47
3.1. Materials 47
3.2. Experimental facility 49
3.3. Test procedure 50
3.4. Measurement methods 51
3.5. Definition of fuel indexes 52
3.6. Results and discussion 52
3.6.1. Fuel combustion behaviour during lab-scale experiments 52
3.6.2. N gaseous species and aerosols formation 62
3.6.3. Selected fuel indexes 65
3.7. Summary 68
4. Gasification of poultry litter in a lab-scale bubbling fluidised bed reactor 70
4.1. Materials 70
4.2. Experimental facility 73
4.3. Test procedure 74
4.4. Measurement methods 75
4.5. Performance analysis 76
4.6. Effect of temperature on gasification performance and tar evolution - Results and discussion 76
4.6.1. Composition of the product gas 77

4.6.2. Gas yield, carbon conversion efficiency (CCE), cold gas efficiency (CGE), and lower calorific value (LCV) 78
4.6.3. Tar evolution and composition 80
4.6.4. Agglomeration 86
4.7. Effect of equivalence ratio (ER) on gasification performance and tar evolution- Results and discussion 87
4.7.1. Composition of the product gas 88
4.7.2. Gas yield and carbon conversion efficiency (CCE) 90
4.7.3. Lower calorific value (LCV) and cold gas efficiency (CGE) 91
4.7.4. Tar evolution and composition 92
4.7.5: Mass balance 96
4.8. Summary 97
5. Modelling and techno-economic analysis of a combined heat and power (CHP) plant running on poultry litter 100
5.1. Description of steam boiler coupled with screw expander 101
5.2. Modelling of steam boiler coupled with screw expander in Aspen plus 102
5.3. Simulation results of steam boiler coupled with screw expander 106
5.4. Description of thermal oil boiler coupled with ORC 107
5.5. Modelling of thermal oil boiler coupled with ORC in Aspen plus 108
5.6. Simulation results of thermal oil boiler coupled with ORC 110
5.7. Economic evaluation 111
5.8. Summary 114
6. Conclusions and recommendations for further work 116
6.1. Conclusions 117
6.2. Recommendations for further work 120
APPENDIX 123
REFERENCES 134

List of tables

Table 2.1: Classification of tar based on Milne et al. [77] 27

Table 2.2: Tar classification based on Paasen and Kiel [78] 28

Table 2.3: Parameters related to the different gasifier designs [72] 36

Table 3.1: Ultimate and proximate analysis of feedstock. 48

Table 3.2: Chemical composition of ash for the three tested fuels 49

Table 3.3: Chemical composition of residual ashes after the test runs 64

Table 4.1: Ultimate and proximate analyses of all tested fuels. 71

Table 4.2: Chemical composition of PL and PL/BW ash 72

Table 4.3: Process conditions of the experimental tests 77

Table 4.4: Identified tar compounds together with the retention times and classification according to Milne et al. (1997). Chromatogram from the experimental test at 700 °C and ER 0.21 was chosen to identify the tar compounds 81

Table 4.5: Summary of operating conditions of experimental tests 88

Table 4.6: Identified tar compounds with the chromatographic retention times 93

Table 4.7: Mass balance for all tested fuels 97

Table 5.1: Input parameters and assumptions of system 1 105

Table 5.2: Performance indicators of the CHP system based on steam boiler -screw expander 107

Table 5.3: Input parameters and assumptions of system 2 110

Table 5.4: Performance indicators of the CHP system based on PL combustion-ORC 111

Table 5.5: Economic factors and indices for the economic evaluation 113

Table 5.6: Economic feasibility of the system 114

List of figures

Figure 1.1: Global primary energy production by source 1

Figure 1.2: Different types of solid biomass [7] 2

Figure 1.3: Global meat production in million tons during the period 2016-2019 [11] 3

Figure 2.1: Different steps of anaerobic digestion process [40] 14

Figure 2.2: Potential applications from biogas utilisation [39]. 16

Figure 2.3: Moving grate furnace. 1: Screw feeder, 2: Moving grate, 3: Primary air, 4: Secondary air, 5: Post combustion chamber, 6: Heat exchanger, 7: Cyclone, 8: Ash removal. Adopted from [61]. . 21

Figure 2.4: Schematic representation of the different stages of gasification process [72]. 29

Figure 2.5: Schematics of an updraft (left) and a downdraft fixed bed gasifier (right) [86]. 32

Figure 2.6: Schematic of fluidised bed gasifiers. a) Bubbling fluidised bed, b) Circulating fluidised bed. 34

Figure 2.7: Schematic of entrained flow gasifier. Adopted from [88]. 35

Figure 2.8: Schematic representation of different types of reactor employed for fast pyrolysis. Adopted from [50]. 40

Figure 2.9: Different applications of pyrolysis products [96] 41

Figure 3.1: Scheme of the lab-scale reactor, including measurement setup and positions of the thermocouples. 50

Figure 3.2: Mass loss over time during SP combustion 53

Figure 3.3: Fuel bed temperatures over time during SP combustion. 54

Figure 3.4: Release of main gases over time during SP combustion. 55

Figure 3.5: Evolution of N gaseous species over time during SP combustion. 55

Figure 3.6: Air ratio and flue gas flow rate during SP combustion vs time 56

Figure 3.7: Mass loss over time during PL combustion. 57

Figure 3.8: Fuel bed temperatures over time during PL combustion. 57

Figure 3.9: Release of main gases over time during PL combustion. 58

Figure 3.10: Evolution of N gaseous species over time during PL combustion. 58

Figure 3.11: Mass loss over time during PL/WC combustion. 59

Figure 3.12: Fuel bed temperatures over time during PL/WC combustion. 60

Figure 3.13: Release of main gases over time during PL/WC combustion. 60

Figure 3.14: Evolution of N gaseous species over time during PL/WC combustion. 61

Figure 3.15: Ash residues after combustion. PL (left) and PL/WC (right) 62

Figure 3.16: Release of N gaseous species related to nitrogen content of the fuel 63

Figure 3.17: Release rate of volatile and semi-volatile elements in the gas phase. 64

Figure 3.18: Amount and concentration of estimated aerosol emissions. 65

Figure 3.19: Particulate emissions (PM1) vs concentration of aerosol forming elements present in the fuel. PM1 emissions for Bark, Straw, Maize residues, Poplar, Grass pellets, Waste wood result from tests in real scale plants and have been taken from Sommersacher [108]; PM_1 emissions of PL, PL/WC, and SP, tested in this work are estimated values. 67

Figure 4.1: Lab-scale experimental facility at ECN part of TNO, Netherlands 1: Hopper, 2: Screw feeders, 3: Pre-heater, 4: Gasifier, 5: Cyclone, 6: Valve, 7: Hot filter, 8: Cold filter, 9: Flare 74

Figure 4.2: Effect of temperature on the evolution of (a) dominant gas compounds and (b) minor gas compounds (constant ER = 0.21) 78

Figure 4.3: Effect of temperature at ER = 0.21 on a) gas yield and CCE (b) CGE and LCV 79

Figure 4.4: Effect of temperature on total GC-detectable tar, secondary, alkyl tertiary and PAH tertiary tar group at an ER of 0.21 83

Figure 4.5: Effect of temperature on the evolution of the most abundant individual tar compounds at an ER of 0.21 85

Figure 4.6: (a) Indication of agglomeration at ER 0.25 and temperature 750 °C (test 7 in Table 2) (b) Agglomerate removed after the shutdown of the gasifier 87

Figure 4.7: Evolution of the major gas species as a function of ER. 90

Figure 4.8: Effect of ER on a) Gas yield and b) CCE 91

Figure 4.9: Effect of ER on a) LCV and b) CGE 92

Figure 4.10: Tar groups classified according to Milne et al., 1998 and total GC- detectable tar as a function of ER. 95

Figure 4.11: Yield of individual tar compounds as a function of fuel at the lowest ER.....96

Figure 5.1: Schematic overview of the CHP plant based on steam boiler and screw expander.....102

Figure 5.2: Schematic overview of system 1 model developed in Aspen plus.....103

Figure 5.3: Schematic overview of the CHP plant based on biomass boiler and ORC.....108

Figure 5.4: Schematic overview of system 2 model developed in Aspen plus.....109

Nomenclature

Symbols	Description
C	Carbon
Ca	Calcium
CH_4	Methane
Cl	Chlorine
CO	Carbon monoxide
Cu	Copper
CO_2	Carbon dioxide
H_2O	Water
HCl	Hydrogen chloride
HCN	Hydrogen cyanide
K	Potassium
KCl	Potassium chloride
K_2SO_4	Potassium sulphate
K_2CO_3	Potassium carbonate
MDM	Octamethyltrisiloxane
Mg	Magnesium
N	Nitrogen
Na	Sodium
NaCl	Sodium chloride
Na_2CO_3	Sodium carbonate
NH_3	Ammonia
N_2O	Nitrous oxide
NO_x	Nitrogen Oxides
Na_2SO_4	Sodium sulphate
O_2	Oxygen
P	Phosphorus
Pb	Lead
PM_1	Particulate matter with diameter <1 µm
P_2O_5	Phosphorus pentoxide
S	Sulphur
Si	Silica

SO_x	Sulphur oxides
Zn	Zinc
ZnO	Zinc oxide

Abbreviations	**Description**
a.r.	As received
BEIS	Business, energy, and industrial strategy
BEST	Bioenergy and Sustainable Technologies
BRISK2	Biofuels Research Infrastructure
CGE	Cold gas efficiency
CHP	Combined heat and power
daf	Dry ash free
d.b.	Dry basis
ECN	The Energy Centre of the Netherlands
EGR	Exhaust gas recirculation
EPC	Electrostatic precipitator
EU	European Union
FID	Flame ionisation detector
FTIR	Fourier-transform infrared spectroscopy
GC	Gas chromatography
GJ	Giga joule
GWP	Global warming potential
ICP	Inductively coupled plasma
IEA	International Energy Agency
kWh	kilowatt-hour
LCV	Lower calorific value
mg	Milligram
min	Minutes
NPV	Net present value
ORC	Organic Rankine cycle
O&M	Operation and maintenance
PAH	Polycyclic aromatic hydrocarbons
PBP	Payback period
PJ	Peta joule

PL	Poultry litter
ppm	Parts per million
RHI	Renewable heating incentive
sec	Seconds
SP	Softwood pellets
SPA	Solid phase adsorption
TCI	Total capital investment
TFC	Trilateral flash cycle
TFN	Total fuel nitrogen
UK	United Kingdom
VS	Volatile solids
WC	Wood chips

1. Introduction

1.1. Background

Fossil fuels are still the predominant means for satisfying the global energy demand, whereas the share of renewable resources is still limited (Fig.1.1). However depletion of fossil fuels along with the associated emission of greenhouse gases considered as the root cause of global warming, make urgent the need for further exploitation of renewables [1]. According to the Paris agreement signed in 2015, 195 countries across the world committed to jointly take global climate action, with the ultimate goal to limit global warming to well below 2 °C above pre-industrial levels by 2100. In addition, the EU28 committed to 32% of energy consumption by 2030 to be generated form renewables, with a consequent 40% reduction in GHG emissions compared to 1990 levels [2].

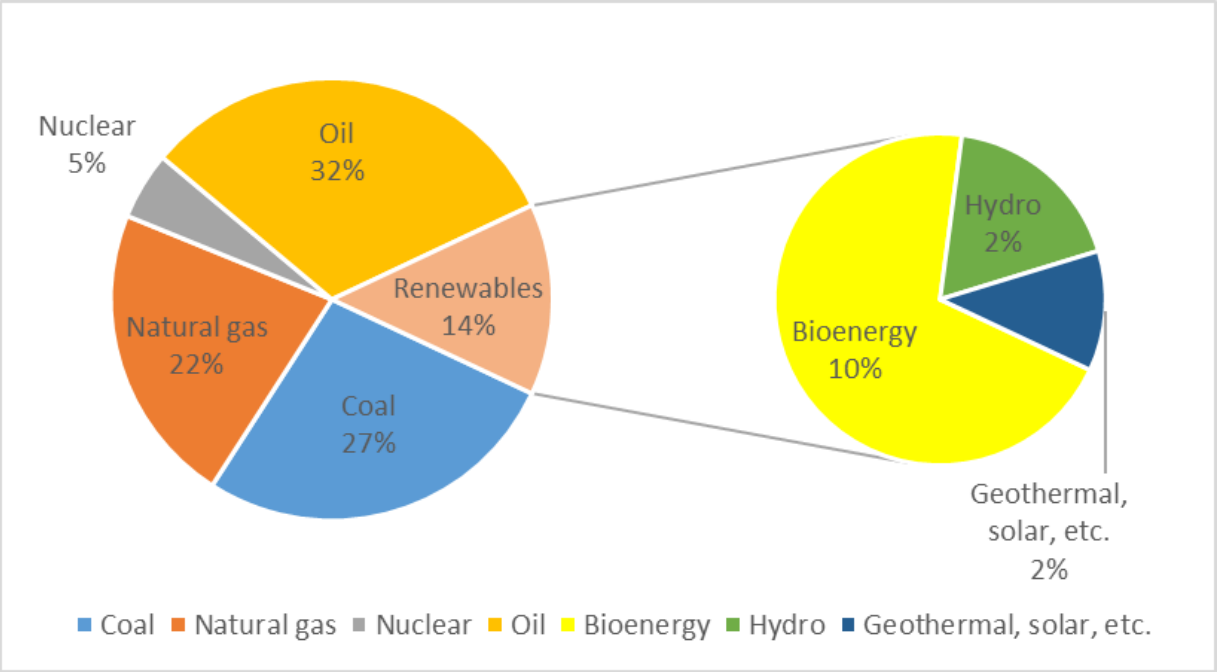

Figure 1.1: Global primary energy production by source [1]

Among the renewable resources, bioenergy has gained a lot of attention recently. According to a statistical report produced from Bioenergy Europe [3], bioenergy accounts for 63% of the energy produced by renewables within the EU-28. The largest share of bioenergy is used for heating purposes in industrial and household sectors (75%), while the rest is equally distributed between biofuel production for the transportation sector and electricity generation [3]. The source of

bioenergy is biomass which according to the EU directive is defined as "*The biodegradable fraction of products, wastes and residues of biological origin from agriculture (including vegetable and animal substances), forestry and related industries, including fisheries and aquaculture, as well as the biodegradable fraction from industrial and municipal waste*" [4]. The main reasons explaining the renewed interest in biomass are its environmentally friendly nature and the vast production potential. Particularly, biomass is considered as a CO_2-neutral fuel since the amount of CO_2 released during combustion of biomass is the same as the one absorbed from the atmosphere during the photosynthesis process [5]. However, there is always some net addition of CO_2 released in the atmosphere, stemming from the utilisation of fossil fuels during the phases of production, handling, and transportation of biomass. Furthermore, there is a large variety of biomass feedstock widely available across different regions of the world that can be sourced locally (Fig.1.2), boosting local economies while assuring security of supply [6].

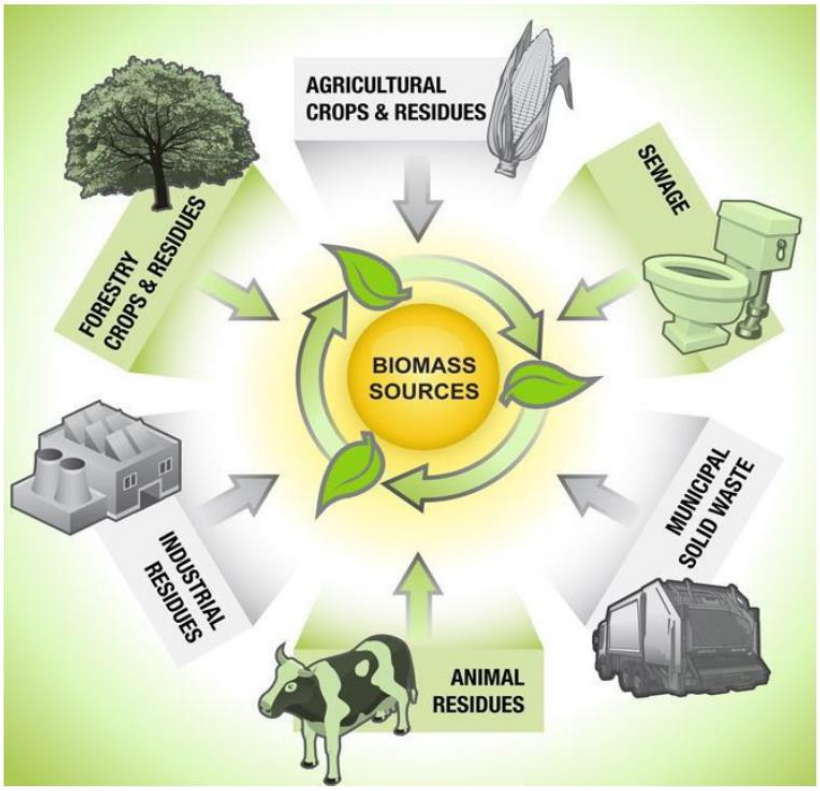

Figure 1.2: Different types of solid biomass [7]

In the EU-28, most of the biomass consumed in energy applications derives from wood, accounting for 70% in year 2017 [8]. The rest is covered by biomass originating from agriculture (18%) and the organic fraction of municipal waste (12%). The main categories of woody biomass

are forest main products (e.g., stem wood, short rotation wood), primary forest residues (e.g., tops, branches, and leaves), by-products from forest industries (e.g., sawdust, wood chips, and mill residues), wood pellets, and waste wood resulting from construction and demolition sites. From all the categories mentioned above, by-products of wood industries represented the largest share in energy applications during 2015, namely 34%, followed by main products at 29% [9]. However, increased production costs of woody biomass, regional availability mainly at areas close to forests or relevant industries, along with high transportation costs from the forest or industrial area to the end-users, have risen the research interest on alternative biomass types such as agricultural residues. There are three categories of agricultural residues: a) residues resulting from food crops after processing (e.g. husks, shells, and kernels); b) residues left in the field after the completion of the agricultural activity (e.g. straw after cereal production) and, c) animal husbandry [4].

1.2. Meat production

Meat production shows a continuous upward trend over the past decades (Fig. 1.3). Population increase, rising income, urbanization, along with the growing need for high value proteins, have shifted society's patterns from plant based to animal food diets. In 2019 the global market of meat production amounted to approximately 330 million tons. Poultry meat constituted the highest share of the global production, followed by pork, and beef and veal [10].

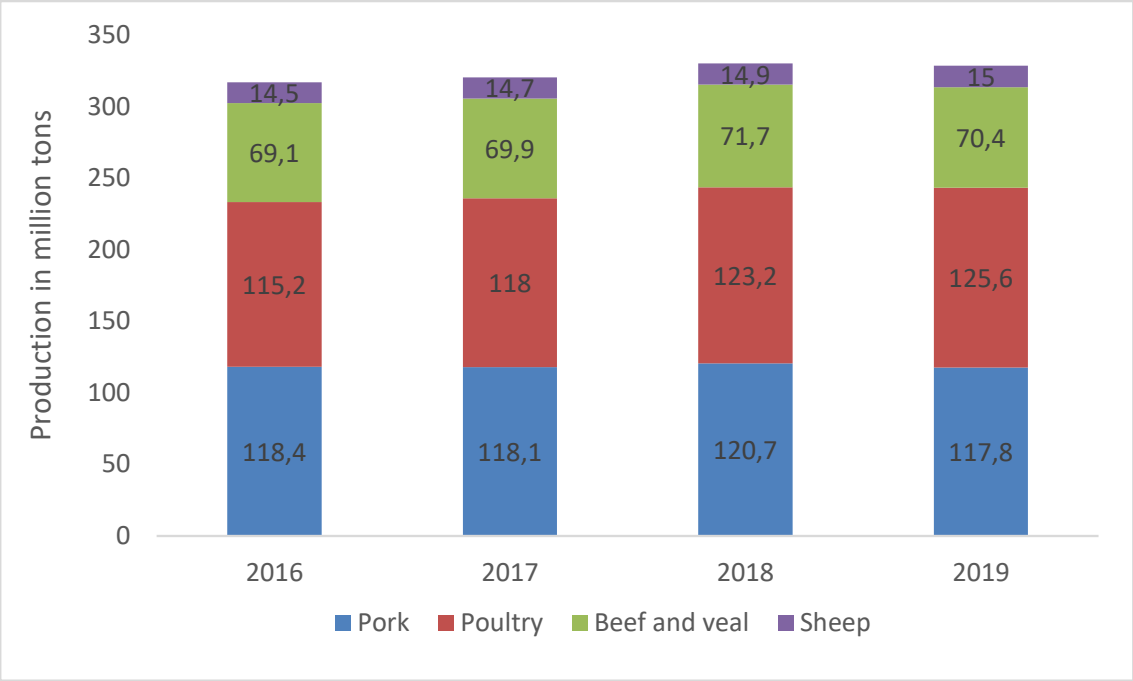

Figure 1.3: Global meat production in million tons during the period 2016-2019 [11]

Among the different meat segments, poultry is predicted to have had the highest growth rate. Poultry production has grown substantially throughout the years, transforming poultry to a very popular commodity. Particularly in the EU, the production reached a new high of 15.2 million tons in 2018. Approximately 70% of this amount resulted from six member states, specifically Poland (16.8%), United Kingdom (12.9%), France (11.4%), Spain (10.7%), Germany (10.4%), and Italy (8.5%) [11]. Compared to the other meat segments, it displays some significant advantages that make poultry meat attractive to the consumers. Firstly, poultry meat is considered to have a better nutritional image than beef and pork. Especially after the spreading of diseases in bovine animal populations, e.g., the Bovine Encephalopathy crisis in the United Kingdom (UK), consumers shifted their preference from red meat (especially beef) towards poultry, since it was considered as a healthier option. Furthermore, the fact that poultry meat is considered as inexpensive compared to other meat products constitutes another important factor that favours its consumption [12]. In addition, the growth rates of poultry species have improved significantly due to betterments in genetics, agriculture, and extensive use of mechanical equipment in processing plants. Back in 1925, the average time period for raising a broiler (small chicken) of 1.13 kg weight, was on average 112 days, while today only 40 days approximately are needed, for the production of a broiler weighting 2.1 kg [13]. From the producer's perspective, poultry production is a more credible option, in terms of feed efficiency. Specifically, 3.1 kg of feed is needed for the production of 1kg of broiler meet, whereas 6.2 kg and 24 kg of feed are required per kg in the case of pigs and non-dairy cattle, respectively [12]. The absence of restrictions due to religion regarding poultry consumption, as in the case of pork in the Muslim culture, as well as a great variety of further processed products such as chicken nuggets and chicken ham, play also an important role to the expansion and popularity of poultry meat production [13,14].

1.3. Poultry litter management practices

The growing demand for poultry meat creates significant amounts of poultry litter (PL) as a by-product. PL is a blend of excreta (manure), waste feed, bedding material (e.g., straw, sand), dead carcasses and feathers. It also contains smaller amounts of plant nutrients like phosphorus (P), potassium (K), nitrogen (N) as well as traces of other elements like copper (Cu), zinc (Zn), along with pesticides, pharmaceutical substances and microorganisms [15]. Its amount depends on the moisture content, the type of bedding material used and the frequency of poultry shed clean-outs [16]. In a recent study by Dalolio et al. [17], it was reported that the amount of PL produced ranges between 1.75 and 5.7 kg of PL/bird over a 42-day production cycle. Taking into account that in

2018, on a monthly basis approximately 80 million birds, mostly chickens were slaughtered in the UK alone [17], this could generate between 140,000-456,000 tonnes of PL.

Nowadays, there are different PL management practices being applied. In particular, PL is rich in elements with high nutritional value (nitrogen, phosphorus, potassium) and therefore it is either spread directly to the land as a fertiliser enhancing crop production, or it may replace part of the mineral fertilisers, hence decreasing their environmental impact [18,19]. Moreover, PL is used as a soil amendment altering its physical and chemical structure (e.g., organic matter content, water holding capacity), improving in this manner soil fertility. Especially in lands that have been continuously under cultivation process with subsequent deterioration of land fertility, PL addition has been reported to increase crop yields [15]. PL used as animal feed is another management option, although less common. In most of the cases PL is used as a supplement during winter periods in beef and dairy farms. Prior feeding however, it needs to be pre-processed in order to remove presence of undesirable materials (e.g. plastic, glass) and any pathogenic contaminants like pesticides and drug residues [20].

From all the above PL management practices, use of PL as fertiliser is currently the preferable option. However, due to changes in farming practises, significant environmental concerns have arisen when this method is applied. Increasing demand for meat consumption has shifted livestock production from traditional farming based on small installations to intensive livestock farming units. The latter, although being more efficient and cost effective than traditional farming, results in the accumulation of a large amount of PL within confined areas. Excessive soil fertilisation where the available arable land for litter application as a nutrient source is limited, can lead to eutrophication, nitrate leaching, crop toxicity due to high concentrations of ammonia (NH_3) and nitrates, odours and emissions of greenhouse gases (NH_3, NO_x, N_2O) to the atmosphere [19,21–24]. Excess nitrogen is one of the main causes of water pollution in Europe, forcing member states to implement the Nitrates Directive (1991) in order to prevent it. Under this directive, EU member states are required to adopt measures such as limiting the spreading of livestock waste to comply with the rule of 170 kg of nitrogen/hectare per year, minimise the storage capacity of animal waste, and monitor the concentration levels of nitrates in the water with the maximum limit being 50 mg/litre of water [25].

1.4. Basis of the research

Increased environmental concerns described previously and strict regulations regarding the application of PL as a fertiliser, necessitate the implementation of alternative strategies regarding PL management. In this context, conversion of PL into renewable energy can be a viable option. PL is considered a fuel of low energetic value due to the high ash and moisture content. Its lower calorific value (LCV) ranges between 8.75 GJ/tonne and 14.27 GJ/tonne on as received basis [26] and therefore the estimated potential energy for UK from PL varies between 1.22 PJ to 6.5 PJ (Peta joule). Considering its energy potential, PL can be utilised as a renewable feedstock for bioenergy production, while at the same time reducing the emissions caused from its over application as fertiliser. In a poultry farm, energy is used for lighting, ventilation, heating and cooling, and operation of the production equipment (feeding, sanitation). In north climates heating is the largest energy consumer in a poultry farm mainly needed to maintain the indoor temperature of the sheds at the desired levels. In order to achieve an efficient poultry growth, the temperature within the poultry house should be kept at 33 °C in the beginning of the growing cycle, whereas it should be decreased to 21 °C towards the end. Therefore, depending on the starting date there is a unique heating/cooling load that should be applied in poultry houses [1]. The energy requirements of a poultry farm are usually satisfied from boilers running on propane and electricity supplied from the grid. A study regarding the energy consumption of poultry farms in the UK has reported an average energy demand of 0.39 kWh/bird [27]. Nevertheless, fluctuations in energy prices may force farm owners to reduce ventilation rates in order to maintain the heat within the poultry houses and decrease energy consumption. This practise of poor ventilation may lead to build-up of ammonia concentration and poultry overheating, resulting in poultry discomfort [28].

In this context, valorisation of PL for onsite energy generation can be an effective solution for satisfying the energy demand of a poultry farm. Currently two different pathways regarding the conversion of animal waste to energy are exploited, biochemical and thermochemical conversion. The choice of technology depends on the feedstock properties, the desired end product, economic feasibility and environmental regulations [29]. The slow production rate of the anaerobic digestion process, the need for a feedstock with high moisture content (moisture content of PL varies significantly from batch to batch and has relatively high solid content) and related high capital costs make this method less attractive for PL treatment [30,31]. Thermochemical conversion seems a promising option for PL treatment, since it can reduce the volume of the waste by 80-95%, upgrade PL to higher value products (e.g. bio-oil, synthetic natural gas), destroy pathogens due to

high operating temperatures, whilst also offering the possibility of electricity, heat generation, and biofuel production [32].

Thermochemical conversion routes are divided into three core technologies, combustion, gasification and pyrolysis. In the former, feedstock is oxidised in excess amounts of air, producing combustion products (CO_2, H_20, SO_2, NO_x, etc.) and heat. On the contrary, gasification takes place in partial oxidised regimes, generating a gas consisting of CO, H_2, CH_4, along with higher hydrocarbons, alkali metals and impurities. In pyrolysis the feedstock is decomposed in a complete oxygen-free environment, producing solid, liquid, and gaseous compounds depending on the operating conditions. It should be noted that combustion is already proven and commercialised, whereas gasification and pyrolysis technologies are still in their development and pilot scale of application and pose different challenges that need to be addressed prior to their further deployment at commercial scale.

All of the thermochemical conversion technologies are able to generate power when coupled with prime movers such as steam turbines, steam engines, internal combustion engines, gas turbines, fuel cells, etc. However, during this process a large amount of heat needs to be rejected due to thermodynamic limitations, decreasing the overall plant efficiency. Therefore, valorising the rejected heat generated as a by-product of electricity generation has gained increased attention in recent years. The simultaneous production of heat and power using a single fuel as energy source is known as combined heat and power production (CHP) and is realised by the implementation of a network of heat exchangers capable of capturing the maximum possible amount of the rejected heat. The electrical power can either by utilised onsite or supplied to the grid, while the thermal energy is mostly valorised onsite covering the needs of process steam, or hot water. According to Eksi et al. [33] from a total of 3696 plants running on wood chips, 21% are CHP plants, with the rest being mainly plants producing only heat.

Different benefits arise if the concept of CHP is applied. Particularly, the overall efficiency is greater than a plant running on electricity or heating mode alone, reaching 60-85%. On the contrary a Rankine cycle installed to generate power only, doesn’t exceed efficiencies of more than 30% in the range between 0.5-100 MW [33]. Moreover, the total amount of fuel consumed in CHP systems is less than the fuel needed to produce the same amount of power and heat but in separate systems. This fact offers substantial energy savings, while improving the economics of the plant, as long as there is a significant and stable heating demand justifying the installation of a CHP system [34]. The environmental footprint is also greatly improved when utilising CHP systems since less

fuel is needed and thus the emissions of greenhouse gases are reduced. It is reported that for every electric MWh produced by CHP plants, 1,000 tons of carbon emissions are avoided [33].

Distributed energy generation can be further enhanced through the implementation of CHP systems. In commercial facilities like poultry farms, a CHP system can be installed onsite utilising the available PL and thus avoiding energy losses in the transmission network. Additionally, it can benefit the farm owners from reduced purchased fuel costs and at the same time mitigate the environmental effects resulting from the utilisation of conventional fossil fuels. From a waste management perspective also, animal waste conversion to energy can help the farm owners avoid transportation and waste disposal costs, while preventing the waste from ending up in landfills or to lands that have limited capacity to absorb fertiliser application.

1.5. Research objectives

Manure spreading in land is currently the most common approach employed by poultry farmers to deal with the amount of waste generated onsite. However, challenges pertaining to the environmental impact resulting from over fertilisation of croplands, along with the fluctuation of energy prices, make urgent the need to explore alternative poultry waste management options. Currently limited research has been conducted on different pathways alternative to fertilisation and landfilling, such as thermochemical conversion, biogas, and composting. The present work aims to address some of the gaps pertaining to thermochemical conversion of poultry waste by investigating two different thermochemical routes, namely combustion and gasification.

The specific objectives of each study are as follows:

1) To provide a detailed overview of the state-of-the-art technologies related to energy recovery from waste, along with literature review findings of those technologies using poultry litter as a fuel input.

2) To investigate the combustion behaviour of poultry litter compared to a blend of a poultry litter with wood chips, and softwood pellets alone. Thermal decomposition of fuels over time, gaseous compounds including N-gaseous species, temperature regimes in the reactor, and estimation of aerosol emissions were analysed based on the data extracted after the completion of the experiments.

3) To assess the impact of process parameters (temperature and equivalence ratio) on the gasification performance of poultry litter, blend of poultry litter with beech wood and beech wood

on its own. Derived experimental data provided information on product gas composition, calorific value, efficiency of the gasification process, and evolution of tar compounds.

4) To develop combined heat and power (CHP) models in the Aspen plus simulation platform based on the combustion of poultry litter. Two different prime movers were compared, namely a steam screw expander and an Organic Rankine Cycle (ORC), in terms of power output, CHP system efficiency, and economic feasibility of the proposed configurations.

The experimental study on combustion of poultry litter was performed at BEST – Bioenergy and Sustainable Technologies research institute located in Graz, Austria. A lab-scale fixed bed reactor operating on a batch mode was employed, while the poultry litter used in the experiments was supplied from a local poultry farm.

Experiments on gasification of poultry litter were conducted at the Energy Research Centre of the Netherlands (ECN part of TNO). An air blown fluidised bed reactor with silica sand as bed material was utilised for the experimental tests. Poultry litter was transported to the research institute from a poultry farm located in Finland, while beech wood and silica sand were supplied by the research institute.

The analysis of the CHP systems based on combustion of PL was performed in the Aspen Plus simulation platform. Input data to the simulation were from an existing poultry farm in the UK and from the open literature.

1.6. Thesis structure

The thesis consists of 6 chapters and their content is summarised below:

Chapter 1: The introduction of the thesis addressing the increased interest in bioenergy nowadays, with a special focus on agricultural residues, namely the by-product of poultry farming known as poultry litter. Current poultry litter management practices are described, along with alternative treatment methods such as thermochemical conversion of poultry litter and its potential as fuel for energy generation.

Chapter 2: This chapter provides a detailed overview of the state of the art of waste to energy technologies. Additionally, a literature review is conducted based on those technologies running on poultry litter, in regard to their operational characteristics, strengths, and limitations.

Chapter 3: This chapter details the lab-scale experimental tests of poultry litter combustion, including description of the experimental facility, measurement methods, test procedures and interpretation of results. The content of this chapter was published in the Elsevier journal 'Fuel'. The title and the name of authors are given below.

Giannis Katsaros; Daya S Pandey; Peter Sommersacher; Stefan Retschitzegger; Norbert Kienzl; Savvas Tassou. Combustion of poultry litter and mixture of poultry litter with woodchips in a fixed bed lab scale batch reactor. DOI: 10.1016/j.fuel.2020.119310

Chapter 4: This chapter details the lab-scale experimental tests of poultry litter gasification, including description of the experimental facility, measurement methods, test procedures and interpretation of results. The content of this chapter was published in two different Elsevier journals, 'Waste Management' and 'Fuel'. The titles and the names of the authors are given below.

Giannis Katsaros; Daya S Pandey; Alen Horvat; Lydia E Fryda; Guadalupe A Almansa; Savvas A Tassou; James J Leahy. Gasification of poultry litter in a lab-scale bubbling fluidised bed reactor: Impact of process parameters on gasifier performance and special focus on tar evolution. DOI: 10.1016/j.wasman.2019.09.014.

Giannis Katsaros; Daya S Pandey; Alen Horvat; Lydia E Fryda; Guadalupe A Almansa; Savvas A Tassou; James J Leahy. Experimental investigation of poultry litter gasification and co-gasification with beech wood in a bubbling fluidised bed reactor – Effect of equivalence ratio on process performance and tar evolution. DOI: 10.1016/j.fuel.2019.116660

Chapter 5: This chapter consists of steady state modelling of combined heat and power (CHP) applications based on combustion of poultry litter and two different prime movers, namely a steam expander and an Organic Rankine Cycle (ORC). The movers were used to investigate energy performance in terms of power production and system efficiency. Techno-economic analysis of the investigated CHP systems is also presented.

Chapter 6: The general summary and conclusions of the work are presented here, together with recommendations for future work in the research area.

2. Energy recovery from waste

This chapter focuses on the different technologies in regard to alternative waste treatment and energy recovery. Currently two different pathways exist, namely biochemical (anaerobic digestion, composting) and thermochemical conversion route (combustion, gasification, pyrolysis). The choice of technology depends on the feedstock properties, the desired end product, economic feasibility and environmental regulations [29]. In the following sections, a detailed description of the technologies is given, including positive aspects and limitations of each technology. Additionally, a thorough literature review is presented with findings related specifically to the use of poultry litter (PL) as a fuel input to these technologies.

2.1. Waste management hierarchy

According to the European directive regarding waste prevention and management [35], the waste hierarchy should be applied in the following order: prevention, preparing for re-use, recycling, energy recovery, and disposal. The first priority for a sustainable waste management system is the prevention of waste. This can be achieved through more efficient methods of product production (using less material in manufacturing), or by using the product for a longer period of time. The re-use of products such as plastic bags or clothes, instead of throwing them away as waste, is the second preferable option based on the hierarchy pyramid. In case the products cannot be re-used, emphasis is given on recycling. Recycling is a well-known method which raises public awareness related to environmental issues. On the other hand, it has the drawback that in many cases high amounts of energy are needed during the recycling processes to convert a waste material into a new product. The fourth option relates to energy recovery. Combustion (incineration) and anaerobic digestion are the most commercially available methods for energy recovery from waste, whereas other technologies are still at deployment stage. Last option and least favorable is the waste disposal in landfills. This method is the oldest and can have serious negative impacts on the release of the greenhouse gas methane (CH_4) to the environment. Furthermore, leachate derived from the breakdown of biodegradable waste, contains chemical and heavy metals that can pollute groundwater and soil of the nearby areas [36]. Another major drawback is the area which is bounded for landfilling that could be used alternatively for agricultural purposes. Especially nowadays, due to the fast-growing population and the associated increase in the amount of generated waste, the demand for land intended for waste disposal is expected to show a continuous increase, if priority is not given to disposal methods higher up in the waste hierarchy.

2.2. Biochemical treatment technologies

2.2.1. Anaerobic digestion

Anaerobic digestion is a biochemical process, during which microorganisms decompose biodegradable material in oxygen free environment. The output of the process is the production of biogas consisting mainly of CO_2 and CH_4, along with traces of other substances. Virtually all biomass types are suitable for anaerobic digestion, except some lignified compounds, e.g., wood, due to their low rate of anaerobic decomposition. Nowadays, most of the plants utilise animal manure and slurries stemming from cattle, pigs and poultry production facilities. Other biomass types suitable for anaerobic digestion are energy crops such as grain and grass crops, maize, residues from harvesting (leaves of sugar beets), food waste and municipal biowaste [37,38].

With regard to the scale of biogas plants, small scale plants are considered the ones with capacity up to 500 kW, satisfying energy requirements locally, with the possibility also to sell excess electricity to the grid. In this type of plants agricultural waste or energy crops are mostly applied as feedstock. On the contrary, large scale plants (>500 kW), co-digest different types of feedstock and they are capable of producing more than 1.8 million m^3 of biogas yearly, when exploiting feedstock of 20,000 tons/year. Methane upgrading and subsequent feeding to the grid is also possible with large scale plants [39].

2.2.1.1. Anaerobic digestion process

Anaerobic digestion is a multistep process as depicted in Fig. 2.1. The different steps are discussed briefly below.

- Hydrolysis: During hydrolysis, large organic polymers are broken down into sugars, amino acids and fatty acids. It is considered as a rate limiting process, mostly when the feed consists of particulates, and low performance of this step can deteriorate the efficiency of the overall process.
- Fermentation: Following hydrolysis, sugars and amino acids produce organic acids, alcohols and H_2 with the aid of fermentative microbes. Fermentation is not a rate-limiting process but it causes reduction in the pH values.

- Acetogenesis: During the microbial process of acetogenesis, organic acids and alcohols are converted to acetic acid, H_2 and CO_2. The only case that it is becoming rate limiting is in very high-rate processes.
- Methanogenesis: This is the final step of anaerobic digestion process. It involves two processes: a) aceticlastic methanogenesis during which 70% of CH_4 is produced and b) conversion of H_2 to CH_4. Methanogenesis occurs in pH values ranging between 6.5 and 8.

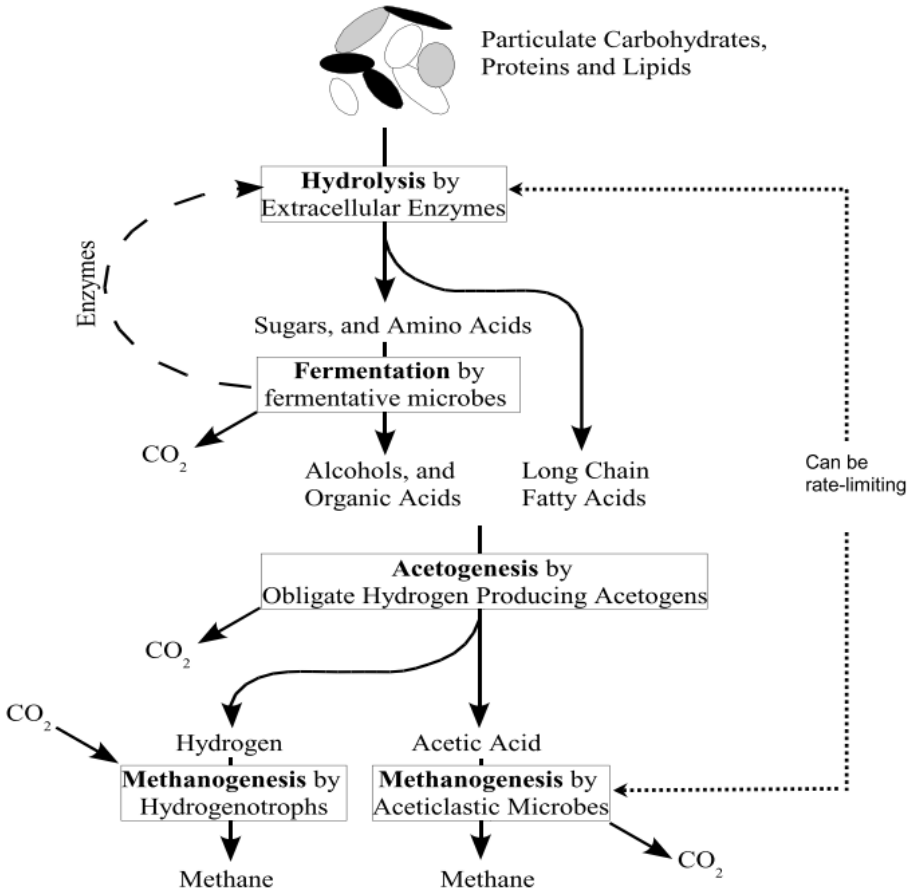

Figure 2.1: Different steps of anaerobic digestion process [40]

Anaerobic digestion can be divided into two categories based on the solid concentration of the feed, namely wet and dry anaerobic digestion. In the former category, the solid concentration is below 10%, whereas in dry digestion it ranges between 15% and 35%. The most usual configuration of a digester is the vertical continuous stirred tank, which is employed in approximately 90% of the biogas plants located in Germany, being the country with the largest number of biogas plants globally. Stirring is necessary in order that microorganisms come into contact with the feed, but also to keep constant temperature levels inside the digester. It is realised

by using mechanical or hydraulic mixing, with mechanical stirring being applied in most cases. Furthermore, wet digestion operates continuously, whereas in the case of dry digestion, both batch and continuous processes are employed. It is worth noting that wet digestion is the predominant method in the agricultural sector [38].

A very important parameter that can influence substantially biogas production, is the operating temperature within the digester, which should remain constant during the process. Generally, digestion takes place either at temperatures between 35-42 °C (mesophilic conditions) or between 45-60 °C (thermophilic conditions). In case of thermophilic conditions, the process is both faster and more efficient, since the growth rate in methanogenic bacteria is higher, and a shorter retention time of the feed is required. Nevertheless, during thermophilic conditions, the risk for NH_3 inhibition is larger, since the toxicity of the specific substance rises with increasing temperatures and can cause the wash out of microbial population. In addition, the concentration of volatile fatty acids will increase, causing a reduction in the values of pH, which should remain between the values of 6.8-7.2 for optimum CH_4 formation [41]. Furthermore, thermophilic processes are less resilient to temperature fluctuations, compared to the mesophilic which are able to accept temperature differences of ± 3 °C without a substantial decrease in the production of CH_4 [38]. Other parameters influencing the biogas production is the composition of feed (proteins and sugars display high values of CH_4 yield), retention time, continuous or batch configuration, single or two stage anaerobic digestion and feedstock pre-treatment [39].

2.2.1.2. Biogas and digestate utilization

A general overview of biogas potential applications is presented in Fig. 2.2. Biogas is considered a versatile renewable fuel, able to substitute fossil fuel consumption in electricity and heating generation, as well as in transportation sector [42]. Following production, biogas has to be cooled and dried immediately. Furthermore, if the concentration of hydrogen sulphide (H_2S) is higher than 250 ppm, cleaning is required before it is supplied to the power conversion technologies in order to avoid corrosion of surfaces [37]. Cleaning is usually performed by air injection, which oxidises H_2S.

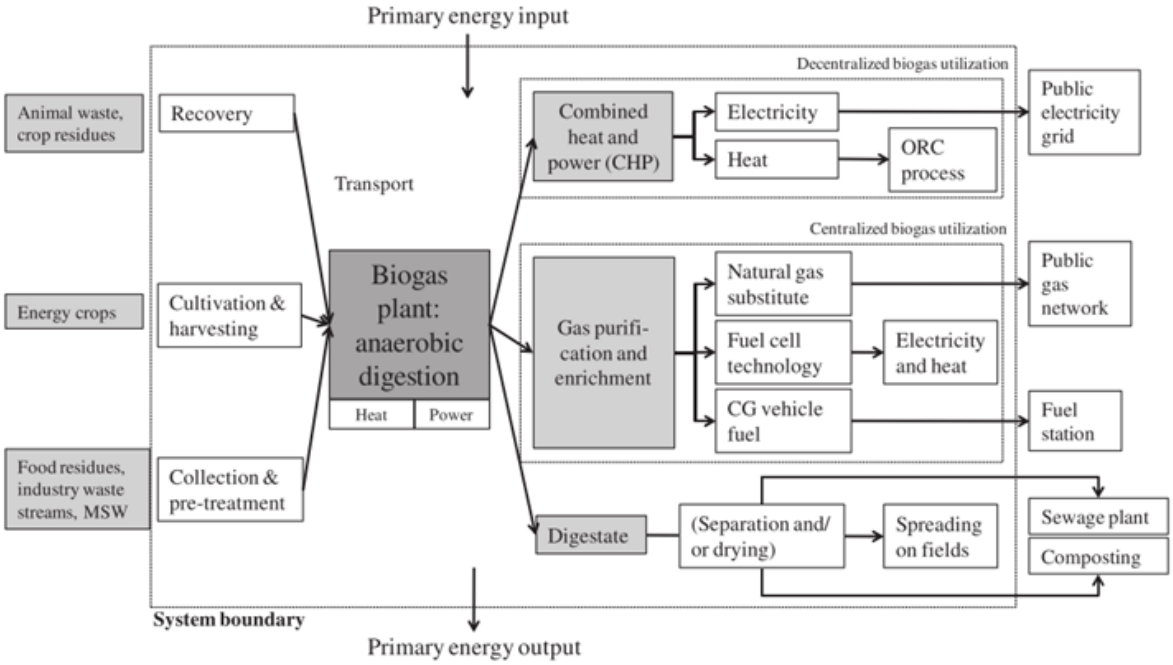

Figure 2.2: Potential applications from biogas utilisation [39].

Biogas can also be upgraded to biomethane and afterwards either injected to natural gas grid, or used as a fuel in the transportation sector. Upgrading requires the removal of CO_2 and other gas contaminants, so as the biomethane in its final concentration to consist of more than 95% CH_4 [38]. Methods commonly used for the removal of CO_2 include water or organic solvents scrubbing, and pressure swing adsorption by applying activated carbon [43].

Digestate is the remaining material after the completion of the anaerobic digestion. It can be separated into its solid and liquid phases, by applying solid-liquid separation technologies such as slope screens or screw-press separators. It is reported that separation can lead to the reduction of transportation requirements by up to 60%. Moreover, if drying process also follows, then the requirements can be reduced by another 25% [39]. Solid fraction can be used as alternative of chemical fertilizers, or as bedding material needed in livestock farms. Liquid fraction on the other hand can be re-used in the anaerobic digestion process, spread out to growing crops, or alternatively transported to a sewage treatment plant for disposal.

Regarding the challenges for further biogas development, biogas is characterised by low energy content and therefore increased feedstock volumes are required for an adequate biogas output. In most cases until now, biogas systems utilize waste streams (sewage and animal residues) and thus

they are most suited for distributed power generation. The overall efficiency of biogas plants can be greatly enhanced, if there is a need for the use of the heat generated during the process. Other measures that can contribute to the growth of the number of biogas plants are better process efficiency, new high-tech components for mixing and monitoring, and better process control [38].

2.2.1.3. Anaerobic digestion of poultry litter

Interest in anaerobic digestion of PL has been reflected on a number of publications recently. Most of the researchers have studied the co-digestion of PL with other substrates (e.g., energy crops, crop residues) rather than individually. Mixing PL with wetter substrates consisting also of higher carbon content, balances the C/N (Carbon/Nitrogen) ratio, pH, and dry matter content [44,45]. C/N ratio is a very important parameter in the co-digestion process. High values of the specific parameter may lead to fast nitrogen degradation resulting in low biogas yields. On the contrary, low values may affect negatively the methanogenesis step [44].

In the study of Rahman et al. [44], poultry droppings were co-digested with lignocellulosic biomass (wheat straw and meadow grass) by applying five different mixing ratios under mesophilic conditions (35 ± 1 °C). The authors argued that biogas yield and methane potential were significantly higher compared to those obtained from mono digestion of the tested fuels. Particularly, in the case of poultry droppings mixed with wheat straw, the maximum methane potential was 330 NL/ kg of VS (normal litre/volatile solids) obtained at 70:30 mixing ratio, while the respective one of poultry droppings mixed with meadow grass amounted to 340 NL/ kg VS at a 50:50 ratio.

Li et al. [45] studied the anaerobic co-digestion of chicken manure and corn stover under wet, semi solid and solid state conditions. Wet conditions imply that the solid content of the substrate is <10%, while for solid state conditions the solid content of the feedstock is >15%. The semi solid conditions fall between the 10% to 15% range. The authors concluded that the production of methane significantly increased in the case of the mixture compared to the digestion of the single substrates. The highest methane yield was obtained at 75:25 mixing ratio in wet conditions, providing a value of 218.8 NL/kg VS.

Wang et al. [46], investigated the effect of feedstock composition and C/N ratio on methane yield, when co-digesting dairy manure, chicken manure, and wheat straw. The findings revealed that

methane yield was higher in case of co-digestion rather than individual digestion. Moreover, as the C/N ratio increased, the methane potential increased until a maximum point and then declined. The maximum methane potential of 247.5 mL/kg VS was observed in the blend of dairy and chicken manure at a 40.3:59.7 ratio and a C/N ratio of 27.2:1.

In the study of Zhang et al. [47], the authors investigated the co-digestion of chicken manure with three different types of feedstock, namely wheat straw, corn stalks and rice straw under mesophilic conditions (35 ± 1 °C). Seven different mixing combinations were tested to obtain the optimum mixing ratio in terms of biogas and methane yields at a retention time of 60 days. Higher biogas yields were observed during co-digestion treatments, compared to the mono digestion of the substrates. Blend of chicken manure with corn stalks at 50:50 ratio obtained the highest biogas and methane yields, 817 mL/g VS and 383 mL/g VS respectively.

2.3. Thermochemical treatment technologies

2.3.1. Combustion

Combustion is the most developed technology for biomass utilisation having reached already a commercialisation level. It can be described as an exothermic chemical reaction between a fuel and an oxidant (air, pure oxygen) occurring at a relatively high temperature environment. During combustion C and H contents of the fuel are oxidised producing heat and forming CO_2 and H_2O along with traces of other gaseous elements (NO_x, SO_2, unburnt hydrocarbons, aerosols). The main parameter of the combustion process is the air equivalent ratio (ER) or lambda (λ), defined as the ratio between the actual amount of oxidant supplied in the reactor and the amount of oxidant needed for stoichiometric combustion. In order to ensure complete burnout of the fuel, air equivalent ratio acquires values higher than one (ER>1). Combustion takes place in three stages, namely a) heating and drying of feedstock, b) devolatilisation and char gasification, c) combustion of char.

Heating and drying of feedstock: Moisture content is a very significant factor affecting the efficiency of the combustion process. High levels of moisture lead to poor ignition conditions, lower combustion temperatures, reduced energy content, and the need for larger equipment related to flue gas treatment [48]. Inside the reactor moisture starts to evaporate at temperatures >100 °C, utilising the heat derived from the combustion zone. For fuels with high moisture contents, pre-

drying of the fuel before being fed in the combustion reactor is essential in order to ensure satisfactory combustion unit operation without penalising the thermal efficiency.

Devolatilisation and volatile combustion: Devolatilisation also called the pyrolysis stage occurs in the early stages of combustion initiating at temperatures between 160-250 °C. Due to thermal decomposition, the fuel releases light permanent gases (non-condensable gases), primary tar (condensable gases) and char (solids). In the next step, volatiles (permanent gases and tar) are oxidised producing CO_2, CO, H_2O, CH_4, H_2 and other hydrocarbons. Char gasification and oxidation is also present during this stage, but at a lower conversion rate since the reactions are slower compared to volatiles oxidation [49].

Char combustion: Char (fixed carbon) consists of carbon and ash from the biomass which generally contains inorganic minerals and alkali metals. Due to the fact that it's burning rate is much slower compared to volatiles, it is important to ensure that the carbon particles are not elutriated before being fully converted into gaseous products [50]. The main product in this stage is CO_2 resulting from direct oxidation of C or partial oxidation of CO.

2.3.1.1. Environmental issues during the combustion process

Although combustion of woody biomass is considered to be well developed, this is not the case for agricultural residues when applied as fuels in combustion units. The reasons are the distinct differences in their composition compared to wood biomass, which may pose challenges during the pre-processing and combustion stages [48]. For example, during combustion of agricultural residues high in ash content such as the PL, the volatile and semi-volatile elements contained in the ash (S, Cl, K, Na, Zn, Pb) are partly released into the gas (flue gas) phase. These elements are taking part in homogeneous reactions and form aerosols (particles with a diameter less than 1 μm known also as PM_1). Among the various compounds found in ash, K (potassium) has the highest impact on aerosol formation, since it is usually found in higher concentrations compared to the other ash forming elements [51,52]. Release of particulate emissions pose significant threat to the environment and human health, and as a result, flue gas cleaning equipment is installed in order to reduce or eliminate the aerosols emitted to the atmosphere.

High nitrogen content in PL originating mainly from animal feed, leads to elevated NO_x (NO, NO_2) emissions, which are linked to serious environmental pollution (acid rain and photochemical

smog). Additionally the formation of N_2O is also favoured in the presence of high nitrogen content, contributing to the greenhouse effect and ozone layer depletion in the stratosphere [53].Three different pathways exist as regards NO_x formation, namely thermal-NO_x, prompt-NO_x and fuel-NO_x. The first two become important when the operating temperature exceeds 1300 °C. However, this is not the case for biomass combustion, where the temperatures normally range between 900-1000 °C. Therefore, the predominant mechanism for NO_x emissions is the conversion of fuel nitrogen to NO_x, depending on the initial concentration of nitrogen in the fuel and the process conditions [49,54]. Release of nitrogen during fuel decomposition involves complex chemistry but generally fuel nitrogen is released mostly during the devolatilisation phase and is converted into HCN, NH_3, NO and small percentages of N_2O and NO_2. Some part of nitrogen is converted also during charcoal burnout, mainly as NO [55].

Concentration of sulphur (S) found in PL is higher than in wood and may also pose emission issues during combustion. The specific compound can vaporise and form sulphur oxides (SO_2 or SO_3) that if released to the atmosphere, can react with water vapor forming sulphuric acid (H_2SO_4). According to EU commission regulations [56] the emissions limits for SO_x during on farm combustion must not exceed 50 mg/Nm^3 (dry gas, 11% O_2). This is because, S compounds can mobilise the inorganics contained in the ash (mostly potassium) to form aerosols (K_2SO_4) through the vaporisation-condensation mechanism of ash formation [26,57–59].

Carbon monoxide (CO) and unburnt hydrocarbons (C_xH_x) are products of incomplete combustion. CO is a toxic gas, colourless and without smell, and its presence acts as an indicator of the combustion quality. From the various unburnt hydrocarbons that may be present in the flue gas due to incomplete combustion, methane (CH_4) is one of the most known since it contributes to the greenhouse effect [60].

2.3.1.2. Reactor types

Two main types of combustion furnaces exist, fixed bed systems and fluidised bed systems. The main features of each technology are presented below.

Fixed bed combustion systems

Fixed bed combustion systems comprise of a fuel bed resting on a grate which can be of fixed, moving, rotating, or vibrating type. In Figure 2.3. a typical layout of a fixed bed combustion

system is illustrated [61]. The fuel is fed by a screw feeder on a moving slopping grate and is being consumed as it travels along the grate. Primary air is supplied below the grate and passes through the fuel bed initiating the different stages of combustion process (drying, pyrolysis, etc.). Secondary air is injected in order to ensure complete burnout of the combustible gases generated in the primary zone. This concept known as air staging, requires primary air to be less than the stoichiometric (air ratio between 0.7-0.9) and has been proved to contribute significantly to the reduction of NO_x emissions [61,62]. Also, a cyclone is employed to remove fine solid particles entrained in the flue gases.

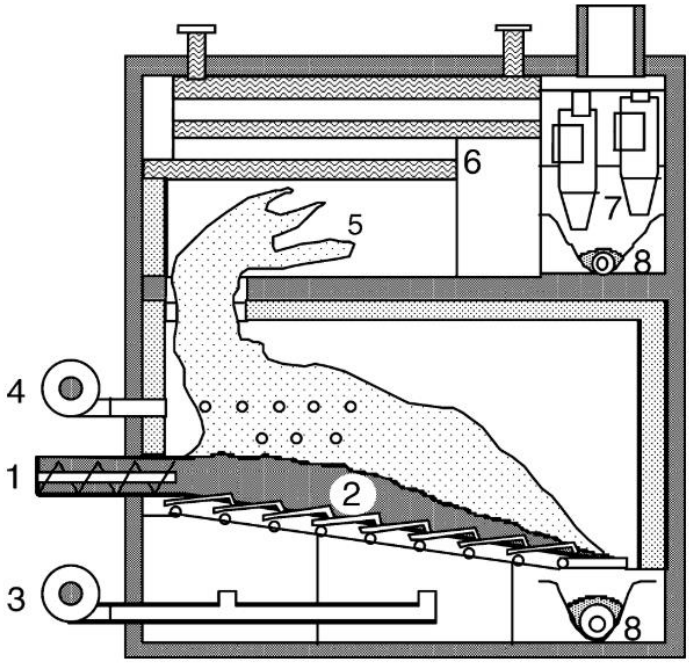

Figure 2.3: Moving grate furnace. 1: Screw feeder, 2: Moving grate, 3: Primary air, 4: Secondary air, 5: Post combustion chamber, 6: Heat exchanger, 7: Cyclone, 8: Ash removal. Adopted from [61].

Fixed bed technology has been widely employed over the years, since it displays a number of significant advantages. First, fixed bed systems are able to handle fuels characterised by heterogeneity with large particle sizes and moisture contents up to 65%. Moreover, the dust load in the flue gas is low, resulting in smaller sizing of equipment required to capture the entrained solid particles. Further advantages are the investment costs, which for plant capacities <10 MW_{th} are comparatively low, and the fact that fixed bed systems are insensitive to agglomeration issues. On the contrary, fuel mixing with air is not very effective, resulting in instabilities on the fuel bed. To overcome those instabilities high amounts of additional air is needed, a fact that decreases the

combustion efficiency but also enhances the NO_x formation [60,62]. Complete char burnout may also not be possible in fixed bed combustion systems, leading to significant amounts of carbon left with the bottom ash, or entrained with the flue gases, causing erosion on the boiler surfaces.

Fluidised bed combustion systems

In fluidised bed combustion systems, fuel mixed with bed material (usually sand) is placed on a perforated plate. The initially stationary solid mix is brought into fluidisation state, when coming into contact with a fluidising medium (air, nitrogen) penetrating the perforated plate at high velocities. In such systems, the gravitational force exerted on the solid particles, is offset by the upward movement of the fluidising medium [63]. The velocity of the fluidising air determines the configuration of the combustion reactor, i.e., bubbling, or circulating. In the former type, the solid particles are just held into suspension by the fluidising medium. In the latter type, the velocity of the fluidising medium increases further resulting in a continuous decrease in the concentration of solid particles as the height above the fuel distributor increases. A fraction of the solids is even entrained with the gas stream outside the reactor, and therefore a cyclone is employed in order to capture the solid particles, which are then returned back to the fuel bed via pipes.

Fluidised bed systems display significant advantages over fixed bed systems. First, they offer very intense mixing between the solid particles (fuel and bed material) and the fluidising medium, leading to temperature uniformity across the reactor. Secondly, due to the intense motion of the fluidised bed, a wide range of fuels can be combusted with different sizes, shapes, moisture contents, and calorific values. Moreover, the high heat capacity of the fluidised bed allows operating temperatures ranging between 850-950 °C, a fact that eliminates the formation of thermal NO_x [62]. Additionally, fluidised bed systems have no moving parts, therefore the maintenance costs are significantly reduced compared to moving grate technologies [50]. An important drawback of the fluidised bed technology, however, is the high dust load on the flue gas, and the consequent requirement for solid separation equipment (cyclones, filters). Additionally, corrosion risk of the internal surfaces is higher compared to fixed bed technology, due to the high velocities acquired from the solid particles. The agglomeration phenomenon is also of great importance in fluidised systems, especially when combusting fuels with high content in alkali metals (potassium and sodium). These substances, when reacting with silica contained in the bed material, may form low eutectic compounds that melt, resulting in serious instability in the operation of the combustion reactor [64].

2.3.2.3. Combustion of poultry litter

Quian et al. [65] investigated the production of electricity from co-combustion of poultry litter with natural gas. The experiments were performed in a lab-scale swirling fluidised bed coupled with a 1 kW Stirling engine. The authors studied the effect of different parameters (primary air ratio, fuel mixing ratio w/w%, height of secondary air injection point) on the electricity production, gaseous emissions, and fly ash composition. Air ratio was varied between 0.04-1.54. The authors suggested that primary air ratio should lie between 0.79-1.08 to decrease both NO_x and CO emissions, while producing 905 kW of electrical power. Furthermore, reaching a 4.51 fuel mixing ratio by increasing the poultry litter mass, was found to decrease both NO_x and SO_2 emissions. Three different heights for secondary air injection were tested (650 mm, 850 mm, and 1100 mm) and the findings revealed that 850 mm was the ideal height to decrease emissions, since at this condition oxygen distribution was more effective and residence time was increased. High amounts of phosphate (10%) and potassium (6%) showed the suitability of poultry litter ash as soil amendment.

Abelha et al.[66] studied the combustion behaviour of poultry litter mixed with peat in a lab-scale fluidised bed reactor. The authors reported that if the moisture content exceeded 25%, problems associated with feeding occurred leading to unstable conditions. Air staging was found to have a reducing effect on both CO and NO_x emissions. Emissions of SO_2 were reported to be very low, due to the low sulphur content in the poultry litter, and also due to the high presence of calcium (Ca) which retained sulphur in the bed ash. High levels of potassium were observed in the cyclone ashes, indicating the volatility of the specific compound in high temperature environments. Leaching tests of heavy metals present in the cyclone ashes showed a small tendency for leaching, making poultry litter ash suitable for agricultural purposes.

Lynch et al. [51] investigated the ash agglomeration and deposition mechanism during combustion of poultry litter under fluidised bed conditions. The authors reported that the generated ash consisted predominantly by a coarse fraction of crystalline ash consisting of alkali-Ca-phosphates and a fine fraction of particulate K_2SO_4 and KCl. Bed agglomeration was coating induced, composed of two distinct layers. The inner layer with thickness ranging between 0.05-0.09 mm resulted from the reactions between the gaseous potassium and the silica sand, forming K-silicates. The outer layer was loosely bound and consisted of fine particulate ash resulted from char. Deposition on the equipment downstream characterised by low temperature regions, occurred through the vaporisation-condensation mechanism.

Topal et al. [67] conducted a theoretical study investigating the performance of a tri-generation (TG) system based on the combustion of poultry litter mixed with coal. The system composed of steam boiler, steam turbine, and a single stage absorption chiller. The authors reported that both energy and exergy efficiencies were lower in the tri-generation mode compared to CHP system alone. Gross electrical output was in the range of 250-260 kW for a fuel input of 400 kg/hour, while the emissions were slightly reduced when the system operated in a TG mode.

Zhu et al. [68] studied the co-combustion of poultry litter and sawdust with natural gas in a swirling fluidised bed reactor. Carbon combustion efficiency, temperature distribution profiles, and release of gaseous emissions were measured against different primary excess air ratios, secondary air ratios, and secondary air injection heights. The findings suggested that carbon combustion efficiency was 10-15% higher in case of sawdust, due to the high ash and low volatile contents of poultry litter, under fixed amounts of primary excess air and secondary air. The bed temperatures of sawdust and poultry litter exactly above the feeding point were 875 °C and 865 °C respectively, while in the freeboard the temperature was higher for poultry litter. These observations indicated that most of the sawdust is burnt in the bed, whereas combustion of poultry litter occurs mainly in the freeboard due its lower volatile content. Regarding the height variation of the injection point of secondary air, it was reported that when the primary excess air was <25%, the carbon combustion efficiency decreased, while the opposite trend was observed for values of primary excess air >25%. Moreover, the authors argued that temperature has a little effect on NO_x missions. On the contrary increased values of primary excess air cause a significant increase in NO_x emissions, because of higher availability of oxygen.

The first plant utilising poultry litter as a fuel, was commissioned at Eye, Suffolk in 1992, by the company Fibropower. It is believed that it is the first power plant to run on poultry litter globally. The system operates on moving grate technology combusting 160,000 tons of poultry litter/year and thus providing 58 tons/hour steam at 66 bar (gauge) at 450 °C. Electrostatic precipitators are used in order to ensure low dust emissions after combustion process [18]. Recently refurbishment took place in order to add more fuel flexibility to the plant, which is now able to run on mixture of poultry litter with wood waste [69].

Company Fibrowatt built two power stations running on poultry litter. The first one was located in Glanford, Lincolnshire, and started operation in 1993. The plant produces 13.5 MW of electricity generated by steam turbine technology. In 1999 the plant was retrofitted by redesigning the fuel dosing system, installation of advanced spreader stoker and upgrade of furnace and secondary air

system. Retrofitting took place in order for the plant to switch from poultry litter to meat and bone meal [70,71]. Similarly to the plant in Eye, an electrostatic precipitator is exploited to control the dust emissions [18]. The second power plant is located in Thetford, Norfolk, and started operation in 1999. The plant utilises over 400,000 tons of poultry litter generating 38.5 MW electrical power. Instead of electrostatic precipitators, a cyclone and baghouse filter installed in series are used to control the dust emissions. Additionally, in order to mitigate HCl and SO_2 emissions, lime is injected in the flue gas stream between the cyclone and the baghouse filter [18].

2.3.2. Gasification

In the gasification process, a carbon-based feedstock is dissociated in a high temperature environment (700–1500 °C), in the presence of an oxidant under sub stoichiometric conditions. The product of gasification is a combustible gas, known under different names such as "producer gas", "product gas", or "syngas", consisting mainly of CO, H_2, CO_2, CH_4 and a small amount of C_{2+} compounds, along with impurities such as fine particulates, tar, and alkali metals [72]. To maintain consistency, the term product gas will be used, since syngas refers to a gas containing only H_2 and CO [73]. The composition and quality of the product gas depend on feedstock properties, operating conditions, gasifier reactor type, and oxidising medium. Typically, air, steam, oxygen, or a mixture of them are used as gasification oxidants. The most common applied oxidant is air since it is inexpensive and readily available. However, in air gasification the product gas is diluted by N_2 (up to 60%), resulting in a lower calorific value (LCV) ranging between 4-7 MJ/Nm^3 [72]. On the contrary, when pure oxygen is used, the product gas is free of N_2 with LCV of 10-15 MJ/Nm^3. The drawback of gasification with oxygen are the high investment costs needed for air separation units, making it suitable only for large scale applications. Oxidation with steam generates a product gas with high H_2 concentration and N_2 free. The LCV ranges between 15-20 MJ/Nm^3. However, external energy is required for the production of steam [74].

Gasification is considered as a more flexible technology compared to combustion, since the product gas can be utilised in a wide range of applications, being that heat and power generation, biofuel production, and chemicals [75]. Moreover, the fact that gasification takes place in oxygen deficient environment, favours the production of CO and H_2 at the expense of CO_2 and H_20. Also, N and S are converted mainly into NH_3 and H_2S, avoiding in this way the formation of NO_x and SO_x compounds. The volume of gas produced from gasification is also lower compared to

combustion for the same fuel input, resulting in more compact equipment and fewer additional costs [50]. On the other hand, product gas from gasification contains solid particles that are entrained with the gas flow and that need to be removed prior utilizing the product gas in downstream applications. Additionally, the formation of alkali metals at temperatures higher than 700 °C may create issues related to corrosion of metal surfaces due to their condensation. However, the largest technical obstacle that hinders further development and commercialisation of gasification technology is the presence of tar in the product gas.

2.3.2.1. Challenges of tar during biomass gasification

Tar is a mixture of complex hydrocarbons which may condense in the process installation if the temperature drops below the tar dew point. Condensation of tar leads to the formation of a black and sticky material which causes system malfunctioning due to clogging and fouling. Multiple definitions of tar can be found across literature. One of the most representative definition is the one derived from International Energy Agency (IEA) gasification task force which defines tar as ‘‘the organics produced under thermal or partial-oxidation regimes (gasification) of any organic material, are called tar and are generally assumed to be largely aromatic” [76].

Depending on the final utilization of the product gas, tar concentration limits may apply. For example, if product gas is to be used as fuel in internal combustion engines or gas turbines for the generation of electricity and heat, gas cleaning is imperative, a fact that increases process complexity and costs. Suggested tar limits for various power devices can be found in Basu [76]. Indicatively, the tar limit for utilization of product gas in internal combustion engines is 50-100 mg/Nm^3.On the contrary, if the product gas is burnt directly in combustion systems (furnaces, ovens), cooling of gas is not necessary and thus, there is minimum risk of tar condensation and gas cleaning can be avoided. Apart from the total amount of tar present in the gas, the composition also plays a significant role in predicting the tar condensation in downstream applications. In general, the presence of tar compounds with higher molecular weight tends to increase tar dew point and vice versa.

There are two different tar classifications considered, either based on the temperature regime under which tar compounds are formed [77] or based on water solubility, dew point temperature, and aromatic ring number [78]. According to Milne et al. [77], tar is classified into primary, secondary, alkyl tertiary, and tertiary tar groups. Primary tar derives from pyrolysis reactions of lingo-

cellulosic materials at temperatures between 200 °C and 500 °C. Primary tar consists of highly oxygenated compounds such as acids, sugars, alcohols, and ketones [79]. As the temperature increases and with the presence of the gasification oxidant, primary tar releases functional groups and reforms into light non-condensable gases and heavier compounds called secondary tar. Examples of secondary tar are phenols and olefins which remain stable up to the temperature of 700-750 °C. Above 750 °C the secondary tar undergoes rearrangement into tertiary tar by completing the condensation pathway resulting in purely aromatic species [80]. Tertiary tar consists mainly of polycyclic aromatic hydrocarbons (PAHs) such as naphthalene, acenaphthylene, and pyrene. PAHs increase exponentially with temperature due to polymerisation. Alkyl tertiary tar such as methyl naphthalene and biphenyl are intermediates between secondary and PAH tar. The yield of PAHs appears to peak at 850 °C followed by a gradual decrease [80,81]. Tertiary tar is not present in the initial biomass but rather as a product of decomposition and rearrangement of secondary tar. Typically, tertiary and primary tars do not co-exist in the reactor [80,82], nevertheless, in some reactor arrangements this scenario is possible. A complete overview of tar evolution based on the different temperature regimes is given in Table 2.1.

Table 2.1: Classification of tar based on Milne et al. [77]

Up to 500°C	Primary tar	Cellulose, hemicellulose and lignin-derived products such as levoglucosan, hydroxyacetaldehyde, furfurals, methoxyphenols 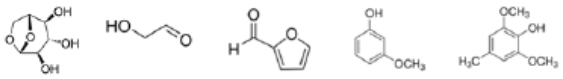
From 500 to 700°C	Secondary tar	Phenolics and olefins 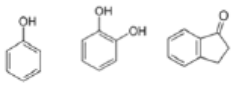
From 700°C upwards	Alkyl tertiary tar	Methyl derivatives of aromatics, such as methylacenaphthylene, methylnaphthalene, toluene, and indene. 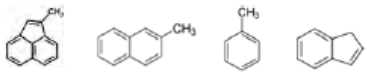
	Condensed polycyclic aromatic hydrocarbons (PAH) tertiary tar	PAH series without substituents, such as benzene, naphthalene, acenaphthylene, anthracene, phenanthrene, pyrene. 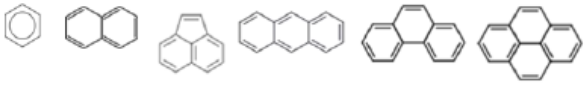

According to the classification proposed by Paasen and Kiel [78] tar is categorised into five different classes (see Table 2.2). Class 1 includes tar compounds that cannot be detected by gas-chromatography (GC) equipment and they are usually found in very small concentrations (<0.1 mg/Nm^3). They are also characterised by high temperature dew point (>200 °C) [83]. Class 2 contains heterocyclic tar compounds highly soluble in water, a fact that poses challenges regarding waste water treatment. Tar compounds belonging to class 3, are hydrocarbons that are not related to condensation, or any water solubility issues. Light polyaromatic hydrocarbons of class 4 are known to condense at high concentrations and intermediate temperatures, whereas class 5 hydrocarbons condense at high temperatures and low concentrations.

Table 2.2: Tar classification based on Paasen and Kiel [78]

Tar class	Tar compounds
Class 1: GC-undetectable	Compounds larger than coronene
Class 2: Heterocyclic *Aromatics*	Compounds such as phenol, pyridine, cresol
Class 3: 1 aromatics ring	Compounds such as xylene, styrene, toluene
Class 4: Light polyaromatic hydrocarbons (2-3 rings)	Compounds such as naphthalene, fluorene, phenanthrene
Class 5: Heavy polyaromatic hydrocarbons (4-7 rings)	Compounds from fluoranthene up to coronene

2.3.2.2. Processes inside a gasifier

Gasification involves four different phases, namely drying, pyrolysis, oxidation, and reduction. Although these stages are usually modelled in series, there is no clear distinction between them and they often overlap [76]. A simplified diagram of gasification process is presented in Fig 2.3, while a brief description of the different phases during biomass gasification is given below. It should be mentioned that when the required heat is provided by external sources, gasification is called allothermal, whereas when heat is provided internally by exothermic reactions occurring within the gasifier, it is called autothermal gasification.

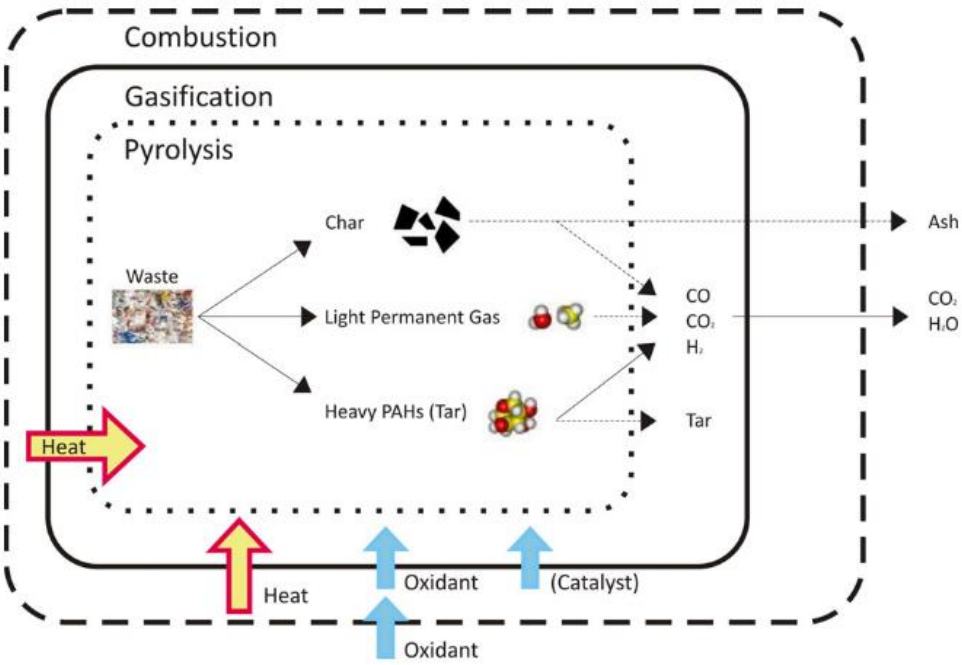

Figure 2.4: Schematic representation of the different stages of gasification process [72].

Drying: Moisture content of biomass is a decisive factor as regards the gasification efficiency. Typical values of moisture for biomass fuels range between 5-35%, but sometimes moisture of fresh biomass after harvesting can reach up to 60% [7,84]. For every kilogram of moisture, 2260 kJ of energy is required to vapourise water. The heat needed in order for the drying to be accomplished is provided by the exothermic reactions occurring within the gasifier reactor. Based on the gasifier type, pre-drying of the fuel before it gets into the gasifier may also be required. This usually happens by an external heat source such as steam or air in temperatures around 150-200 °C. Most gasification systems are able to operate with a moisture content between 10-20% [85].

Pyrolysis: Following the drying process, biomass is thermally decomposed in the absence of oxygen at temperatures between 200-700 °C, releasing light permanent gases (non-condensable at ambient temperature), condensable gases (primary tar) and solid residues (char). The composition and quantities of the pyrolysis products rely on various parameters, such as composition of biomass, temperature, pressure, and heating rate [72]. Permanent gases include H_2, CO, CO_2, CH_4, H_20, but also some minor quantities of C_{2+} hydrocarbons (C_2H_6, C_3H_8, etc.). Primary tar consists of oxygenated hydrocarbons as described in Table 2.1 before**,** whereas char is comprised of unreacted carbon and ash material (inorganics and alkali metals). The overall pyrolysis reaction is described in equation 2.1.

$$Biomass = Permanent\ gases + Tar + Char\ (endothermic) \quad (2.1)$$

Oxidation: Part of pyrolysis parts are being oxidized with the aid of the gasification oxidant, in order to provide the heat necessary for drying, pyrolysis, and gasification endothermic reactions, while maintaining the desired operating temperature of the gasifier. Although partial oxidation involves all the pyrolysis products including tar, it is possible to simplify the oxidation process by considering that only char and hydrogen react with oxygen, as shown below [82].

$$C + \frac{1}{2}\ O_2 \rightarrow CO \quad with\ DH^O = -110{,}5\ \frac{kJ}{mol} \quad (2.2)$$

$$C + O_2 \rightarrow CO_2 \quad with\ DH^O = -398{,}8\ \frac{kJ}{mol} \quad (2.3)$$

$$H_2 + \frac{1}{2}\ O_2 \rightarrow H_2O \quad with\ DH^O = -242\ \frac{kJ}{mol} \quad (2.4)$$

Reduction (gasification): In the reduction phase both homogeneous and heterogenous reactions are taking place in a high temperature reducing environment. The most important are given in equations 2.5-2.8, while it should be noted that all the reactions follow chemical equilibrium. Water gas reaction acetolactic (equation 2.5) and Boudouard reaction (equation 2.6), both increase the concentration of CO and H_2 in the final composition of the product gas. They are both endothermic, implying that their equilibrium shifts towards the formation of products when the temperature increases. Equations 2.7 and 2.8 describe water gas shift and methanation reactions respectively. They are both slightly exothermic, thus they are favoured in lower temperatures. Overall, the reduction phase is considered endothermic, meaning that heat resulting from oxidation reactions is needed in order the reduction phase to be realised. The temperature in the reduction phase is a very significant parameter, affecting char conversion, presence of tar in the product gas, as well as its energy content [82].

$$C + H_2O \leftrightarrow H_2 + CO \quad with\ DH^O = 131{,}3\ \frac{kJ}{mol} \quad (2.5)$$

$$C + CO_2 \leftrightarrow CO \quad with\ DH^O = 172{,}5\ \frac{kJ}{mol} \quad (2.6)$$

$$CO + H_2O \leftrightarrow H_2 + CO_2 \quad with\ DH^O = -41\ \frac{kJ}{mol} \tag{2.7}$$

$$C + 2H_2 \leftrightarrow CH4 \quad with\ DH^O = -74{,}8\ \frac{kJ}{mol} \tag{2.8}$$

2.3.2.3. Gasifier types

Gasification technologies can be distinguished on the basis of: a) the gasification oxidant used (air, oxygen, steam), b) the heat source (allothermal or autothermal gasification, c) the gasifier design, and d) the gasifier operating pressure. From the above classifications, the most common one is the gasifier design. There are three main gasifier designs, namely fixed bed, fluidised bed, and entrained flow gasifiers and their most important aspects are described below [84].

Fixed bed gasifiers

Fixed bed gasifiers are divided into two subcategories, updraft and downdraft gasifiers. In the former type of gasifier depicted in Fig 2.5(a), fuel is inserted at the top of the gasifier and is moving downwards passing through the different gasification zones in the order: drying, pyrolysis, char gasification, and partial oxidation. The gasification oxidant enters the reactor from the bottom, initiating the partial combustion of unconverted carbon (char) in the oxidation zone at temperatures ranging between 1000-1600 °C. Afterwards the hot gas produced from oxidation moves upwards in the reduction zone where the gasification of char descending from pyrolysis zone takes place at temperatures between 600-1000 °C. What follows the reduction zone, is the thermal decomposition of the biomass fuel in the pyrolysis zone (200-600 °C).The product gas is further cooled in the drying zone and as a result its temperature exiting the gasifier is between 200-300 °C [86]. Updraft gasifiers are the oldest type of gasifiers characterised by the simplest design. Due to the upward movement of gases, a large drying zone is created, allowing the utilisation of feedstock with moisture up to 60%, Additionally, updraft gasifiers are easily scalable up to 10 MW thermal input [7]. However, a major drawback of the specific type of gasifier, is the high content of tar in the product gas. Tars are formed in the pyrolysis zone and thus they pass only through the drying zone where the temperature is low and thermal cracking is unlikely to occur. The composition of tar consists mainly from oxygenated compounds as well as light aromatics [86].

In the downdraft design shown in Fig. 2.5(b) the fuel is also fed from the top, while the gasification oxidant is inserted either from the top or the sides. The sequence of the processes based on the specific gasifier design is drying, pyrolysis, followed by oxidation and finally the gasification of char. The product gas moves downwards and exits from the bottom. Biomass fuel is dried and further decomposed in the pyrolysis zone, similarly to the updraft design. Nevertheless, part of the char and tar produced in the pyrolysis zone, are oxidised before entering the reduction zone. Afterwards, the hot gases move downwards passing through the remaining char in the bed where reduction phase occurs. The exit temperature of the produced gas is high between 500-900 °C and it is also characterised by small amounts of tar (mainly aromatic species) due to the effective thermal cracking in the oxidation and reduction zones. However, due to the fact that the hot gas passes through the bed, the particle load exiting with the product gas is higher compared to the updraft gasifier. Moreover, downdraft gasifiers are very sensitive to moisture and particle size parameters. Particularly, moisture shouldn't exceed 25% of the biomass composition and the particle size should be as homogeneous as possible preventing blockages in the throat section [76,86]. Also, due to the limitations stemming from the geometry of the reactor, their maximum size is around 2 MW of thermal input.

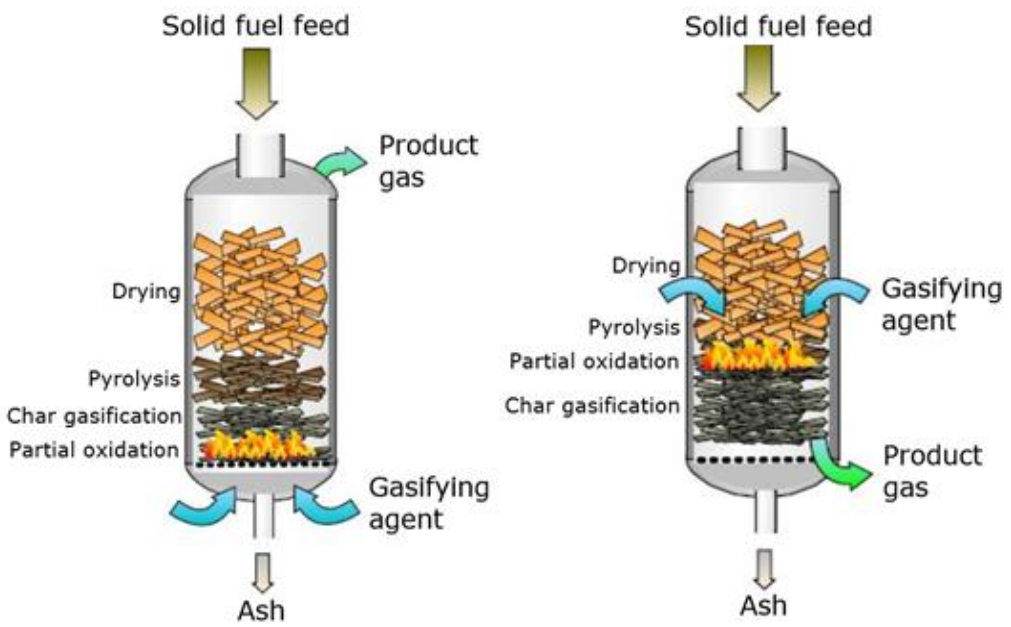

Figure 2.5: Schematics of an updraft (left) and a downdraft fixed bed gasifier (right) [86].

Fluidised bed gasifiers

In fluidised bed gasifiers, the gasification oxidant enters from the bottom of the reactor, penetrating a bed of inert material (typically silica sand or olivine), where the biomass fuel is located. The superficial velocity of the oxidant is significantly larger compared to the minimum fluidisation velocity (the velocity that equals the drag forces of the solid particles to equal their weight) and as a result, the bed acquires a fluid-like behaviour [82]. Due to the intensive mixing of fuel particles with the bed material, the different gasification phases take place in the whole reactor volume, resulting in almost isothermal conditions. The operating temperature of fluidised bed gasifiers falls between 700-900 °C in order to avoid any ash sintering (agglomeration) issues [86,87], a fact that is particularly important for biomass fuels with high ash content. Compared to fixed bed gasifiers, they offer greater fuel flexibility, achieve high heat transfer rates, while they are also suitable in different scale of applications [87]. The tar load ranges between the downdraft and updraft gasifiers, consisting mainly from aromatic species. The explanation for the higher load compared to the downdraft design stems from the fact that aromatic tar species are not exposed in temperatures as high as the respective ones found in the oxidation zone of a downdraft gasifier.

The two different types of fluidised bed gasifiers are schematically presented in Fig 2.6. The main difference between the two designs is the velocity of the fluidising medium. In the bubbling fluidised bed (BFB) gasifier, the velocity of the oxidant medium is low (2-3 m/sec) and thus, only few bed particles can escape from the reactor together with the gas flow. On the contrary, the high velocities (5-10 m/sec) developed in the circulating fluidized bed (CFB) cause the drifting of many solid particles within the gas flow. Therefore, in order to ensure stable operating conditions a cyclone is needed to capture the discharged bed material and char, which are then reintroduced in the gasifier providing heat via partial oxidation.

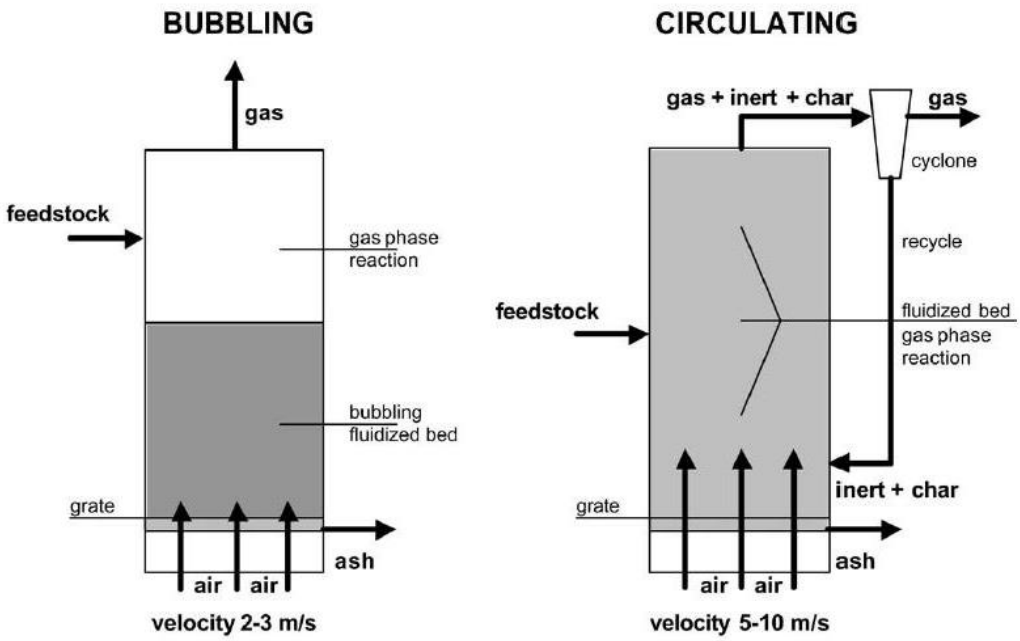

Figure 2.6: Schematic of fluidised bed gasifiers. a) Bubbling fluidised bed, b) Circulating fluidised bed.

Entrained flow gasifiers

Entrained flow gasifiers operate in high pressures (25-30 bar) and they were initially exploited in coal gasification for large scale industrial applications [72]. The gasification oxidant is pure oxygen, leading to increased operating temperatures ranging between 1300-1500 °C, resulting in almost tar-free product gas [82]. The gasifier operates always above the ash melting temperature to maintain ash in the liquid phase. Compared to the other gasifier types, entrained flow gasifiers achieve high carbon conversion, almost tar-free product gas and low methane content in the final composition of the product gas. Although the specific type of gasifiers seems attractive for the exploitation of biomass fuels, short residence time in entrained flow reactors require powder size particles (<1 mm) to ensure complete carbon conversion. Nevertheless, grinding of biomass particles to achieve the required size is an energy intensive process giving rise to high investment costs, a fact that currently limits the use of biomass in this type of gasifiers [7].

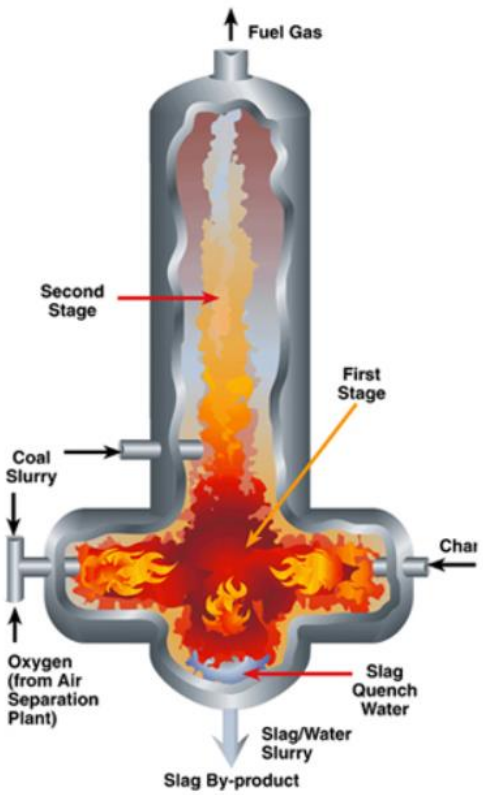

Figure 2.7: Schematic of entrained flow gasifier. Adopted from [88].

Table 2.3 illustrates some important features of fixed and fluidized gasifier designs. In general, downdraft gasifiers are well suited for small scale applications due to physical limitations stemming from the geometry of the reactor. Important preconditions for an efficient performance of a downdraft gasifier are the low percentages of ash and moisture content of the fuel, so as to avoid both clogging and temperature decrease within the gasifier reactor. Updraft gasifiers on the contrary are well applicable for medium-large scale applications and they offer higher fuel flexibility than the downdraft gasifiers. They can accept a high moisture content of the incoming fuel due to the presence of a large drying zone. The drawback of this specific design of gasifier is the high tar content in the produced gas, a fact that makes essential the installation of an extensive gas cleaning equipment. Fluidised bed gasifiers are characterised by high heat exchange rates and isothermal conditions across the gasifier reactor due to very effective mixing between the fuel and the bed material. Furthermore, they offer great fuel flexibility and they can be employed in a wide range of application scales. Tar content is higher compared to downdraft gasifiers but lower than the updraft gasifiers. Entrained flow gasifiers are designed for very large-scale applications, whereas the fact that fuel particles must be sized below <1 mm, make them unfavourable for biomass applications.

Table 2.3: Parameters related to the different gasifier designs [72]

Parameters	Updraft	Downdraft	Bubbling	Circulating	Entrained
Moisture	< 50	< 20	< 55	< 55	<15
Particle size (mm)	<100	<100	<150	<100	<1
Ash content d.b. (%)	15	5	25	25	20
Ash melting point (°C)	>1250	>1000	>1000	>1000	>1250
Application area (MWth)	<2	2-10	5-100	5-100	>50

2.3.2.4. Gasification of Poultry litter

Interest in PL valorisation as a gasification feedstock together with the specific challenges of this fuel is reflected in a number of publications in the recent years, however, very few are the actual installed systems.

Pandey et al. [29] studied the effect of limestone addition to prevent agglomeration while gasifying PL in a lab-scale fluidised bed reactor. The authors reported that by adding 8% w/w limestone, agglomeration did not occur below 800 °C compared to the case without limestone where agglomeration was observed at 750 °C. The optimum conditions (maximum carbon conversion, gas yield, and cold gas efficiency) were achieved at an equivalence ratio (ER) of 0.25 and temperature 800 °C, resulting in a product gas with LCV of 4.52 MJ/Nm^3.

Di Gregorio et al. [89] investigated the effect of ash composition on PL gasification in a pre-pilot reactor by comparing two batches of poultry manure taken from an industrial poultry farm. The experiments were carried out at different ERs (0.27–0.4) and temperatures (700–800 °C). The findings revealed the role of ash composition, since all the process parameters were significantly reduced in the batch with the higher ash content. In particular, increase of ash content from 17.2% to 25.1% and higher fractions of calcium, potassium, and phosphorus, reduced cold gas efficiency (CGE) from 0.63 to 0.33 and the specific energy from 2.1 to 1.1 kWh/kg$_{fuel}$.

Priyadarsanet al. [90] co-gasified coal with cattle and poultry manure in a fixed bed gasifier operating in batch mode. Compared to coal test run, the blends displayed higher CO_2 and H_2

concentrations, whereas the LCV for all tested fuels was in the range 4.5-5.12 MJ/kg on a dry basis.

Font Palma et al. [91] studied six different model-based energy integration schemes based on a small scale gasifier coupled with gas turbine technology for onsite power generation. The findings revealed that CGE and exergetic efficiency ranged between 58.4–79.5% and 46.8–65.7% respectively. The preferred 200-kW system configuration including heat recuperation from the gas turbine exhausts and pressurised air before being fed in the gasifier resulted in electrical efficiencies between 26% and 33.5%.

Huang et al. [92], performed a technoeconomic feasibility analysis of generating biochar, electricity and heat production from PL using a model developed in ECLIPSE software. The authors concluded that gate fees, carbon credits and renewable energy certificates greatly influence the breakeven selling price of produced biochar.

Cavalaglio et al. [93] studied the installation of an innovative 300 kW thermal power gasification plant installed on a poultry farm located in central Italy. Further to the real plant monitoring, an Aspen Plus v.8.0 model was developed by the authors to predict the outlet product gas composition and its LCV which was found in the range 3–5 MJ/m^3 for an ER of 0.2.

Taupe et al. [24] studied an updraft gasification system installed at a farm with capacity of 40 kg/h. The ash melting temperature was 639 °C, therefore the operating temperature of the gasifier was kept around that value to avoid any agglomeration issues. Cold gas efficiency (CGE) of 0.26 and carbon conversion efficiency (CCE) of 0.44 were reported, reflecting the negative impact of low operating temperature on the process performance parameters. The LCV of the clean product was reported to be 3.39 MJ/Nm^3.

2.3.3. Pyrolysis

Pyrolysis is the thermal decomposition of biomass in a complete oxygen free environment. It is a complex process where both simultaneous and successive reactions take place, when external heat is applied in the absence of a reactive agent. The outputs of pyrolysis are solid matter (biochar), condensable vapours (bio-oil) and permanent gases. Although these products are always present, their final proportion in the final product is dependent on various process parameters, such as

temperature within the reactor, heating rate of the feedstock, particle size, pressure, and reactor configuration [94].

2.3.3.1. Types of Pyrolysis

Generally, pyrolysis can be classified in three categories, namely slow, fast, and flash pyrolysis, based on the applied heating rate. A brief description of the different types is given below.

Slow pyrolysis

Slow pyrolysis is divided into two categories, carbonisation and conventional pyrolysis. The former type is applied from ancient years, resulting in the production of char. It is performed at low temperatures (~400 °C), very low heating rates, and the fuel residence time can be very long (in the order of days). Char is mostly comprised of carbon (~ 85%), but also hydrogen, oxygen, and inorganic ash constituents may be present. The LCV of char is around 32 MJ/kg, significantly higher than the LCV of biomass itself. In conventional pyrolysis, biomass is heated slowly at a moderate temperature (400-600 °C). Vapour residence times are in the order of minutes (5-30 minutes), while the heating rates range between 0.1-1 °C/s [95]. Char, bio-oil, and gas are all produced during conventional pyrolysis. [76].

Fast pyrolysis

In fast pyrolysis, the decomposition of feedstock occurs rapidly, resulting in the production of vapours and smaller amounts of biochar and gas. Following condensation, a dark brown homogenous liquid is formed, with LCV between 13-18 MJ/kg on a wet basis [76]. The yield of the liquid acquires higher values than in slow pyrolysis, while the remaining yields of biochar and gases can be utilized in order to provide the necessary heating, minimizing in this manner the waste streams of the process. The main characteristics of fast pyrolysis are the high heating rates ranging between 100-1000 °C/sec and the short residence times of hot vapours (< 2 seconds) in order to avoid secondary reactions. Rapid cooling of the produced vapours and control of temperature inside the reactor at ~500 °C [76,96,97] are essential for maximising the bio-oil yield. Other important features for an effective fast pyrolysis process are small particle sizes < 2 mm

[40], drying the feed to <10% moisture, and fast separation of bio-oil from biochar material due to its catalytic effect on vapours cracking [96].

Flash pyrolysis

Flash pyrolysis is characterised by very short vapour residence times (< 1 sec), very high heating rates, small particle sizes (<0.2 mm) and temperatures < 650 °C inside the reactor [76]. It is reported that bio-oil yields up to 75% can be achieved when flash pyrolysis is applied [95]. On the other hand, problems associated with the specific pyrolysis type relate to thermal instability of the bio-oil, presence of solid particles in the bio-oil, and increase in its viscosity due to the catalytic action of char.

In summary, maximizing biochar production requires low temperatures, high residence times and large particle sizes. On the contrary, moderate temperatures, short residence times and smaller particle sizes, favour the production of bio-oil at high yields. Finally, high temperatures and longer residence times result in high gas yields.

2.3.3.2. Fast pyrolysis reactors

The most important part of an integrated pyrolysis system is the reactor. Fixed bed reactors are the oldest type of reactor, mainly utilised in slow pyrolysis applications due to low heating rates and long vapour residence times. However, for fast pyrolysis applications different type of reactors are employed (see. Fig. 2.8). Fluidised bed reactors are the most commonly used, due to the fact that it is a well understood technology, providing good temperature control, high heat transfer rates and are easily scalable [76]. The operational principles and characteristics of fluidised bed technology have been described in previous sections and thus they will not be repeated. It should be mentioned that residual char and fraction of the produced gas are burned in a combustor providing the heat needed for the pyrolysis process, as well as creating fluidising conditions. The residence time for char and vapours depends on fluidising medium's flow rate, and for bubbling fluidised beds (BFB), it is generally higher for char compared to vapours. Since char is known to act as catalyst in vapours cracking into lighter molecules, a cyclone is employed in order to separate it fast from the pyrolysis products [96]. Circulating fluidised bed (CFB) reactors, have the same operating principles as BFB reactors, except that the fluidisation velocity is higher, resulting in higher

attrition of char and bed material entrained with the gas flow. CFB, are more suited for larger throughputs compared to BFB [76,96].

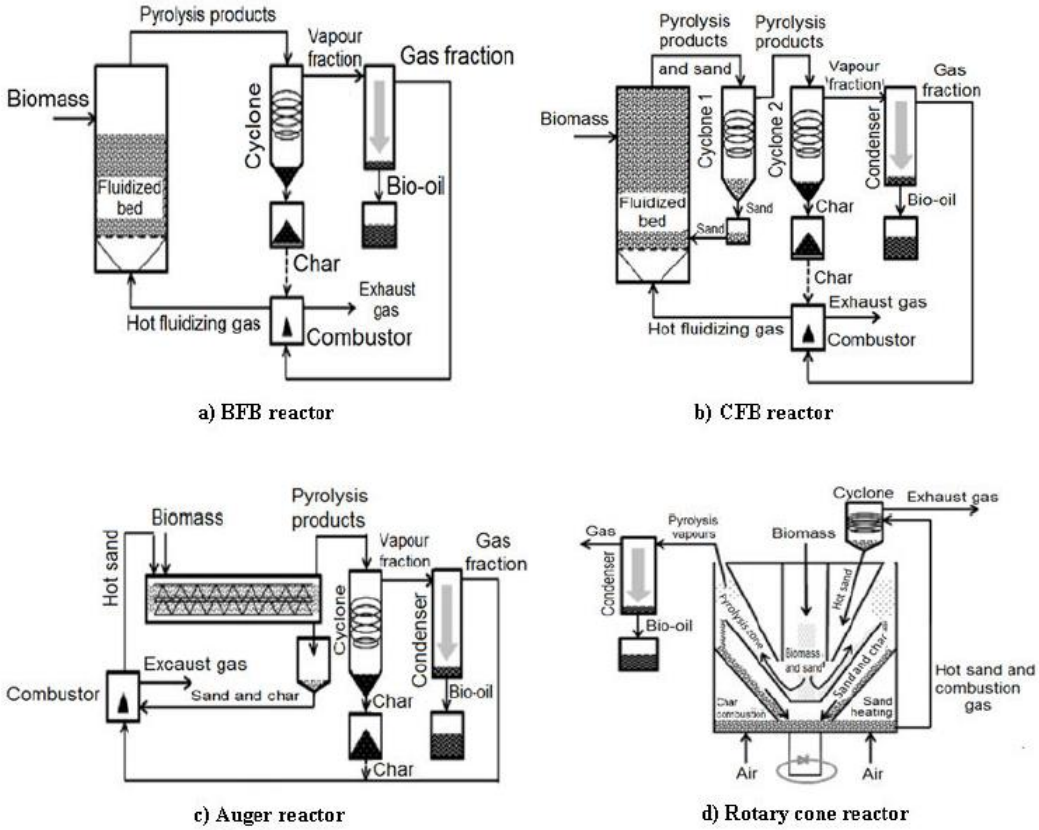

Figure 2.8: Schematic representation of different types of reactors employed for fast pyrolysis. Adopted from [50].

In auger reactors, biomass moves in a heated cylindrical tube by auger means, rather than using fluids. Vapour residence times ranging between 5-30 seconds have been reported, resulting in lower bio-oil yields compared to fluidised bed reactors. [96]. In rotary cone reactors, biomass mixed with sand are introduced in the bottom of a rotating cone (360-960 revolutions/minute). Centrifugal forces drive biomass and sand upward along the wall and due to the very effective mixing, biomass is heated rapidly. A significant advantage of the specific type of reactor, is the much less requirements for a carrier gas compared to fluidising bed technology. Moreover, high

bio-oil yields ranging between 60-70% on a dry feed have been reported [96]. However, upscaling maybe challenging due to the complex geometry [95].

2.3.3.3. Outlook of pyrolysis process

In Fig.2.9 the different applications of pyrolysis products are illustrated. Bio-oil can substitute fuel oil or diesel used for power generation purposes, or can be further upgraded to transportation fuel or chemicals. Additionally, gas output can be directly utilized for process heating, or can be combusted in order to produce part of the heat required for pyrolysis. Solid residue char is comprised mostly from carbon, along with small percentage of hydrogen and inorganic species, and can be exploited in fertiliser applications. Currently there is a limited number of pyrolysis plants installed globally. Most of the plants are pilot scale for research and demonstration purposes, while only few of them are actually located in industrial sites where energy is produced.

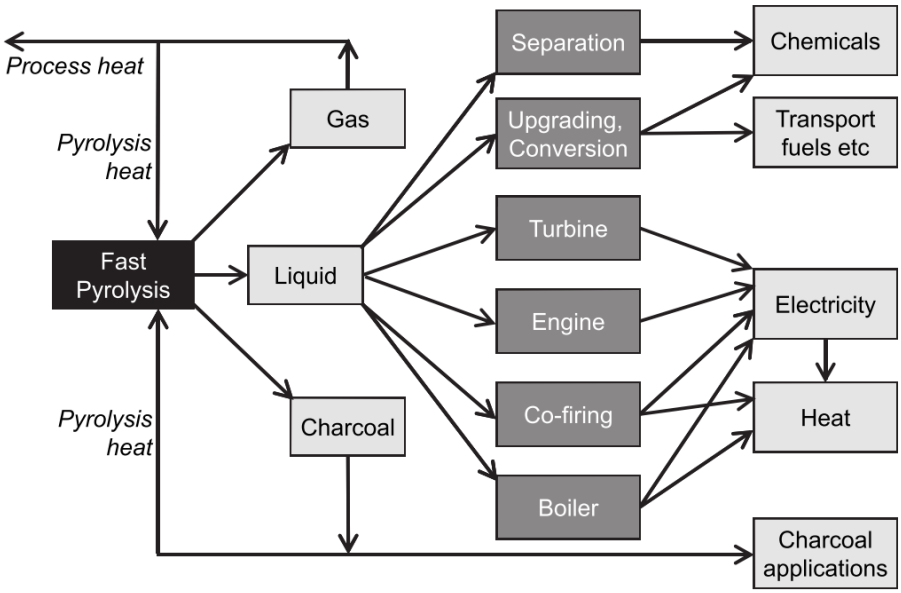

Figure 2.9: Different applications of pyrolysis products [96]

Focusing on bio-oil product, its LCV is around 17 MJ/kg, which is 60% of the LCV of diesel on a volume basis [40]. Albeit a lot of research has been conducted related to further development of bio-oil as an alternative fuel in power generation, its application is still limited. Some of the

challenges related to the utilization of bio-oil as a fuel are its moisture content, low volatility, high viscosity, and acidity. Presence of moisture in the bio-oil results both from the initial moisture present in the feedstock, along with the moisture produced during pyrolysis reactions. It ranges between 15-30% depending on feedstock and process conditions, and its presence has a deteriorating effect on LCV, while it delays also the ignition in combustion applications. As described above, water in bio-oil composition is undesirable and therefore it can be removed through vaporisation and phase separation. However, bio-oil cannot be completely vaporised and if it is heated at 100 °C or higher, it reacts immediately producing a solid residue with 50% fraction of the original liquid [96]. Viscosity of bio-oil varies between 35-1000 cp (centipoise) at 40 °C depending on the biomass feedstock and process conditions. Increased values of viscosity give rise to high pressure drops in the pipes, resulting in increased pumping costs. However, compared to oil derived from petroleum products viscosity decreases faster with temperature, and consequently if preheating is applied then the bio-oil is easily pumpable. Furthermore, bio-oil has an acidic nature, since it comprises of large amounts of organic acids, resulting in a pH between 2-3. Consequently when bio-oil comes into contact with surfaces made from carbon steel or aluminium, it becomes highly corrosive [96,98].

Currently research on fast pyrolysis focuses on the modifications needed on power conversion technologies, taking into consideration carbon deposition, surface corrosion and combustion efficiency. Furthermore, more efficient char separation techniques, which will eliminate the presence of solids in the bio-oil composition is also of particular interest. As regards bio-oil upgrading, research is directed towards physical (e.g., hot vapour filtration to reduce ash and alkali content), and catalytical pathways (e.g., hydrotreating to remove oxygen as water) in order to increase the quality of bio-oil and make it suitable for transportation fuel, or for the production of chemicals.

2.3.3.4. Pyrolysis of poultry litter

Baniasadi et al. [99] investigated the amount and composition of pyrolysis products, during slow pyrolysis of poultry litter in a fixed bed reactor at the temperature range 400-800 °C. The highest bio-oil yield was observed at 550 °C consisting of fatty acids, phenols, nitrogen-compounds, whereas water was also present. Char yield showed a high energy content, decreased with temperature, whereas it retained most of the sulphur contained initially in the feedstock. Atomic ratios H/C and O/C were measured to be four times smaller compared to the raw feedstock,

evidencing the suitability of char in soil amendment applications. On the other hand, high viscosity, acidity, and aging effects should be considered prior utilising bio-oil in downstream applications (power generation, biofuels). The energy transfer analysis showed that one-third of the heating value of the poultry litter was transferred to the organic liquid condensate and roughly the same was retained in the char.

Kim et al. [100] performed experiments on fast pyrolysis of poultry litter in a fluidised bed reactor. Silica sand was used as a bedding material and nitrogen as the fluidising medium. Two different poultry litter samples were tested at temperatures ranging between 450-550 °C with 50 °C intervals. The findings revealed low yields of bio-oil, between 20-26% due to the high ash content, with a higher heating value (HHV) between 27-30 MJ/kg at 500 °C. Additionally, char yields were found to be in the range 37-44%, while gas yields were between 33-42%. No clear conclusion could be drawn regarding the effect of temperature on the pyrolysis products of the two poultry litter samples. Inorganic constituents of ash such as potassium, calcium and phosphorus were mostly retained in char, a fact that makes char a suitable candidate in fertiliser applications.

Azargohar et al. [101] studied the characteristics of biochar derived from different biomass feedstocks including wheat straw, sawdust, and poultry litter, under fast pyrolysis conditions at a mobile pyrolysis unit. Three temperatures were tested, 400 °C, 475 °C, and 550 °C respectively. Results revealed that poultry litter displayed the highest concentration of inorganic elements (~200000 ppm) among the fuels. O/C ratio was decreased for all fuels with rising temperature. The ratio was the lowest in case of poultry litter due to the lower carbon content. According to the authors, biochar from poultry litter is suitable more for agricultural applications rather than utilising it for activated carbon, due to the high presence of inorganics in its composition.

Ro et al. [102] performed slow pyrolysis experiments in a pilot scale reactor. The authors tested chicken litter, swine solids, and mixture of swine solids at a temperature of 620 °C and heating rate of 13 °C/sec. The HHV of produced gas coming from poultry litter pyrolysis, was the lowest among the tested fuels, approximately 15 MJ/m^3 under standard conditions. Biochar poultry litter displayed HHV of 13 MJ/kg, close to the one of low rank coal (16 MJ/kg) due to the high ash content, while the carbon recovery in the biochar was estimated to be around 55%. Approximately 50% of the energy contained initially in the feedstock was retained in the biochar and 25% in the produced gases.

Simbolon et al. [103], studied the slow pyrolysis of various bedding materials (hay, straw, rice husk, wood shavings) mixed with poultry litter at 50:50 mass ratio. The fuel input to the reactor was 100 grams, and the three tested temperatures were 350 °C, 400 °C, 450 °C. The highest char yield (~67%) resulted from rice husk mixed with poultry litter at 350 °C, due to the high ash content of the specific fuel blend. Furthermore, char yield was reported to decrease with rising temperatures for all tested fuels. The highest bio-oil yield resulted from wood shavings-poultry litter blend (~44.5%), consisting of organic acids, fatty acids, and polyaromatic hydrocarbons. The same blend displayed also the highest HHV and energy content, a fact that according to the authors, was in line with the highest carbon and lowest ash contents among the tested fuels.

Simbolon et al. [104] also investigated the effect of temperature on poultry litter under fast pyrolysis conditions. The experiments were conducted in a Pyroprobe 5200 reactor in the temperature range 400-600 °C. The authors reported that biochar yield decreased with increasing temperature from 62% to 40%, while the highest bio-oil yield of 23% was found at 600 °C. Moreover, the maximum gas yield was observed in the highest temperature, consisting mainly of CO_2.

2.4. Summary of findings

Nowadays, there is a growing interest in alternative technologies suitable for treating poultry and recover energy. Converting poultry litter into biogas via anaerobic digestion is an option, although it seems less attractive for a number of reasons. Firstly, the specific technology is best suited for highly degradable biomass fuels with increased moisture content as well. However, for fuels with high solid contents such as the PL, significant amounts of water are needed in order to create slurry material suitable for digestion. This would create a wastewater stream that needs to be cleaned prior to disposal, while it would also affect the size of the plant, since the volume of the digesters will increase in order to be able to handle certain amount of fuel [44]. Furthermore, high nitrogen content found in PL composition, may increase NH_3 concentration, exceeding the levels needed for microbial growth and thus further inhibiting the digestion process. For all the above reasons, the biochemical route suggested for PL treatment, is a challenging option for implementation at farm scale level.

On the other hand, the thermochemical route seems an attractive alternative for efficient poultry litter management. Within this framework, combustion technology is by far the most commercially

available, with a number of existing large-scale plants running on PL, the oldest one being installed back in 1992, in the UK. With regard to the other two technologies within the thermochemical route, namely gasification and pyrolysis, the technologies are still in the development stage. In the following chapters, experiments performed at a lab-scale both on combustion and gasification of PL are thoroughly discussed.

3. Combustion of poultry litter in a lab-scale fixed bed reactor

Experiments have been conducted in a batch fixed bed lab-scale reactor to investigate the combustion behaviour of three different biomass fuels, poultry litter (PL), blend of PL with wood chips (PL/WC) and softwood pellets (SP). Due to the fact that Brunel University London doesn't have the necessary facilities to conduct experiments on combustion technology, the latter took place at BEST-Bioenergy and Sustainable Technologies research institute located in Graz, Austria, within the framework of BRISK2 (Biofuels Research Infrastructure). BRISK2's main activity is to provide researchers access to state-of-the-art biological and thermal biomass conversion facilities across Europe [105]. The measurements were performed by the research institute's personnel utilising the available equipment, whereas the analysis of the gathered data was performed afterwards at Brunel University London. In the following sections, a thorough description will be given with regard to the methods and equipment used, as well as the results derived from the experimental tests, providing useful insights related to the thermal decomposition behaviour of the fuels, the formation of N gaseous species, the release of ash forming elements and the estimation of aerosol emissions.

To the best of the author's knowledge, fixed bed lab-scale combustion experiments running on PL had not been investigated before submitting the thesis. The conducted experiments have given valuable insights in terms of volatile elements release rates, potential of aerosol formation, development of N-gaseous compounds during devolatilisation phase, etc. All this data can be used as input to CFD modelling tool and help in the proper design of a fixed bed combustion system running on PL. Also, it needs to be highlighted the fact that fluidised bed reactors being another common technology type used in combustion, are typically used for plants > 20 MWth. This is too large for a poultry farm. For small to medium scale plants such as poultry farms, fixed bed reactors are a more economic option for the farm owners and also easier to operate compared to fluidised bed reactors.

3.1. Materials

PL was collected from a local farm producing eggs and it was partially dried and pelletised at a particle size range of 6 mm before being fed into the reactor. Wood chips (WC) and softwood pellets (SP) were provided by the research institute where the experiments took place.

Compared to woody biomass (in this case SP), PL is characterised by lower concentrations of C and H, whereas N, Cl, and S, are present in higher fractions. It also contains significantly higher amount of ash, consisting of minerals and metals like phosphorus (P), potassium (K) and sodium (Na). Table 3.1 reports the ultimate and proximate analysis and Table 3.2 the chemical analysis of ash for the three tested fuels. Fixed carbon was calculated by subtracting the percentages of volatile matter and ash from 100%. Similarly, the oxygen content was determined by the difference from the elements presented in ultimate analysis.

Table 3.1: Ultimate and proximate analysis of feedstock.

Type of feedstock	**PL**	**PL/WC**	**SP**
Proximate analysis (% w/w)			
Moisture (a.r.)	10	9.2	7.1
Ash (d.b.)	21.98	13.01	0.33
Ultimate analysis (% w/w, d.b.)			
C	38.03	43.22	49.53
H	4.86	5.08	6.13
N	3.72	2.84	0.05
Cl	0.58	0.42	0.01
S	0.47	0.29	0.02
O	30.36	35.15	45.35
LCV (MJ/kg d.b)	17.21	19.44	17.59

a.r.: as received, d.b.: dry basis

Table 3.2: Chemical composition of ash for the three tested fuels

Ash composition (mg/kg d.b.)	PL	PL/WC	SP
Calcium (Ca)	74600	43700	950
Silicon (Si)	1860	1800	300
Magnesium (Mg)	9450	355	122
Potassium (K)	22700	14600	507
Sodium (Na)	4820	2850	15
Phosphorus (P)	16900	10400	38
Aluminium (Al)	377	358	n.d.
Zinc (Zn)	550	328	12.5
Lead (Pb)	2	3	0.1
Iron (Fe)	766	1010	n.d.
Manganese (Mn)	548	355	n.d.
Copper (Cu)	93	63	n.d.

n.d.: not detected

3.2. Experimental facility

The lab-scale reactor has been designed to represent the burning conditions of a biomass fuel layer on a grate as good as possible. This approach is valid if diffusional transport and mixing effects on the grate can be neglected in comparison to the transport of the fuel along the grate. The validation has been achieved in previous research, which has shown that the fuel transport along the grate can be fluidically characterized by a plug flow in good approximation.

The lab-scale reactor, specially designed for simulating thermal decomposition of biomass under fixed-bed conditions consists of a cylindrical retort (height 35 cm, inner diameter 12 cm). The fuel is loaded in a cylindrical sample holder (100 mm height and 95 mm inner diameter) prior being fed to the reactor. The sample holder is placed on the plate of a scale, which is used to determine the weight loss of the sample and is mechanically separated from the retort by a liquid seal (synthetic thermal oil, Therminol 66). The material used in the reactor wall and sample holder is reinforced silicon carbide, which is inert under reducing and oxidising conditions, thus avoiding any reactions between the wall and the fuel, ash or flue gases. Heated filter and controlled heater are placed in order to avoid condensation of tar in the sample line. These filters remove coarse fly ash and partly

aerosol particles and ensure that these particles do not enter in the gas analysers. The temperature of the heaters and filter is set to 180 °C.

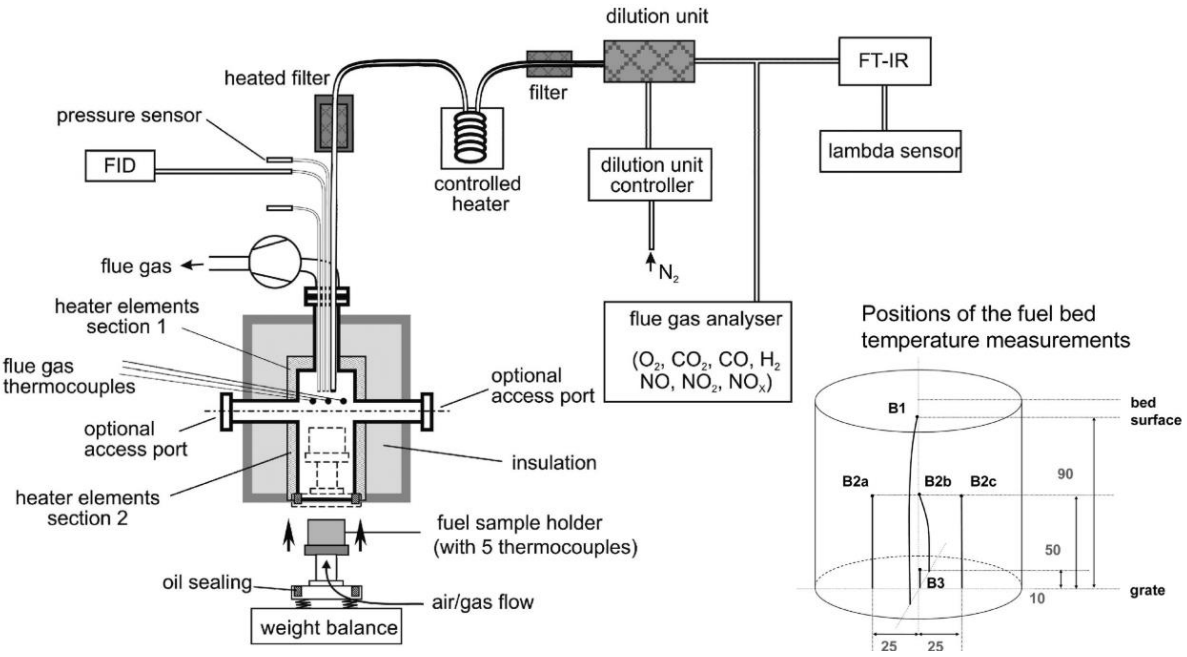

Figure 3.1: Scheme of the lab-scale reactor, including measurement setup and positions of the thermocouples.

3.3. Test procedure

Before the start of an experiment, fuel was dried to ≤10% moisture on a wet basis (a.r) and a sub-sample was sent for chemical analysis. Afterwards the fuel was inserted into the cylindrical holder, while the reactor's lower and upper parts were pre-heated by electrical means at 450 °C and 750 °C, respectively. When the preset temperatures were achieved, the fuel sample was inserted in the reactor where rapid heating occurred, similar to conditions of a real scale fixed bed combustion systems. Dry air (21% O_2 and 79% N_2 by volume basis) was supplied as an oxidising medium through the grate at a constant flow rate of 30 l/min. Three tests of identical conditions for all the tested fuels were performed to ensure repeatability. Measurements were taken at 2 second intervals and the total duration of the experiments ranged between 30-60 min depending on the fuel density and moisture content. At the end of each experiment, residual ash was removed and sent for chemical analysis.

The weight loss of the fuel sample was continuously monitored during the experimental process (drying, devolatilisation, gasification and charcoal combustion). The concentration of the produced gases and the formation of NO_x precursors were also measured. Furthermore, the data derived from the chemical analysis of fuel and residual ash, as well as the weight loss measurements of the fuel and the ash sample were used to calculate the elemental release rate into the gas phase, by calculating the mass balances of relevant elements (S, Cl, K, Na, Zn, Pb). Since the chemical analysis is robust, any observed deviation in the mass balance of the elements was considered to result from the entrainment of the ash particles with the flue. The formula used to calculate the release rate is given below.

$$Release\ rate\ (\%) = \left(1 - \frac{mass\ of\ element\ in\ the\ residual\ ash}{mass\ of\ element\ in\ the\ fuel}\right) * 100 \qquad (3.1)$$

Once the release rate of aerosol-forming elements has been determined, it is possible to estimate the aerosol formation potential. In particular it is considered that elements K, Na, P and Zn form K_2SO_4, KCl, Na_2SO_4, NaCl, P_2O_5, and ZnO. Moreover, if there is not enough S and Cl to bind K and Na, the formation of carbonates K_2CO_3 and Na_2CO_3 is also possible [106,107]. If it is assumed that the whole S reacts with K and Na to form sulfates, the maximum aerosol formation potential can be estimated, whereas if all the Cl is assumed to be bound with K and Na, the minimum aerosol emission can be determined. The difference is attributed to the fact that sulfates have higher molecular weight than chlorides. However, it is important to state that the particle losses due to condensation and subsequent deposit in reactor walls as well as gaseous emissions of S (SO_x) and Cl (HCl) were not considered in the analysis. Therefore, the results might be overestimated, but can provide a proximate evaluation of aerosol emissions potential.

3.4. Measurement methods

The following measurements and analyses were performed during each of the combustion test runs: a) Weight loss of the fuel sample over time, b) Concentrations of flue gas species over time (CO_2, H_2O, CO, CH_4, NH_3, HCN, N_2O and basic hydrocarbons), c) O_2 detection, d) total amount of hydrocarbons (C_xH_y), e) temperature measurements over time, f) fuel and ash analysis. Gas analysis was performed by FTIR method and by using a multicomponent gas analyser. Similarly, oxygen concentration was measured with the multicomponent gas analyser and a lambda sensor.

The goal of applying different methods was to check the consistency of the resulted data. Since data was very comparable among the different methods, the results from multicomponent gas analyser were considered. Moisture content has been determined by measurement of weight loss during drying at 105 °C until a constant weight has been reached, according to standard BS EN 14774-1. The determination of C, H, N contents has been performed according to standard BS EN 15104 by fuel combustion, followed by gas phase separation in a gas chromatograph and measurement in an elemental analyser. Content of Cl has been determined according to BS EN 15289 by introducing a digestion step based on bomb combustion in oxygen and absorption in NaOH followed by ion chromatography (Shimadzu LC 20). The content of S in the fuel has been determined by multi-step pressurized digestion of the samples, and consequent detection applying either inductively coupled plasma-optical emission spectroscopy (ICP-OES) (Arcos, Spectro), or ICP-MS (Agilent 7700x), depending on the element's content and detection limits.

3.5. Definition of fuel indexes

Fuel indexes were applied as a pre-evaluation step regarding typical combustion related problems when new fuels are introduced. Their determination is based on fuel chemical analysis, chemical reactions between ash forming elements and interactions between different group of elements. Moreover, their validation was performed via dedicated combustion tests on lab, pilot and real scale facilities [107,108]. The indexes being considered in this work are as follows: a) N content in the fuel as indicator for NO_x emissions potential b) K+Na+Zn+Pb to estimate the potential of aerosol emissions, c) molar ratio (Si+P+K)/(Ca+Mg) for determining the ash melting behaviour and d) molar ratio 2S/Cl for the prediction of corrosion on boiler surfaces.

3.6. Results and discussion

3.6.1. Fuel combustion behaviour during lab-scale experiments

This section describes the test runs conducted on the SP in order to have a complete overview of the experimental procedure, before summarising the relevant results of the combustion of PL and blend of PL/WC. Figures 3.2 and 3.3 show the mass decrease of SP, and the temperatures at different positions in the reactor over the complete duration of the test run. A fuel mass of 410 grams was inserted in the preheated reactor and the total duration of the experiment lasted approximately forty minutes. Initially the drying process occurred which can be identified by

moderate mass decrease, low temperatures in the fuel bed and the release of H_2O. After approximately 11 minutes (652 sec) the devolatilisation phase started taking place. During this phase, the reaction front propagates from the top of the bed to the bottom. This causes an intensive mass loss and a sharp increase in the temperature, especially when the main devolatilisation phase starts at ~1000 sec, as observed from the thermocouple's values.

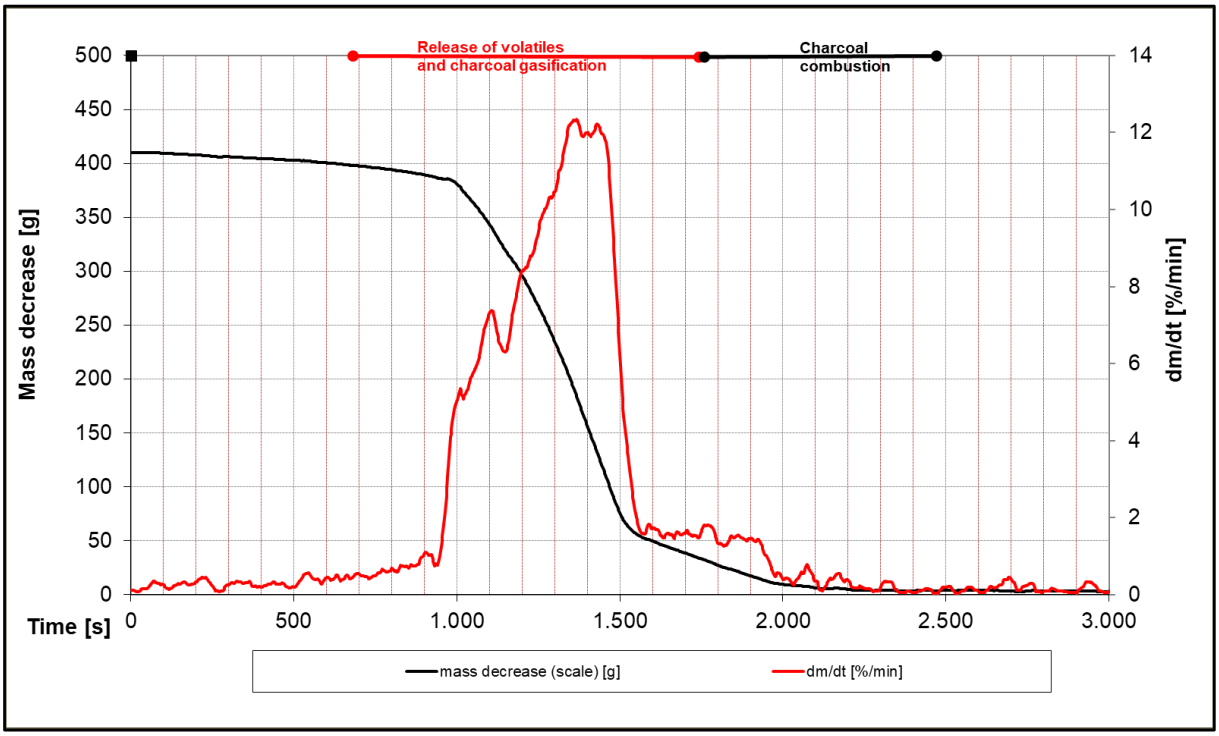

Figure 3.2: Mass loss over time during SP combustion

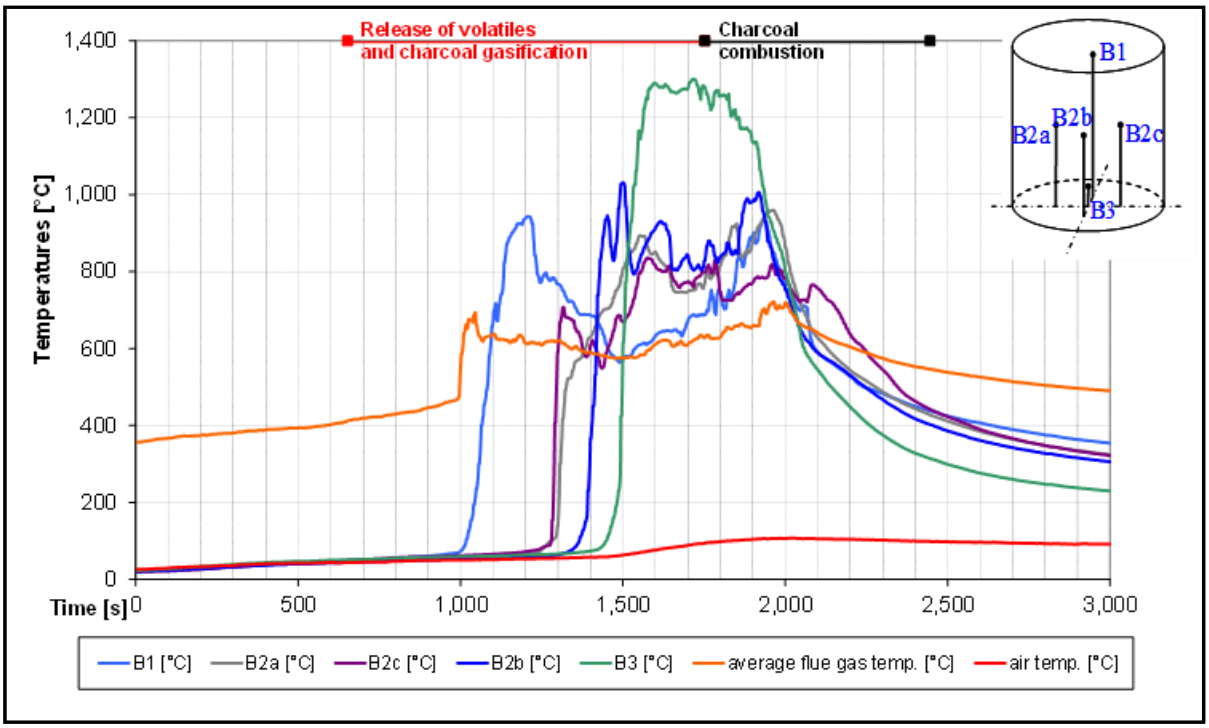

Figure 3.3: Fuel bed temperatures over time during SP combustion.

Figure 3.4 depicts the main gaseous compounds produced, namely CO, CO_2, H_2O, CH_4 and smaller amounts of other hydrocarbons. After approximately 20 minutes (1752 sec) the devolatilisation front reaches the grate and the concentration of CH_4 drops to zero, indicating the end of this phase and the initialisation of charcoal combustion. The latter phase occurs at the bottom of the bed close to the grate and the main product during this phase is CO_2, produced either directly from carbon oxidation or from partial oxidation of CO. It should be noted that the highest temperature is observed in this stage, and in the case of SP test run the maximum temperature reached 1301 °C. The evolution of N gaseous species over time in given at Figure 3.5. As observed, the N gaseous species are mostly released during the devolatilisation phase with the dominant compounds being HCN, NH_3 and NO. Moreover, a second peak in volatiles release is observed during charcoal combustion, with an increase in NO concentration, implying the partial oxidation of N bounded in charcoal.

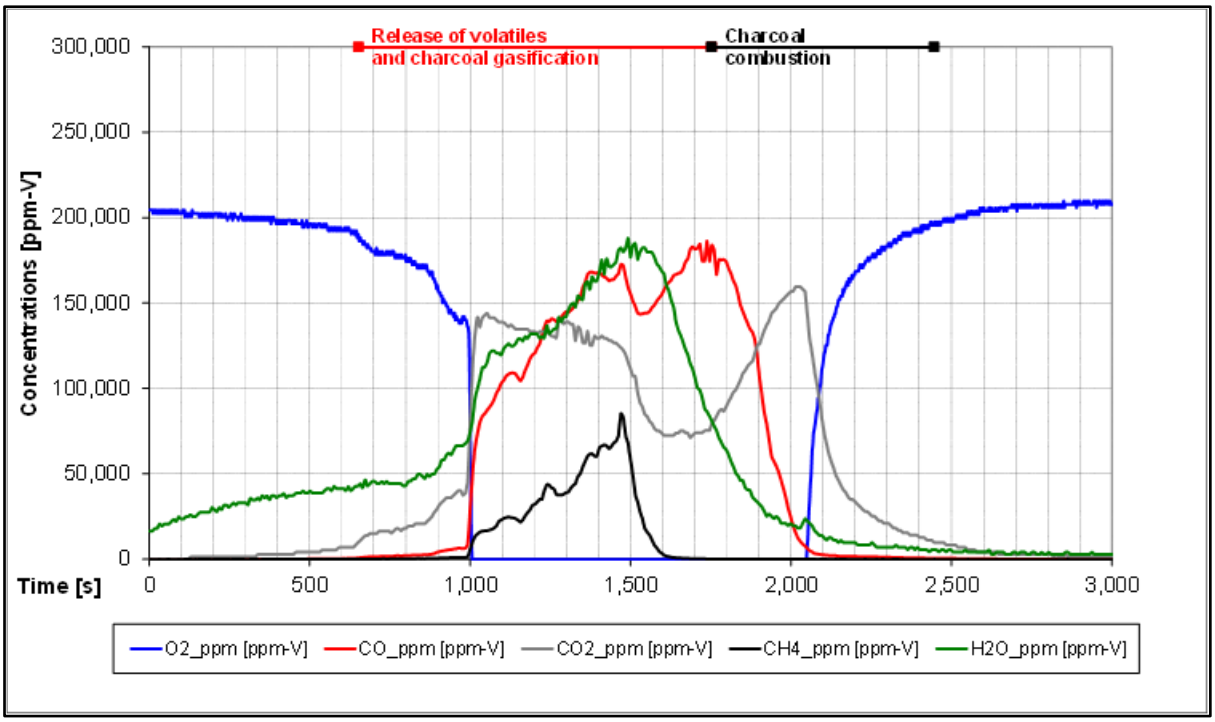

Figure 3.4: Release of main gases over time during SP combustion.

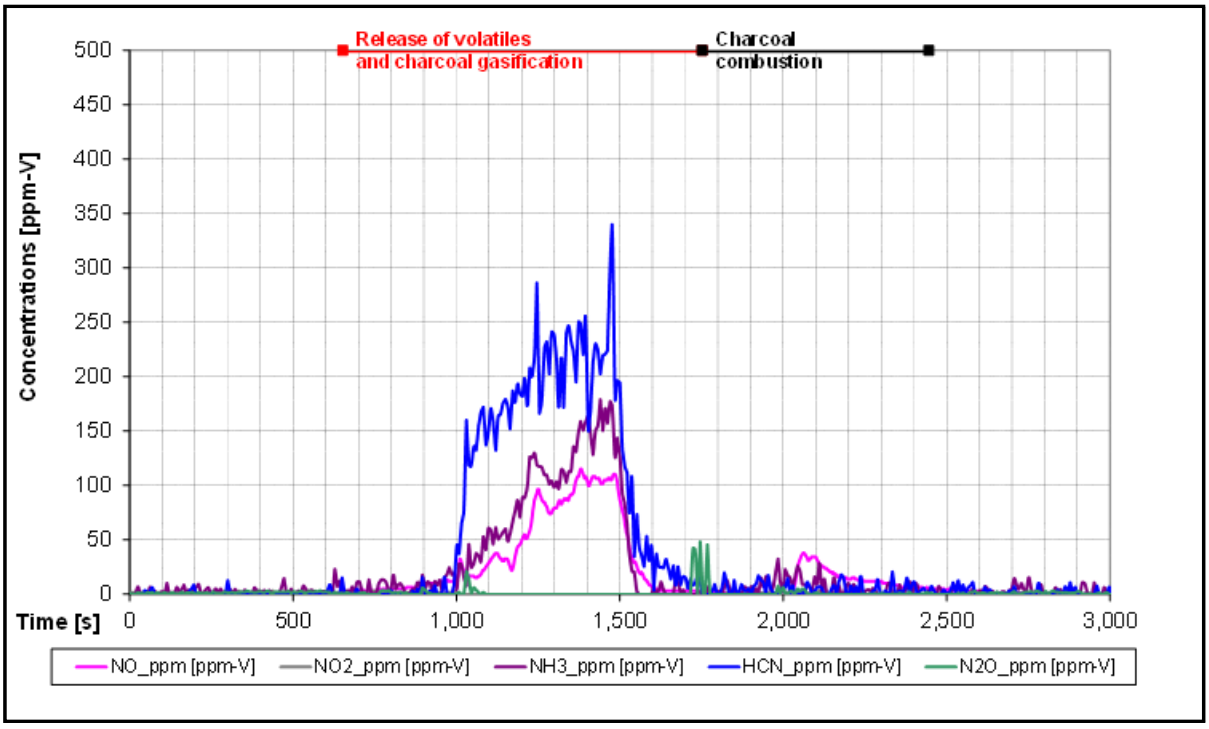

Figure 3.5: Evolution of N gaseous species over time during SP combustion.

In Fig. 3.6 the profile of air equivalence ratio and flue gas flow rate over time is illustrated. Air equivalence ratio (ER) is defined as the ratio between the actual amount of air supplied to the

reactor and the amount of air needed for stoichiometric combustion. The air flow was kept constant at a rate of 30 Nl/min. As observed, at the start of the devolatilisation phase, the oxygen concentration decreases; however, high values of ER ratio are still present. When the main devolatilisation phase starts at (~1000 sec), a sharp reduction in the ER is observed, implying the rapid consumption of oxygen in the oxidation of the devolatilisation products (refer to Fig.3.4). On the contrary, during charcoal combustion phase, ER rises again acquiring values higher than one and keeping the same trend until the end of the experiment. Similarly, the amount of flue gas increases during the release of the devolatilisation products, following a downward trend afterwards.

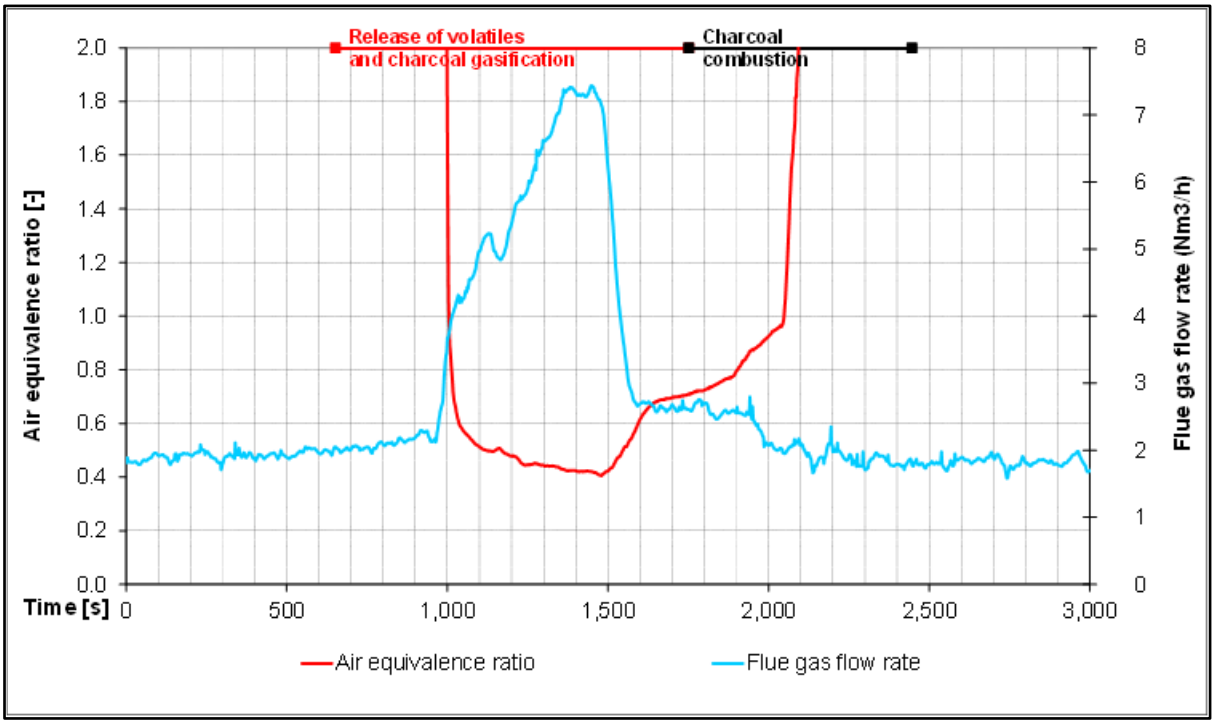

Figure 3.6: Air ratio and flue gas flow rate during SP combustion vs time

Figures 3.7-3.10 show the combustion behaviour of PL. The initial mass of PL inserted in the reactor was 400.5 grams. Compared to SP test run, the drying phase of PL combustion lasted longer (1698 sec) due to comparatively higher moisture content in the PL. The maximum temperature was observed during the beginning of charcoal combustion phase, reaching 1228 °C, while the total duration of PL combustion was 65 minutes. Similar to SP combustion, oxygen is consumed rapidly during the devolatilisation phase. Among the N gaseous species, NH_3 is the compound with the highest concentration followed by NO, both released mainly during the

devolatilisation phase, with a small peak in NO concentration observed also during charcoal combustion.

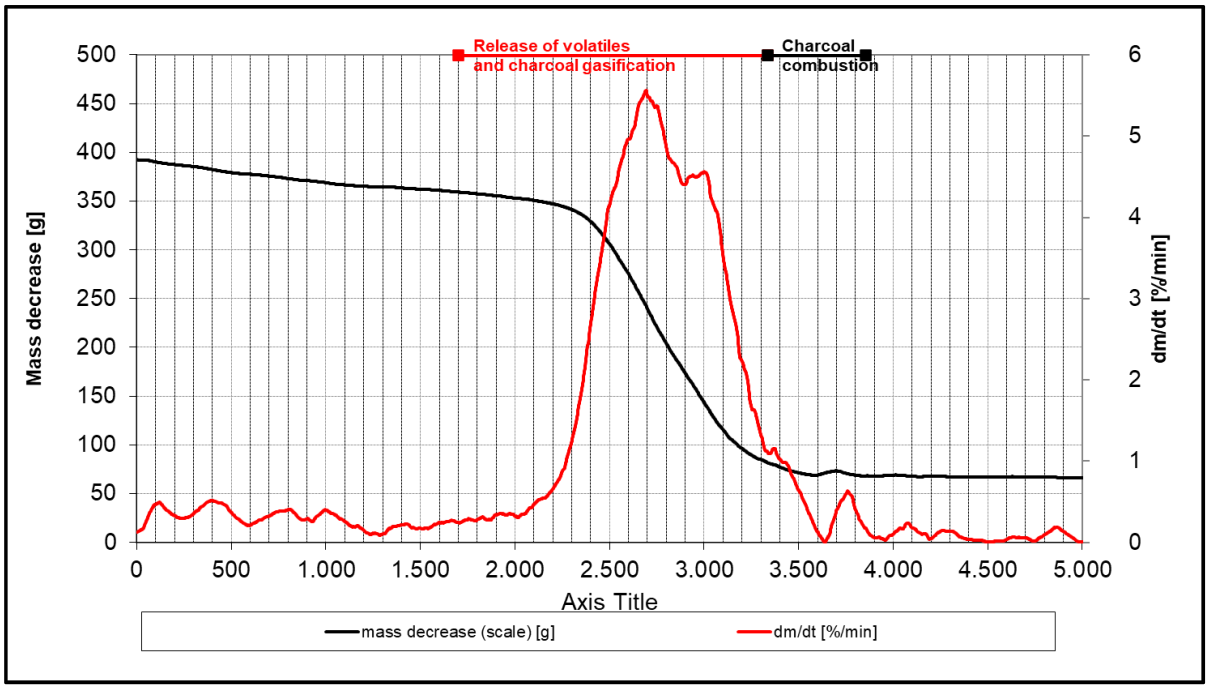

Figure 3.7: Mass loss over time during PL combustion.

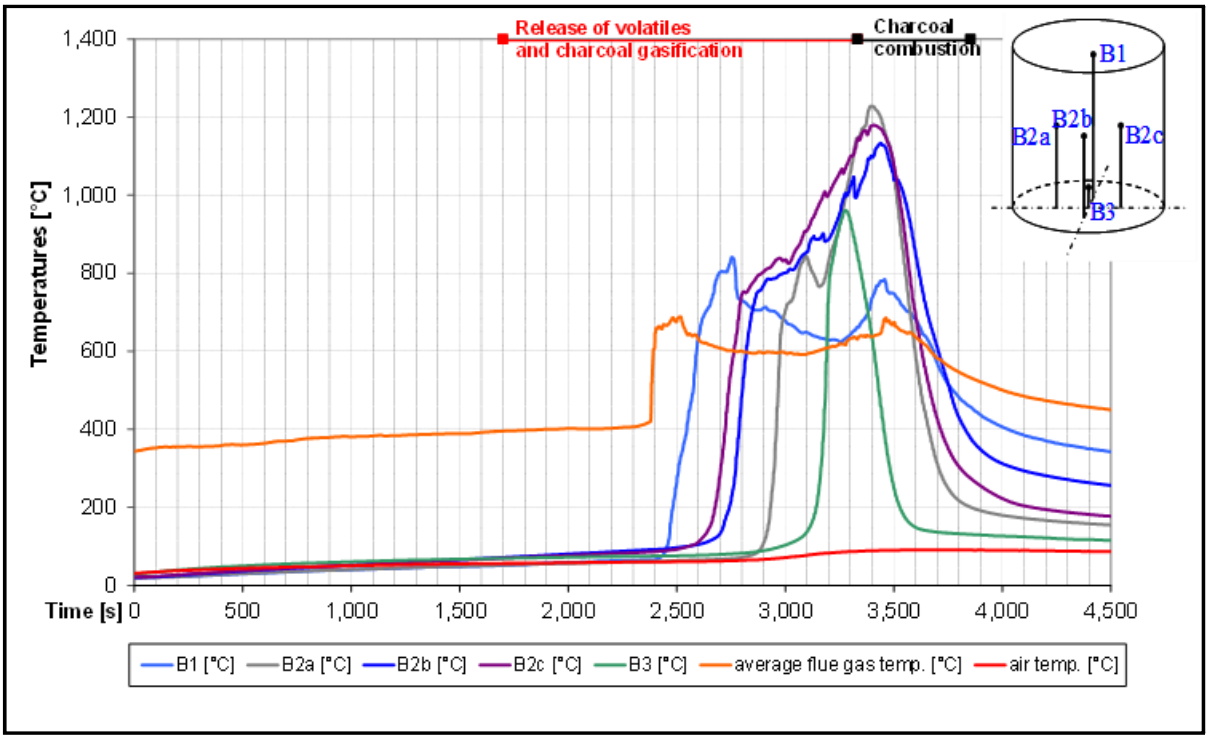

Figure 3.8: Fuel bed temperatures over time during PL combustion.

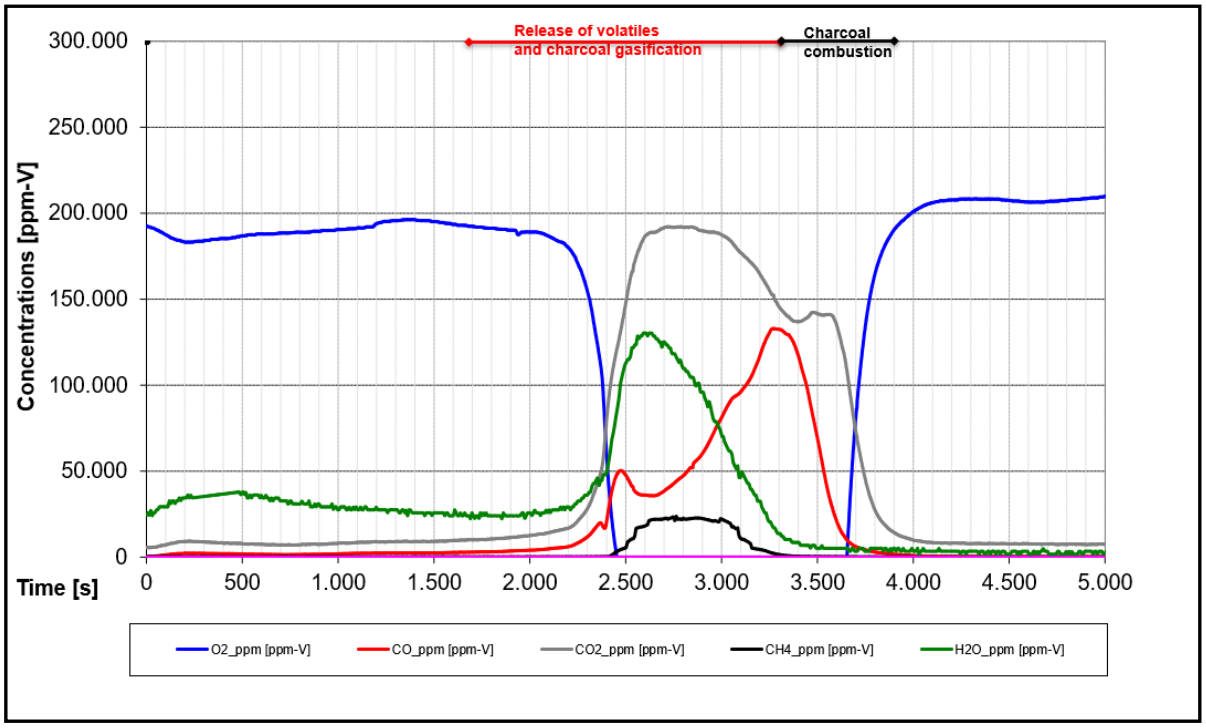

Figure 3.9: Release of main gases over time during PL combustion.

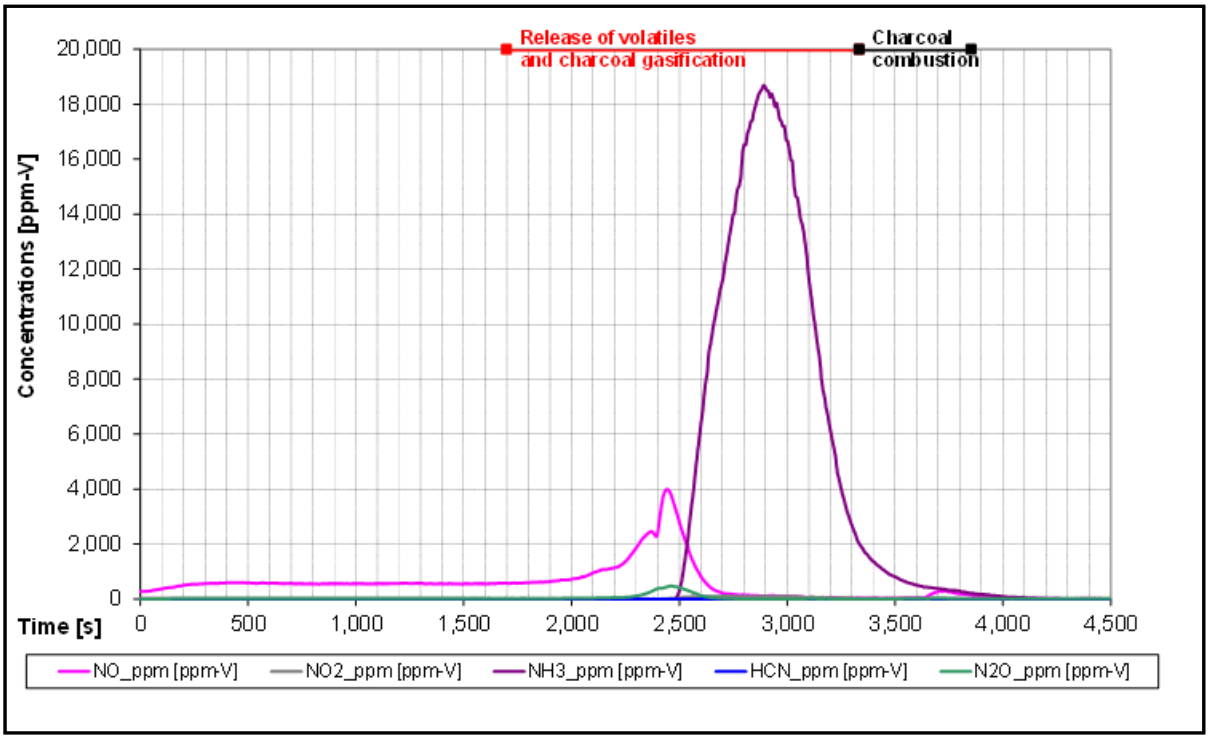

Figure 3.10: Evolution of N gaseous species over time during PL combustion.

Combustion behaviour of PL/WC blend is presented between the Figures 3.11-3.14. Drying lasted approximately 60 seconds since the initial mass was smaller (240.6 grams), due to density differences between the tested fuels. The maximum bed temperature during charcoal combustion was 1041 °C and the total duration of the PL/WC experiment lasted 1560 seconds. NH_3 appeared to be the dominant compound released during devolatilisation phase, in line with the combustion of PL. In contrast to PL and SP, the PL/WC charcoal combustion didn't show a peak of NO concentration.

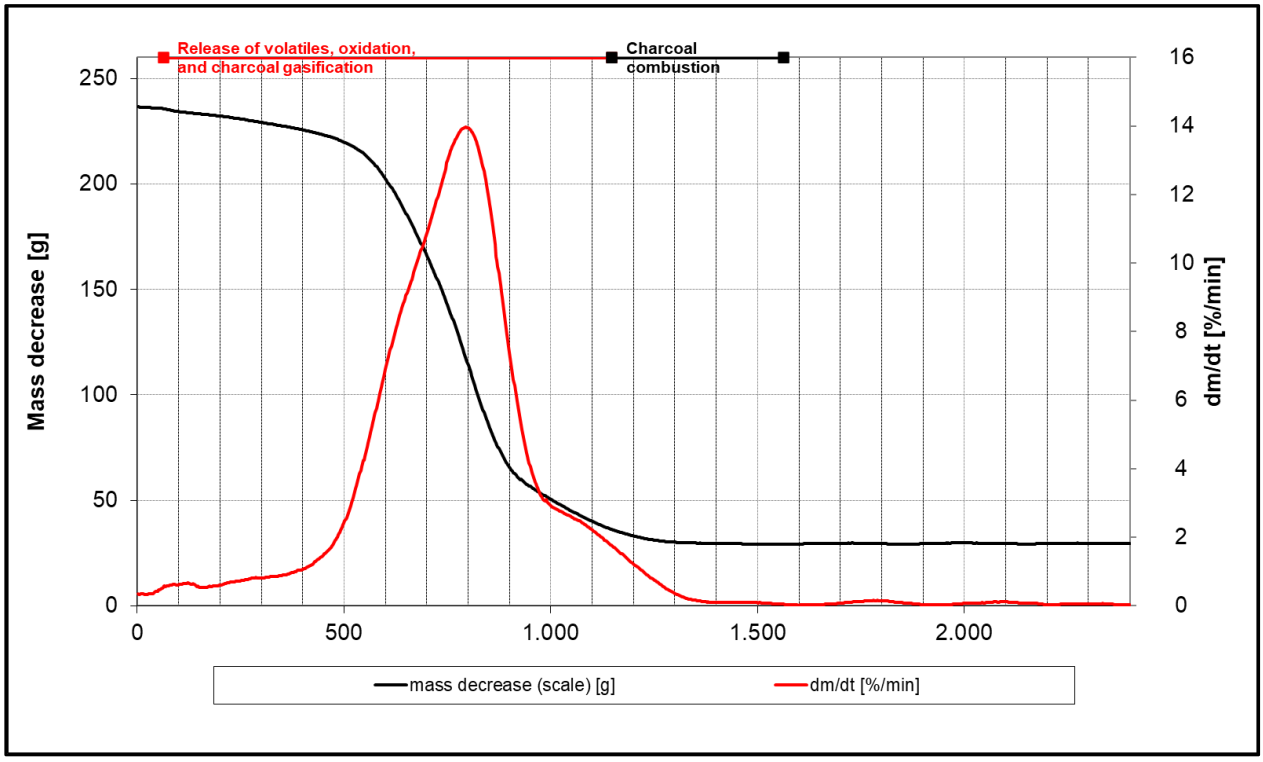

Figure 3.11: Mass loss over time during PL/WC combustion

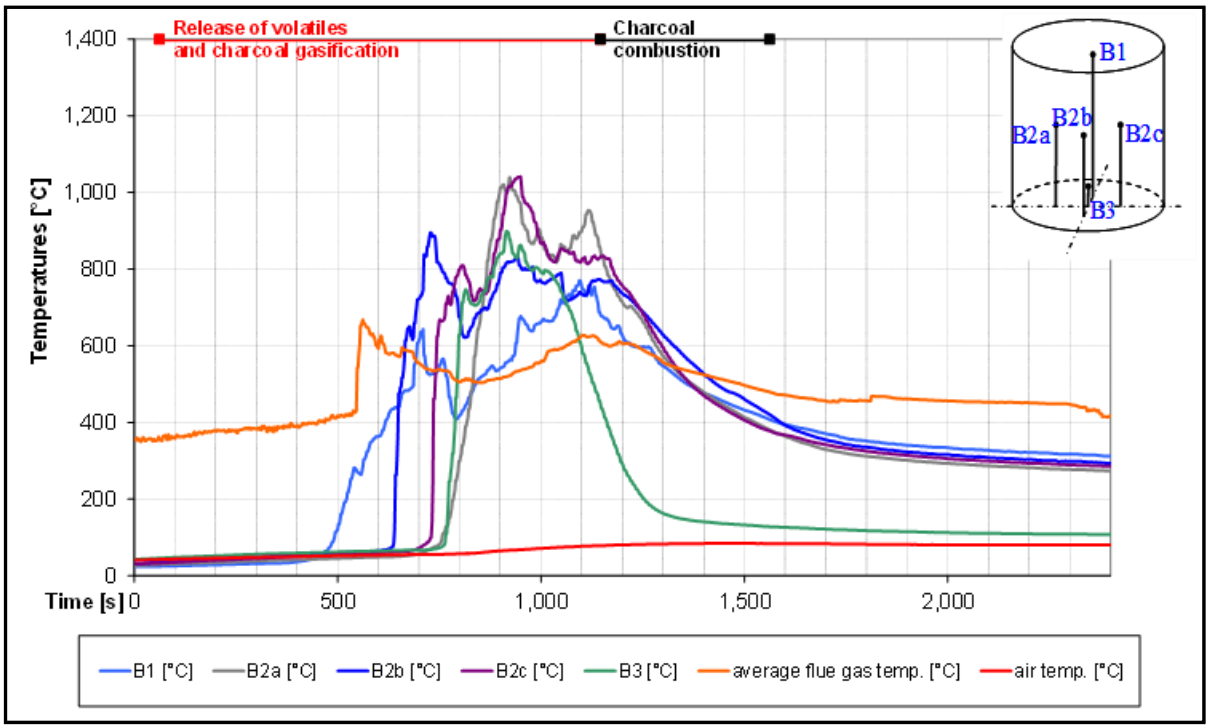

Figure 3.12: Fuel bed temperatures over time during PL/WC combustion.

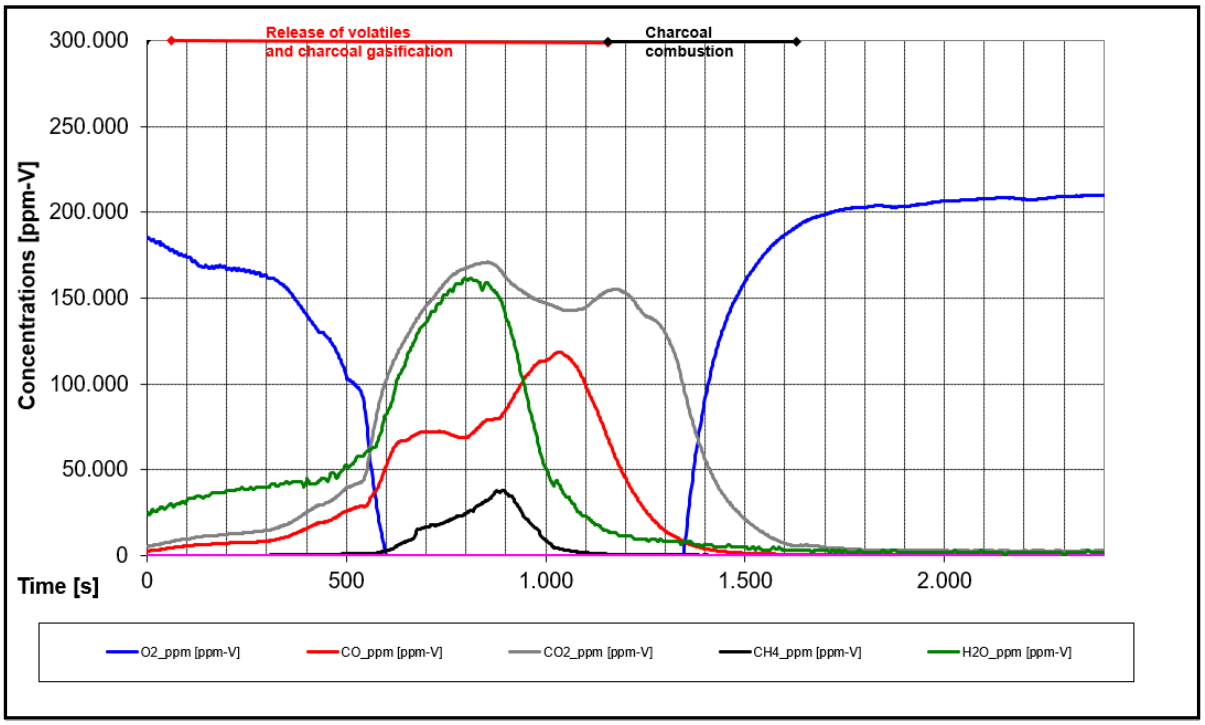

Figure 3.13: Release of main gases over time during PL/WC combustion.

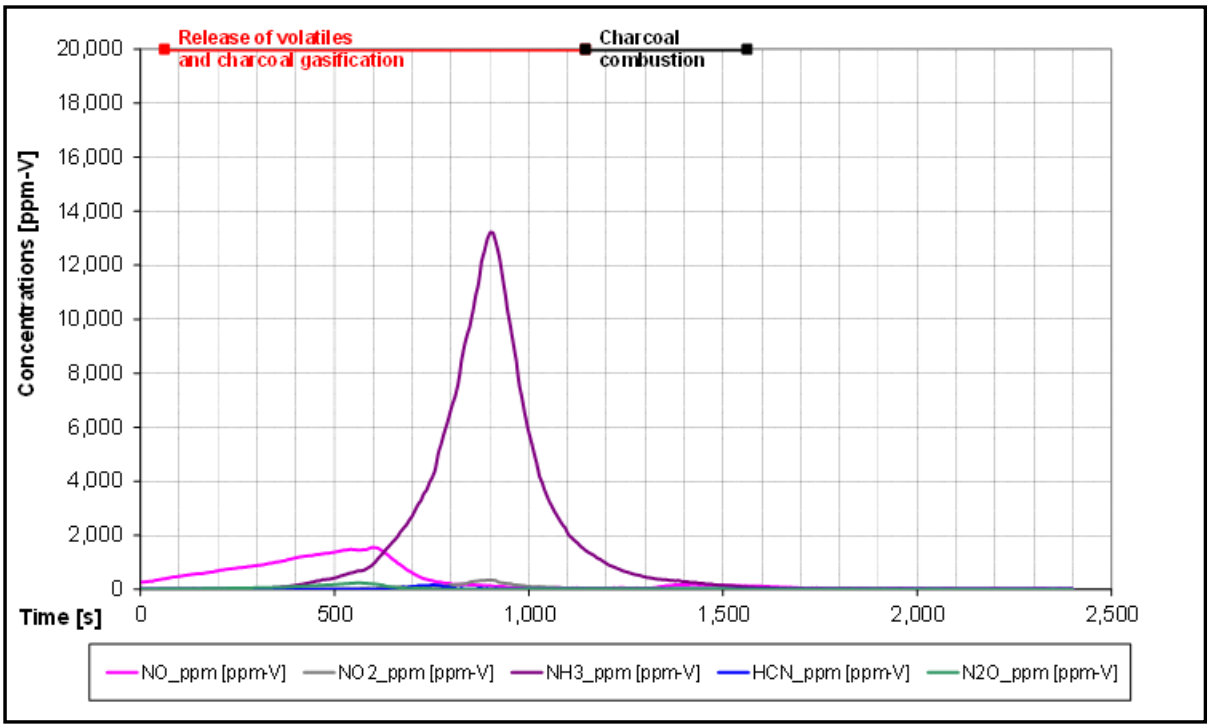

Figure 3.14: Evolution of N gaseous species over time during PL/WC combustion.

Element balances performed based on the fuel analysis data and the process data recorded showed good closures ranging between 80-120%, thus revealing the representativeness of the test runs. Indicatively for fuel PL, the mass balance of elements reads 118% for C, 104% for O and 99.5% for ash.

It should be highlighted that the residual ash after combustion of SP was 1.43 grams (0.35% of the initial fuel mass), whereas in the case of PL and the PL/WC were 69.7 grams (17.4% of the initial fuel mass) and 27.7 grams (11.5% of the initial fuel mass) respectively. The latter fact clearly implies the associated challenges due to high ash content when combusting PL compared to traditional biomass. Representation of ash residues after the combustion of PL and PL/WC is given at Fig.3.15. From the residual ashes of tests with PL no sintered ash particles have been obtained, while the pellet structure was still intact, whereas for PL/WC a similar result has been observed.

Figure 3.15: Ash residues after combustion. PL (left) and PL/WC (right)

3.6.2. N gaseous species and aerosols formation

Initially the conversion rate of fuel bound N into gaseous species is depicted in Fig. 3.16. Total fixed nitrogen (TFN) stands for the sum of fuel bound N in NH_3, NO, HCN, NO_2 and N_2O. N contained in PL is converted by ~40% into NH_3, less than 10% into NO, while the rest (50%) remains in the charcoal. In the case of PL/WC, NH_3 amounts slightly more than 30%, followed by NO (~6%). On the other hand, TFN for the SP reads almost 100%, since N is converted into HCN by 50%, ~30% into NH_3, and ~20% into NO. As observed, NH_3 and HCN are the main nitrogen products released during the devolatilisation phase. Their ratio varies depending on the fuel characteristics, reactor set-up and operating conditions. The conversion of fuel nitrogen from biomass residues and biowastes was investigated and the authors have concluded that N in heterocyclic compounds mostly decompose into HCN, while N found in amino acids and proteins decompose into NH_3 [109]. Indeed, most of the N in the PL derives from the animal feed, excreta, and feathers rather than from the bedding material and this N is chemically incorporated into protein molecules and urea. Therefore, it could be a possible explanation for NH_3 being the dominant compound during PL combustion. However, due to the complex structure of nitrogen, it's not yet possible to draw definite conclusions regarding the ratio NH_3/HCN. In the study of Anca-Couce et al. [49], the authors tested 32 different biomass fuels (woody biomass, agricultural, etc.) in the same reactor of the present study. The authors reported similar amounts of HCN and

NH_3 for woody biomass characterised by low N content, while in some cases (hardwood and stem softwood) HCN showed the highest concentration. Furthermore, in the study of Brunner et al. [106], the authors tested beech woodchips also in the same reactor utilised in the present study and the findings revealed HCN as the compound with the highest concentration (44.5%) during devolatilisation, followed by NH_3 (~20%). Beechwood pellets in the study of Brunner et al. [29] had similar composition with the softwood pellets (SP) tested during the present study, and the findings from both studies are in qualitative agreement regarding the concentration of the N gaseous species during devolatilisation. In both studies the authors reported two different peaks for NO concentration, one at the beginning of the devolatilisation phase and the second one during char oxidation, similarly to the present study.

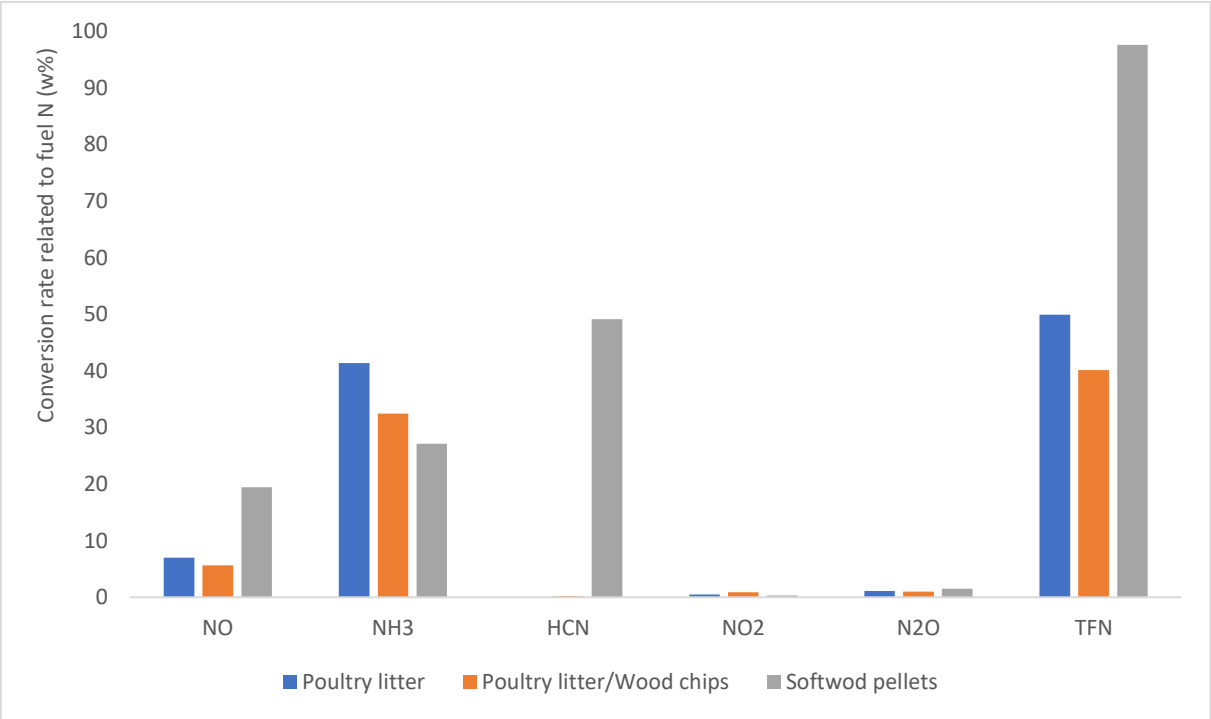

Figure 3.16: Release of N gaseous species related to nitrogen content of the fuel

Fig. 3.17 shows the release rates of the aerosol forming elements in the gas phase, based on their concentrations in the fuel (see Table 3.2) and residual ashes (see Table 3.3). The blend of PL/WC shows the highest release rate of alkali metals K and Na, reaching 50% and 37% respectively. Furthermore, Zn was almost completely released in the case of SP, whereas in the case of the other two tested fuels (PL and PL/WC), Zn release rate was ~60%. Pb was present in minor concentrations, reaching an almost 100% release rate into the gas phase for SP. Cl displayed high

release rates (>80%) for all tested fuels. S illustrated the lowest release rate in the case of PL combustion (~55%) whilst the highest release rate was reported during SP combustion (~93%).

Table 3.3: Chemical composition of residual ashes after the test runs

Ash composition (mg/kg d.b.)	PL	PL/WC	SP
Calcium	328000	305000	277000
Silicon	12700	28400	81600
Magnesium	45300	42200	36400
Potassium	66300	70800	114000
Sodium	18600	17600	3170
Phosphorus	78700	73500	11600
Aluminium	2540	4360	n.d.
Zinc	1250	1320	22.8
Lead	10	10	0.5
Iron	3980	4720	n.d.
Manganese	2240	2180	n.d.
Copper	404	381	n.d.

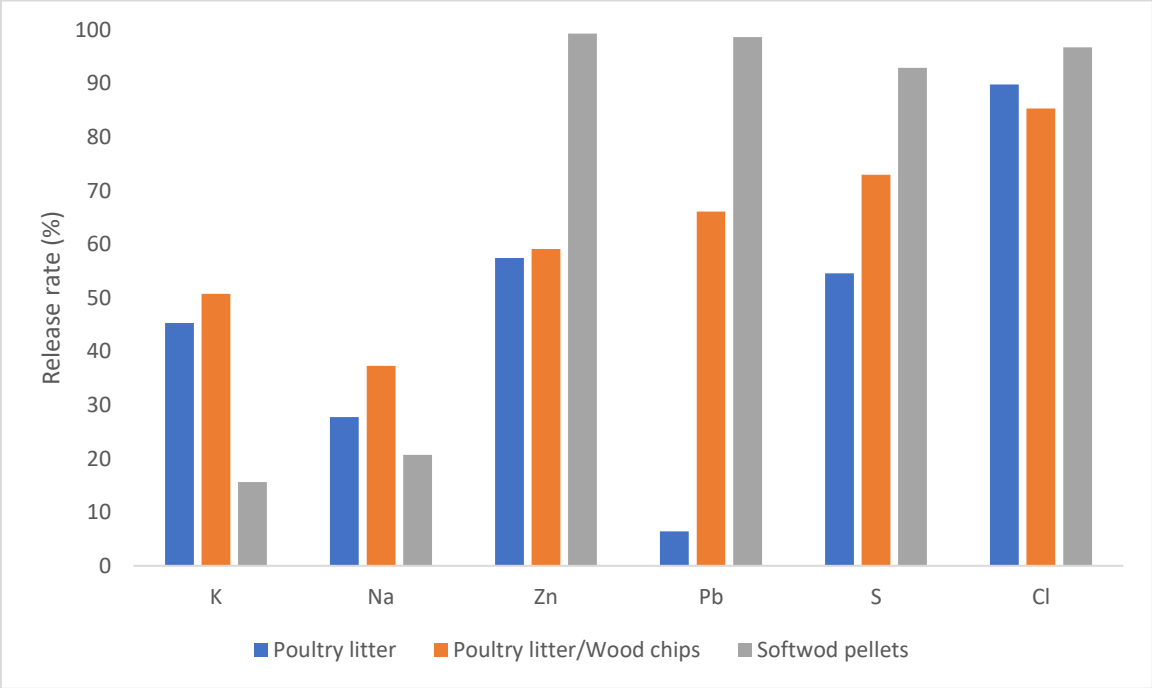

Figure 3.17: Release rate of volatile and semi-volatile elements in the gas phase.

Fig.3.18 illustrates the maximum potential of aerosol emissions from all tested fuels. The maximum estimated aerosol emissions result from the combustion of PL, reaching the value of 2806 mg/Nm^3 (dry flue gas, 13 vol% O_2), whereas for PL/WC a value of 2584 mg/Nm^3 (dry flue gas, 13 vol% O_2) was determined. As expected, the estimated aerosol emissions from SP combustion are negligible with 16.5 mg/Nm^3 (dry flue gas, 13 vol% O_2), due to the low presence of aerosol forming elements initially contained in the fuel. Moreover, it should be highlighted that the aerosol emissions are mainly influenced by the release of potassium in the gas phase. The findings are in line with the work of Sommersacher et al. [107].

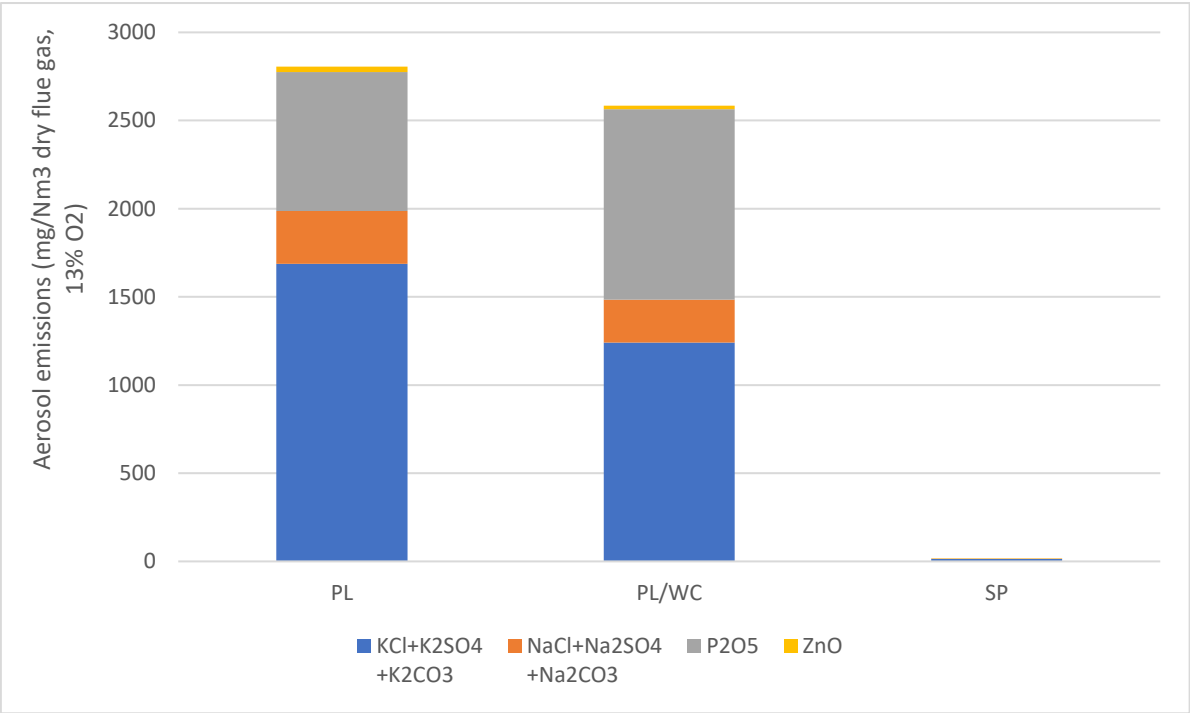

Figure 3.18: Amount and concentration of estimated aerosol emissions.

3.6.3. Selected fuel indexes

NO_x emissions

Generated NO_x emissions are an important factor to be addressed during the operation of biomass combustion plants. Pre-evaluation of a particular fuel can be proven a very effective measure, since it can provide a good estimation if its utilisation in a combustion plant will exceed the emission limits imposed from European regulations, and the consequent mitigation measures that need to be

considered. In the study of Sommersacher et al. [108], data has been derived from test runs of different biomass fuels in grate combustion plants equipped with air staging technology. According to their observations, NO_x emissions are increasing with the N content in the fuel and that fuels with N content >1 wt% (d.b.) tend to produce NO_x emissions >200 mg/Nm^3 (dry gas, 13% O_2). Therefore, based on the fuel index, combustion of PL is expected to generate ~ 400 mg/Nm^3 (dry gas, 13% O_2) at 3.7 wt% (d.b.) N content. The index is considered valid only for the specific type of plant, and furthermore, there is a possibility that the expected NO_x emissions can be lower due to the fact that the main N gaseous compound released during devolatilisation phase is NH_3. It is very likely that the NH_3 will reduce the NO_x emissions and therefore this index cannot be directly applied. However, the index delivers a maximum range of expected NO_x emissions. It should be highlighted that under Commission Regulation (EU, 142/2014), NO_x emissions derived from on-farm PL combustion must not exceed 200 mg/Nm^3 (dry gas, 11% O_2) [56].

Aerosol emissions

A correlation between the production of aerosol emissions and the concentration of aerosol forming elements (K, Na, Zn, Pb) in the dry fuel is depicted in Fig.3.19. Sommersacher et al. tested the fuel indexes of different types of biomass fuels [108] and classified the level of aerosol emission as follows: a) Low PM1 emissions range for an index with value <1000 mg/kg d.b., b) medium PM_1 emissions range for index with value ranging between 1000-10000 mg/kg d.b. and c) high PM_1 emissions range if the index exceeds 10000 mg/kg d.b.

In the current study, index acquires values >10000 mg/kg d.b. in the cases of PL and PL/WC combustion, therefore aerosol emissions above 500 mg/Nm^3 (dry gas, 13 vol% O_2) should be expected. This estimation has been confirmed by the test runs with the lab-scale reactor, where maximum estimated aerosol emissions of 2806 mg/Nm^3 (dry gas, 13 vol% O_2) for PL and 2584 mg/Nm^3 (dry gas, 13 vol% O_2) for PL/WC were determined, as shown in Fig.3.10. The index related to SP combustion is low (535 mg/kg d.b.) and consequently the aerosol emissions are estimated to be in negligible quantities 16.5 mg/Nm^3 (dry gas, 13 vol% O_2). High aerosol emissions can cause high deposition rates on cooled surfaces in a plant (e.g., the boiler) and show the need to consider this aspect when designing a plant. An effective measure to tackle this issue is the installation of an automatic boiler cleaning system. Additionally, the limit of particulate matter emissions stemming from on-farm PL combustion shouldn't exceed 10 mg/Nm^3 (dry gas, 11% O_2) according to European regulations [56]. Therefore, high aerosol emissions determined from PL combustion show the need to equip a plant with flue gas cleaning devices such as electrostatic

precipitators (ESPs) or bag filters, that remove the aerosols from the flue gas with high efficiency before it is emitted into the atmosphere.

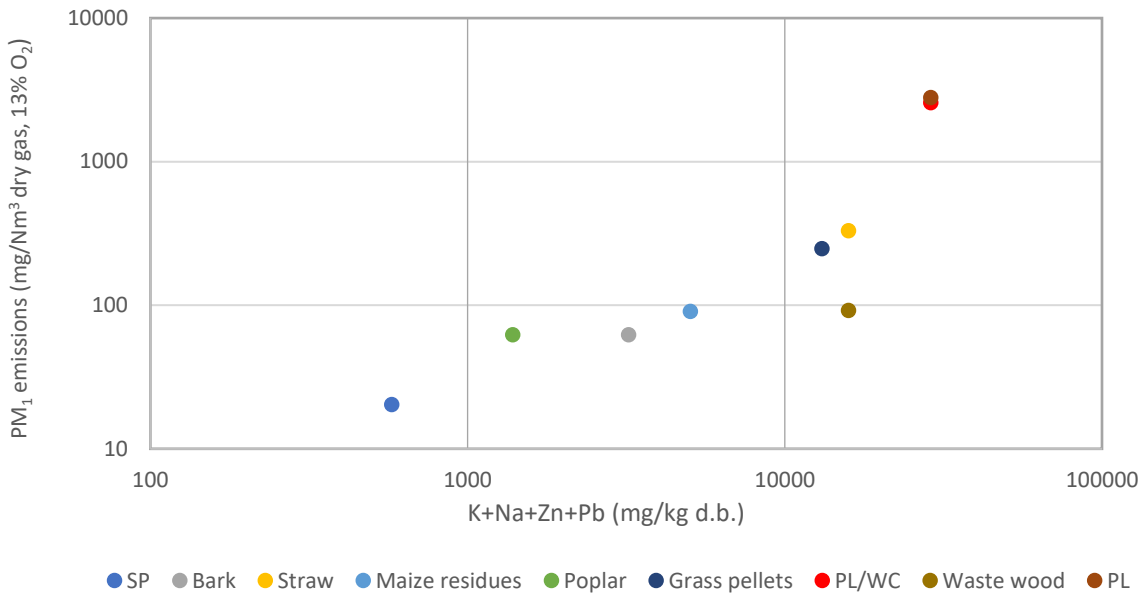

Figure 3.19: Particulate emissions (PM1) vs concentration of aerosol forming elements present in the fuel. PM1 emissions for Bark, Straw, Maize residues, Poplar, Grass pellets, Waste wood result from tests in real scale plants and have been taken from Sommersacher [108]; PM_1 emissions of PL, PL/WC, and SP, tested in this work are estimated values.

Ash melting behaviour

Ash melting behaviour is determined by the molar ratio of Si/(Ca+Mg). It is generally accepted that the presence of Si in combination with K decreases the ash melting temperature, while the opposite is observed when there is an increased concentration in Ca and Mg [29,51,110,111]. However, for fuels with high concentration in P and K, the index is not valid. Therefore, another index is used, Si+P+K/(Ca+Mg), considering also the presence of P and K. In the work of Sommersacher et al, [112], a correlation was developed according to which ash melting temperatures decrease with rising values of the index. The indexes for PL and PL/WC have low values, 0.53 and 0.57 (mol/mol) respectively, and thus high ash melting temperatures should be expected. Indeed, the estimated melting temperatures based on the correlation were found to be ~1335 °C for both fuels, a fact that comes into agreement with the lab-scale experimental observations. Similarly, the estimated melting temperature of the SP was 1315 °C.

Corrosion issues

Regarding the fuel index 2S/Cl (mol/mol), it is known that the presence of Cl is very crucial with reference to corrosion of boiler surfaces. Chlorine induced corrosion is usually realised by the direct attack of gaseous Cl in the form of Cl_2 and HCl, or the deposition of alkali chlorides on the boiler surfaces. The former corrosion mechanism is favoured mainly in high temperature combustion environment, whereas the latter causes the reduction of melting temperature range. Presence of sulphur in the fuel composition, along with adequate residence time and high enough combustion temperature is reported to limit the corrosion effect since alkali chlorides are converted into sulphates, characterised by higher melting temperatures compared to chlorides. On the contrary, if there is not enough time for alkali chlorides to convert into sulphates, then their deposition on the surfaces release Cl which becomes available for corrosion reactions. This mechanism is known as active oxidation [108,113]. If the molar ratio <4, then high corrosion risks should be expected. Furthermore, if the value is >8, Cl concentration in boiler deposits is considered to be negligible, therefore minimising corrosion risks [108,114]. Based on the description above, corrosion risk is much higher in case of PL (fuel index 1.82) and blend of PL/WC (fuel index 1.53) compared to SP (fuel index 6.85).

3.7. Summary

The combustion behaviour of PL, blend of PL/WC and SP, was experimentally studied in a discontinuous lab-scale fixed bed reactor. As regards the N gaseous species, NH_3 showed the highest concentration in cases of PL and the blend, while HCN was the most abundant compound during SP combustion. Almost all N initially bound with the SP was converted into N gaseous species, whereas the corresponding conversion for PL and the blend amounted around 50% and 40% respectively. Easily volatile elements Cl and S illustrated higher release rates, while 15-50% was the range for the release rate of alkali metals K and Na for all tested fuels. Furthermore, the maximum estimated aerosol emissions were estimated during PL combustion, reaching the value of 2806 mg/Nm^3 (dry flue gas, 13 vol% O_2), followed by 2584 mg/Nm^3 (dry flue gas, 13 vol% O_2) in the case of blend (PL/BW). On the contrary, the estimated aerosol emissions for SP combustion were very low. Ash melting temperatures are estimated to be high for all tested fuels, whereas the corrosion risk is greater in the cases of PL and blend combustion, compared to SP.

4. Gasification of poultry litter in a lab-scale bubbling fluidised bed reactor

The objective of this chapter is to describe the experiments conducted in a lab-scale fluidised bed reactor with the aim to investigate the gasification behaviour of three different biomass fuels, poultry litter (PL), blend of PL with beechwood (PL/BW) and beechwood (BW) alone. Similar to the combustion experiments described in chapter three, the gasification experimental campaign was carried out under the framework of the European project BRISK2 (Biofuels Research Infrastructure) [105]. The facilities of the Energy Research Centre of the Netherlands (ECN part of TNO) located in Petten, Netherlands, were employed for the performance of the experiments, due to the absence of appropriate equipment at Brunel University London. The measurements were performed by the research institute's personnel utilising the available equipment, whereas the analysis of the gathered data was performed afterwards at Brunel University London. In the following sections, methods and equipment used are thoroughly described. Furthermore, the analysis of the results obtained from the experimental tests, provide useful information for the assessment of poultry litter as a potential fuel to be employed in the gasification process. In particular, the effect of process parameters on the gasification performance of the tested fuels is studied, along with the evolution of tar compounds in terms of their amount and composition, as well as any challenges that may arise due to the chemical composition of the residual ash, such as the agglomeration phenomenon.

To the best of the author's knowledge tar evolution during PL gasification and co-gasification with woody biomass has never been studied before. The study provides useful insights regarding the amount and composition of the tar, the effect of temperature and ER on tar evolution and how does it compare with respect to lignocellulosic feedstock. This knowledge can be used as input prior to designing a gas cleaning system during gasification of PL. Furthermore, presence of agglomeration phenomenon revealed during one of the experimental tests, showed the operating temperature limitations when using PL in gasification process.

4.1. Materials

PL was sourced from a company in Finland and it was partially dried and sieved to a particle size range of 0.5-0.98 mm before being fed into the reactor. Table 4.1 reports the ultimate and proximate analysis of all tested fuels, whereas the chemical compositions of PL and PL/BW ash

are provided in Table 4.2. It should be noted that chemical composition of ash for BW alone was not measured, since the specific fuel contains negligible quantities of ash and thus no challenges associated to its ash composition were expected. Fuel and ash analysis were conducted externally by a company named Celignis Limited. Fixed carbon was calculated by subtracting the percentages of moisture, volatile matter and ash from 100 %. Similarly, the oxygen content was determined by the difference from the elements presented in ultimate analysis. For the determination of the chemical composition of PL ash (generated at 550 °C according to BS EN 14775) the ash was digested and analysed using an Agilent Inductively Coupled Plasma-optical emission spectrometry.

Table 4.1: Ultimate and proximate analyses of all tested fuels.

Type of feedstock	**PL**	**PL/BW**	**BW**
Proximate analysis (% w/w, a.r.)			
Moisture	9.71	9.94	9.00
Volatile matter	69.60	73.90	80.90
Fixed carbon	20.70	17.90	17.80
Ash	14.30	8.10	1.30
Ultimate analysis (% w/w, d.b.)			
C	42.82	46.76	46.85
H	5.49	5.68	6.30
N	3.90	2.48	0.17
Cl	0.25	0.16	0.01
S	0.60	0.37	0.02
O	32.69	36.44	45.4
LCV (MJ/kg d.b)	16.78	17.37	17.59

a.r.: as received, d.b.: dry basis

The ash contained high concentrations of alkali metals such as K and Na that promote agglomeration and consequently can cause disruption of continuous fluidised bed gasification. These alkali metals along with the high concentration of Cl in PL contribute significantly to the potential challenges associated with fouling, agglomeration and corrosion.

Table 4.2: Chemical composition of PL and PL/BW ash

Ash composition (mg/kg d.b.)	PL	PL/BW
Major components		
Aluminium	1200	336
Calcium	15500	8947
Iron	1600	868
Magnesium	8200	4299
Sodium	4200	1661
Phosphorus	10200	5603
Potassium	27700	12866
Silicon	7300	147
Titanium	95	87.5
Minor components		
Arsenic	<0.5	1.03
Cadmium	0.14	<0.25
Cobalt	1.9	2.28
Chromium	16	40.7
Copper	84	89.8
Mercury	<0.02	0.04
Manganese	600	346
Molybdenum	4.8	7.03
Nickel	16	37.2
Lead	1.5	1.87
Antimony	<0.5	<0.25
Vanadium	4.2	4.29
Zinc	450	238

4.2. Experimental facility

The experimental set up located at the Energy Research Centre of the Netherlands (ECN part of TNO) is illustrated in Fig 4.1. Fuel is fed into an atmospheric bubbling fluidised bed reactor by two mechanical screw feeders under 1 Nl/min (Normal litres/min) flow of N_2 (flush gas) in order to avoid backflow of gases. The reactor consists of two different zones: (i) bed section with an internal diameter of 74 mm and 500 mm height and (ii) the freeboard section with an internal diameter of 108 mm and height of 600 mm. The lab-scale reactor operates in allothermal mode, implying that the desired temperature cannot be achieved by controlling the ER alone. Therefore, external heat source is needed, realised by electrical means under inert conditions. The fluidising medium (a mixture of N_2 and air calculated to achieve a particular ER value while maintaining a constant fluidisation velocity) is adjusted and introduced from the bottom of the reactor through the perforated distributor plate. The fluidising medium is preheated to 160 °C before being introduced into the reactor. The product gas exits the freeboard section passing through a cyclone where entrained particles of char and ash were removed. After the cyclone, part of the raw product gas is sampled for chemical analysis, while the rest is combusted in a flare. Product gas for chemical analysis flows through the hot filter to remove the finest particles that escape from the cyclone. The section downstream the reactor including a hot filter is maintained at 400 °C, preventing tar condensation inside the pipes. Tar and moisture samples were collected via a sampling port located after the hot filter. Successive cold filter removes tar prior to an online micro-gas chromatography (GC) analyser.

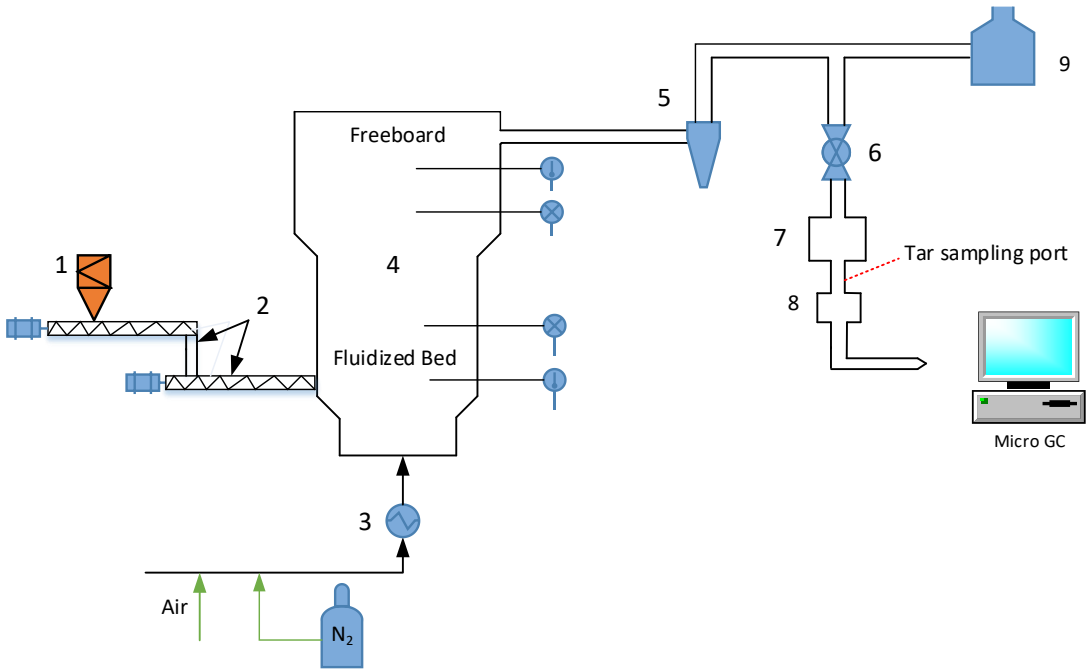

Figure 4.1: Lab-scale experimental facility at ECN part of TNO, Netherlands 1: Hopper, 2: Screw feeders, 3: Pre-heater, 4: Gasifier, 5: Cyclone, 6: Valve, 7: Hot filter, 8: Cold filter, 9: Flare

4.3. Test procedure

Considering the high ash content in PL and possible agglomeration issues, experiments were conducted at lower temperature starting from 700 ºC. Air and N_2 were continuously supplied from the bottom of the reactor at a total flow rate of 12 Nl/min in order to maintain an adequate fluidisation regime while ensuring the set gasification conditions. The minimum theoretical fluidisation velocity at the specified operating conditions was calculated using correlation proposed by [115]. Experiments were conducted at different ERs (adjusting the flow rates of air and N_2) and temperatures whilst keeping the same fluidisation condition (fluidisation velocity 4.2 times the minimum one). To adjust for lower ER, the flow rate of air was reduced while the N_2 flow was increased and vice versa. Sieved silica sand (0.25-0.5 mm) was used as the bed material with bulk and absolute densities of 1422 kg/m^3 and 2620 kg/m^3, respectively. To avoid accumulation of ash in the bed (which would distort the results, due to the potential catalytic activity of certain compounds in the fuel ash), 1.06 kg of fresh silica sand was introduced into the reactor on each test day.

4.4. Measurement methods

Continuous online measurement of product gas composition was carried out by an ABB gas analyser (CO, CO2, CH4, H2, O2) and Varian micro-GC analysis (Ar/O2, Ne, N2, CO, CO2, CH4, C2H2, C2H4, C2H6, C6H6, C7H8, H2S, and COS) [116,117]. The micro-GC measurements took place continuously at 4 min intervals. Neon (10 ml/min) was added as a tracer gas to measure the flow rate of dry product gas enabling the calculation of carbon conversion, gas yield and cold gas efficiency. Neon gas was continuously fed into the reactor and was detected by micro-GC in the outlet product stream (in ppm unit) along with the product gas. The flow rate of the product gas (m3/min) was then determined from the ratio between the neon flow rate (ml/min) and the neon concentration in the product gas (ppm).

The solid phase adsorption (SPA) method was employed for the tar sampling [118]. The SPA protocol coupled with GC detection offers reliable measurement of phenolic and 2-5 rings PAH tar compounds [119,120]. However, SPA is not ideally suitable for the detection of hydrocarbons that are too heavy to pass through GC instrument. Notable deviations were also observed during the measurement of light hydrocarbons such as benzene and toluene. This may be attributed to their high volatility making these compounds difficult to trap on the solid sorbent [121]. Three SPA samples were taken for each test condition. 100 ml of dry product gas was withdrawn from the SPA sampling port with an automatic syringe pump. The amount of total GC-detectable tar as well as the amount of each individual tar compound is expressed as an average of the three repetitive measurements. The SPA tar samples were taken in 2-minute intervals where the tar vapours were either adsorbed on 500 mg of amino propyl silica sorbent. These tars were subsequently desorbed from the amino phase by the addition of 3 x 600 ml of dichloromethane before being analysed by gas chromatography.

An Agilent 7890A GC coupled with a triple-axis MSD 5975C [122] was used for identification of the most abundant tar compounds. A Thermo Scientific Trace 1310 GC with a flame ionisation detector (GC-FID) was used for tar quantification. Tert-butylcyclohexane was added to the tar solutions as internal standard. The GC-FID instrument was calibrated by known concentrations of naphthalene/tert-butylcyclohexane for quantification of tar chromatograms. Total GC-detectable tar reported in this study refers to the sum of tar compounds eluting from thiophene (M ~84 g/mol) to benzo[a]anthracene (M ~ 228 g/mol). Benzene and toluene yields were measured by micro-GC

and presented as permanent gases and not as tar compounds [123]. In this study, the tar yields are reported on a mass basis ($g_{tar}/kg_{feedstock\text{-}daf}$) in order to avoid any dilution effect due to changes in ER. Alternatively, tar yields can be reported on a volumetric basis as $g_{tar}/Nm^3_{dry\ gas}$. The volumetric basis is suitable for industrial developers where upper tar limits with regard to downstream applications need to be met.

4.5. Performance analysis

The process performance parameters analysed in this section as a function of temperature are described below. It should be noted that all calculations were performed on a dry basis and that the concentration of permanent gases includes benzene and toluene but excludes tar compounds. The performance parameters are lower calorific value (LCV) of product gas, cold gas efficiency (CGE), carbon conversion efficiency (CCE), gas yield and tar yield. The gasification performance is usually determined by CGE and CCE. CGE is defined as the ratio between the chemical energy of the product gas and the chemical energy of the fuel input. CCE reads as the ratio between the amount of carbon fed initially in the reactor and the amount of carbon converted into gaseous products.

The quantities of permanent gas compounds are expressed as an average of four consecutive measurements. It is important to mention that the total gas volume includes both the N_2 contained in ambient air, together with the varying external addition of N_2 which is applied to ensure proper fluidisation. Although it was possible to extract some data points at 750 ºC and an ER of 0.25, the data are not presented, since agglomeration occurred immediately after steady state conditions were achieved, and thus the results are not considered reliable. More information on agglomeration will be provided in a following section.

4.6. Effect of temperature on gasification performance and tar evolution - Results and discussion

The effect of gasifier temperature (700-750 °C) at a constant ER of 0.21 on the gasification performance and tar evolution was investigated. Three different ER levels were tested at each temperature (tests 1-3 at 700ºC and tests 5-7 at 750 ºC). Due to time limitations, only one ER was tested at 725 °C (test 4). All the experiments were completed successfully except for the final test at an ER of 0.25 (test 7), where fluctuations of bed temperature and pressure were observed at the

starting phase of the experiment due to bed agglomeration. A summary of the experimental tests is given in Table 4.3.

Table 4.3: Process conditions of the experimental tests

Feedstock	**Poultry litter**						
Test number	1	2	3	4	5	6	7
Fuel flow rate (kg/h, a.r)	0.548	0.548	0.548	0.548	0.548	0.548	0.548
Equivalence ratio, ER (-)	0.17	0.21	0.25	0.21	0.17	0.21	0.25
Air flow rate (Nl/min)	6.05	7.6	9.08	7.6	6.05	7.6	9.08
N_2 flow rate (Nl/min)	5.95	4.4	2.92	4.4	5.95	4.4	2.92
Minimum fluid. Velocity (m/s)	0.033	0.033	0.033	0.033	0.033	0.033	0.033
Superficial fluid. Velocity (m/s)	0.138	0.138	0.138	0.138	0.138	0.138	0.138
Gasifier temperature T (°C)	700	700	700	725	750	750	750

"Fluid." stands for fluidisation

4.6.1. Composition of the product gas

Fig. 4.2 presents the composition of the major gas components as a function of temperature at a constant ER (0.21). The concentrations of H_2, CO and CH_4 increase with temperature, while the CO_2 content shows the opposite trend. These tendencies stem from the fact that higher temperatures favour char gasification reactions ($C + H_2O \Leftrightarrow CO + H_2$, $C + CO_2 \Leftrightarrow 2\ CO$). CH_4 is mainly evolved during the devolatilisation process. Therefore, an increase in CH_4 concentration at higher temperatures might indicate a larger extent of devolatilisation and tar decomposition into lighter molecules such as CH_4. Taupe et al. [24] reported that at higher temperatures the hydrogen content rises because oxygen reacts preferably with carbon forming CO_2 rather than water. On the other hand, the decrease in CO_2 concentration can be attributed to the Boudouard equilibrium ($C + CO_2 \Leftrightarrow 2CO$) [24]. The results obtained are in line with the relevant literature [24,29,124]. The evolution of minor gas components is presented in Fig. 4.2(b). C_2H_4 shows an increasing trend with rising temperature. The decline in ethane (C_2H_6) concentration may be the result of its thermal reforming into C_2H_4 and C_2H_2 at elevated temperatures. C_6H_6 increases slightly with temperature, whilst the concentration of C_7H_8 shows the opposite trend. The increase in C_6H_6 concentration

may be attributed to the conversion of phenols and toluene via demethylation [125,126]). C_6H_6 is a thermally stable compound. For its decomposition, an adequate gas residence time and temperatures above 1100 °C are required [81]. The results of minor gas compounds are in agreement with [127], where the authors investigated the gasification of raw and torrefied *miscanthus x giganteus* at temperatures between 660-850 °C and an ER of 0.18-0.32. Sulphur is present in the gas phase mainly in the form of hydrogen sulphide (H_2S) and carbonyl sulphide (COS). There are likely traces of other S compounds, such as thiophenes and mercaptans present in the gas, but it was not possible to be detected by the measurement equipment. The H_2S increases with temperature while the concentration of the COS is very small and showed almost a negligible change with temperature hence it is not reported in the graph.

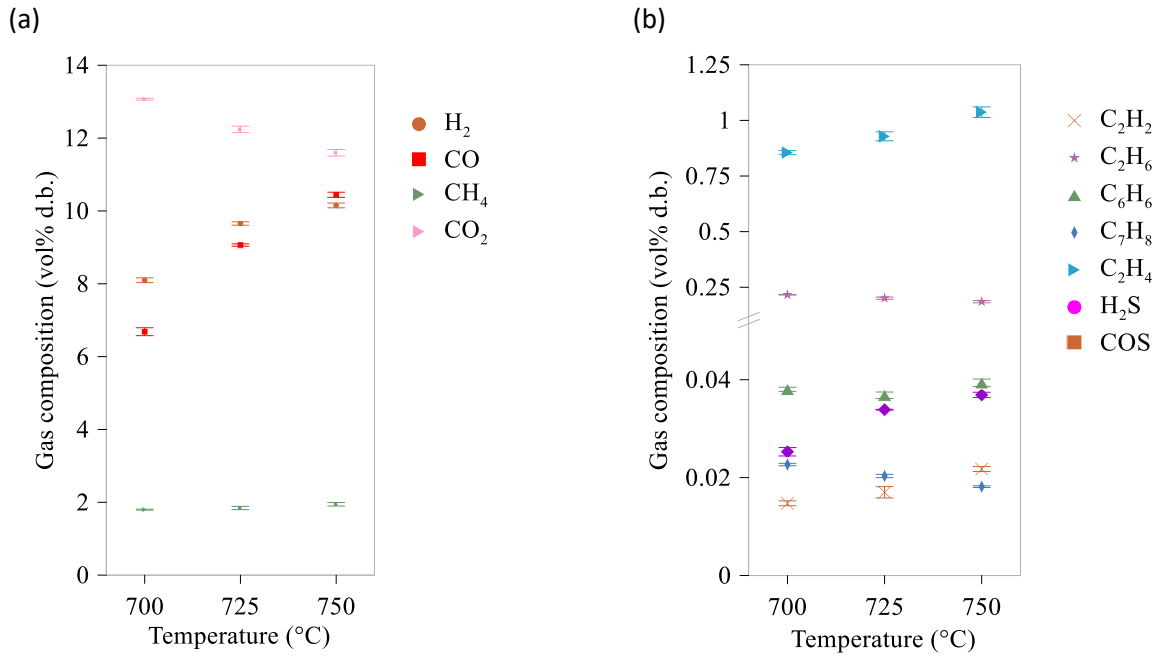

Figure 4.2: Effect of temperature on the evolution of (a) dominant gas compounds and (b) minor gas compounds (constant ER = 0.21)

4.6.2. Gas yield, carbon conversion efficiency (CCE), cold gas efficiency (CGE), and lower calorific value (LCV)

Fig. 4.3(a) shows gas yield and CCE as a function of temperature at a constant ER (0.21). Gas yield is reported on a N_2 and dry ash free basis in order to ascertain the actual gas production without any dilution effects. A gas yield increment of 33 % (from 0.93 to 1.24 N_2 free m^3/ kg

feedstock-daf) correlates with elevated temperature. Higher temperature favours the breakdown of molecular bonds (i.e., char conversion and release of volatiles). CCE also rises with temperature from |67% to 85% (an increase of 27%). It should be mentioned that for the experiment conducted at 750 °C and an ER of 0.21, some extraction of bed material took place prior to the test due to ash accumulation in the bed, which may underestimate the carbon conversion. In industrial gasifiers bed extraction usually takes place in order to prevent agglomeration phenomenon due to the build-up of alkaline metals contained in the ash.

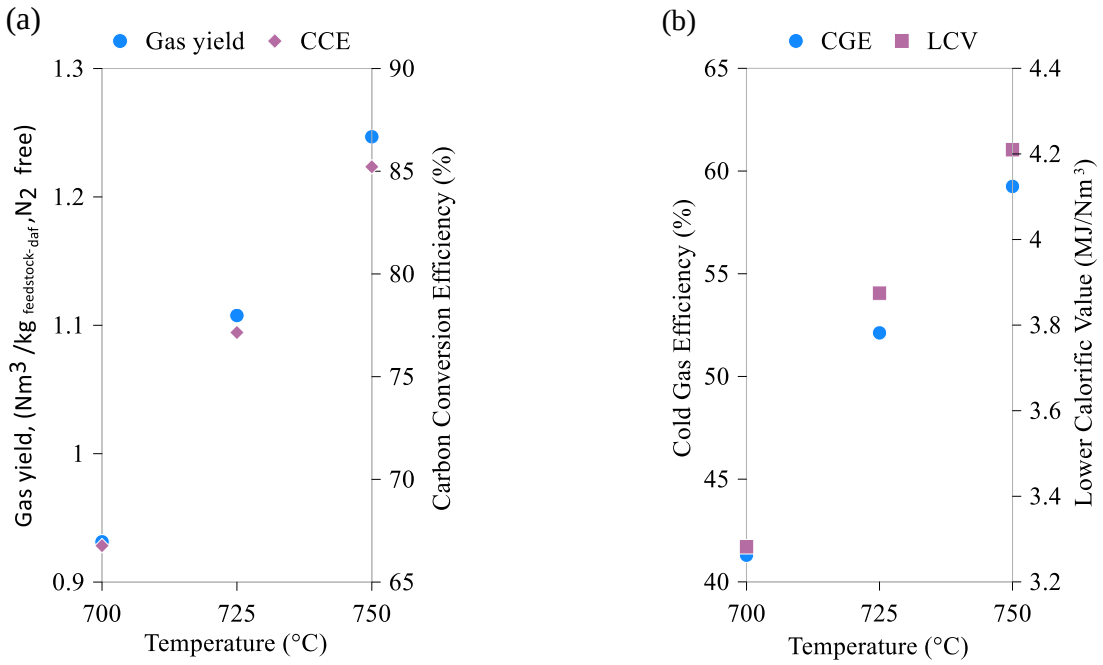

Figure 4.3: Effect of temperature at ER = 0.21 on a) gas yield and CCE (b) CGE and LCV

Fig. 4.3(b) depicts the effect of temperature on LCV and CGE at a constant ER (0.21). The LCV of the product gas rises by 24 % ranging from 3.4 MJ/Nm^3 to 4.2 MJ/Nm^3 as the temperature increases. It is noteworthy to mention that the highest LCV at 750 °C (4.2 MJ/m^3) doesn't exceed the limit of 4.71 MJ/m^3 reported to be suitable for internal combustion engine applications [128]. However, the sum of all tar content represented solely as naphthalene gives LCV of 5.85 MJ/Nm^3. Similarly, Arena and Di Gregorio et al. [129] in their study on gasification of industrial plastic wastes reported a significant increase in the LCV of the product gas when adding up the energy stored in the tar (i.e. naphthalene). Therefore, it is evident that, when tar is removed from product gas, its calorific value reduces significantly. CGE rises considerably with temperature, reaching approximately 60 % at the highest tested temperature. The explanation is based on the increase of

both gas yield and LCV with temperature as described above.

4.6.3. Tar evolution and composition

The identified tar compounds in this work together with their retention times are given in Table 4.4. Compound classification is based on the system proposed by Milne et al. [77] which was described in section 2.3.2.1. Compared to typical lignocellulosic biomass, PL is expected to give lower tar yields due to the lower lignin content in PL with respect to wood. Lignin is considered as a tar precursor leading to the formation of higher amount of GC-detectable tar and PAHs [126,130]. Furthermore, high alkali and alkali earth metal content (e.g., calcium, magnesium, sodium) in PL ash should catalyse tar cracking reactions. The tar composition of PL feedstock also varies with respect to lignocellulosic feedstock. In particular the high nitrogen content found in waste feed, excreta, and feathers, leads to the formation of nitrogen-containing hydrocarbons (pyridine, pyrrole, methyl pyridine).

Table 4.4: Identified tar compounds together with the retention times and classification according to Milne et al. (1997). Chromatogram from the experimental test at 700 °C and ER 0.21 was chosen to identify the tar compounds.

	Compound	Retention time (min)	Tar group
1	Thiophene	2.98	Secondary
2	Pyridine	4.60	Secondary
3	Pyrrole	5.16	Secondary
4	Methyl pyridine	7.28	Secondary
5	Methyl pyrazine	7.50	Secondary
6	Ethylbenzene	8.68	Secondary
7	o/m/p Xylene	8.98	Secondary
8	Phenylethyne	9.18	Secondary
9	Styrene or o/m/p Xylene	9.77	Secondary
10	Iso-dimethyl pyridine	10.72	Secondary
11	2/3/4 Ethenyl pyridine	10.89	Secondary
12	Benzonitrile	13.11	Secondary
13	Phenol	13.65	Secondary
14	o/m/p Methyl styrene	14.58	Secondary
15	Indene	15.06	Secondary
16	o/m/p Cresol	16.12	Secondary
17	Naphthalene 1,2 dihydro	18.37	PAH tertiary
18	Naphthalene	19.36	PAH tertiary
19	Quinoline	20.93	Secondary
20	Isoquinoline	21.15	Secondary
21	2-Methyl naphthalene	22.50	Alkyl tertiary
22	Indole	22.76	Secondary
23	1-Methyl naphthalene	22.94	Alkyl tertiary
24	Biphenyl	24.80	Alkyl tertiary
25	Acenaphthylene	26.48	PAH tertiary
26	2-Ethenyl naphthalene	26.94	Alkyl tertiary
27	Acenaphthene	27.36	PAH tertiary
28	Dibenzofuran	28.18	Secondary
29	Fluorene	29.71	PAH tertiary
30	Phenanthrene	33.99	PAH tertiary
31	Anthracene	34.27	PAH tertiary
32	4h-cyclopenta(def)phenanthrene	36.60	Secondary
33	Fluoranthrene	38.90	PAH tertiary
34	Pyrene	39.59	PAH tertiary
35	Benzo[a]anthracene	43.90	PAH tertiary

The evolution of total GC-detectable tar and associated tar groups as a function of temperature is presented in Fig. 4.4. Total GC-detectable tar accounts for ~1 wt.% of the initial dry and ash free feedstock. For the temperature range tested, the total GC-detectable tar decreased by 24 % (from 5.6 to 4.25 $g_{tar}/kg_{feedstock\text{-}daf}$). Detected but not identified tar compounds account for 20-30 % of total GC-detectable tar. The yield of secondary tar dominates the tar groups while alkyl tertiary tar

is the least abundant category over the entire range of tested temperatures. The alkyl tertiary tar group evolves at 750 - 850 °C as an intermediate between secondary and PAH tertiary tar. At temperatures between 850 - 950 °C, alkyl tertiary tar reforms into unsubstituted PAHs [78]. Since the temperature range investigated was limited to the range 700 -750 °C in order to avoid agglomeration issues it is not possible to verify the evolution profiles of alkyl/PAH tertiary tar in details. However, the yield of PAH tertiary tar group increased by 28 % as the temperature increased from 700 to 750 °C and PAH tertiary tar is expected to increase exponentially at higher temperatures. Two different reaction pathways are proposed for the production of PAH tertiary tar. The first pathway describes cracking of heavier hydrocarbons which were not GC-detectable due to their high molecular weight. The second pathway suggests PAH production via decomposition and subsequent recombination of secondary tar or through isomerisation of unsaturated C_2-C_4 hydrocarbons.

The dew points were calculated using an online tool developed by the ECN [131] to be between 101-105 °C and show minor effects of tested temperatures on its values. However, the high tar dew points confirm the need for gas cleaning if the gas is to be used in internal combustion engines, gas turbines or synthesis processes. The dominant factor determining tar dew point is the yield of the PAH compounds in the product gas. The dew point of PAHs correlates with their molecular mass and concentrations in the product gas. Thus, PAH growth amplifies the risk of tar condensation on the cold surfaces of the gasifier.

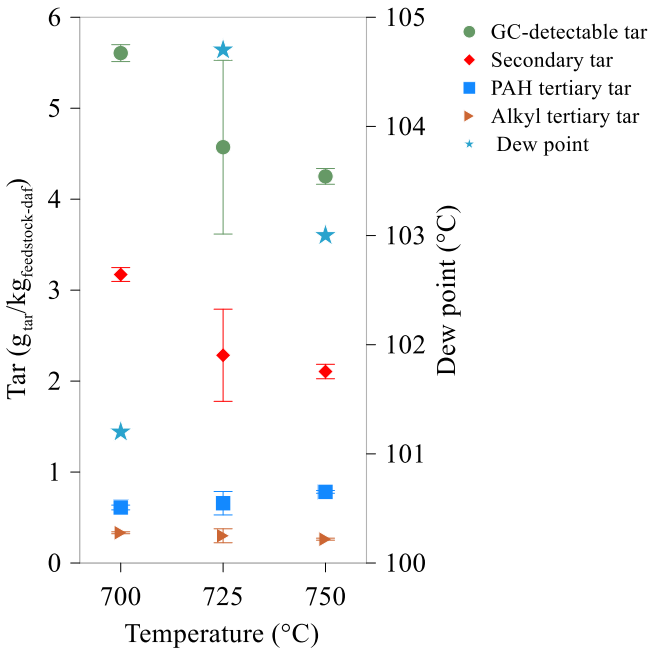

Figure 4.4: Effect of temperature on total GC-detectable tar, secondary, alkyl tertiary and PAH tertiary tar group at an ER of 0.21

Fig. 4.5 shows the evolution of the most abundant individual tar compounds. Secondary tar compounds are represented by oxygen-containing phenolic compounds and substituted one-ring aromatics presented in Fig. 4.5(a), and nitrogen-containing hydrocarbons displayed in Fig 4.5(b). Compounds representing alkyl and PAH tertiary tar groups are shown in Fig. 4.5(c-d), respectively. Note that isomeric compounds such as 1-methyl naphthalene and 2-methyl naphthalene are summed up and presented as a single quantity. Tar data points at 725 °C appear to deviate more than tar data measured at 700 and 750 °C. Such deviation while using SPA method has been reported previously in [132,133]. This could result from inconsistencies in feedstock feeding rate, SPA sampling failures such as leaks and clogs or inconsistent integration of complex tar chromatograms.

Horvat et al. [79] gasified raw and torrefied *Miscanthus x giganteus* at temperatures between 660-850 °C. They reported a peak in phenolic yield at 750 °C when using torrefied feedstock. While testing raw feedstock, phenolic yield decreased steeply at temperature above 715 °C. Dufour et al [125] conducted pyrolysis experiments on wood chips at temperatures 700-1000 °C and a gas residence time of two seconds. Their findings revealed a decrease in phenol and cresol concentrations as the temperature increased. The authors suggested that phenol is converted into benzene, indene and naphthalene via cyclopentadienyl radicals, while cresol transforms into phenol

and toluene through demethylation and dehydration reactions. Willow and beech wood were gasified in a lab-scale fluidised bed reactor. Authors suggested that the conversion of phenol and cresol occurs between 750-850 °C [81]. However, in the present study phenolic hydrocarbons start to decrease earlier at 700 °C. Single-ring aromatics such as styrene and xylenes show a small reduction with temperature, while indene increases slightly. Indene is formed by the decomposition of phenol via cyclopentadienyl radicals. It is probably reformed to either benzene or naphthalene at temperatures higher than the ones tested in the present work, namely between 800-900 °C according to [81,125].

Nitrogen-containing hydrocarbons show different thermal behaviour. Pyridine increases steadily while the concentration of pyrrole reduces significantly. Methyl pyridine shows a very small decrease, down to approximately 0.12 $g/kg_{feedstock-\ daf}$. The opposite trends for pyridine and pyrrole may be attributed to the higher thermal stability of the former compound. Wang et al. [134] investigated the transformation of nitrogen during pyrolysis and combustion of coal in a flow reactor. Pyridine and pyrrole were considered as model compounds while measuring the amount of H_2 and HCN in order to identify their thermal stability. The findings revealed that that pyridine appeared to be more stable generating high amounts of HCN at 825 °C, while the respective temperature for pyrrole was at 775 °C.

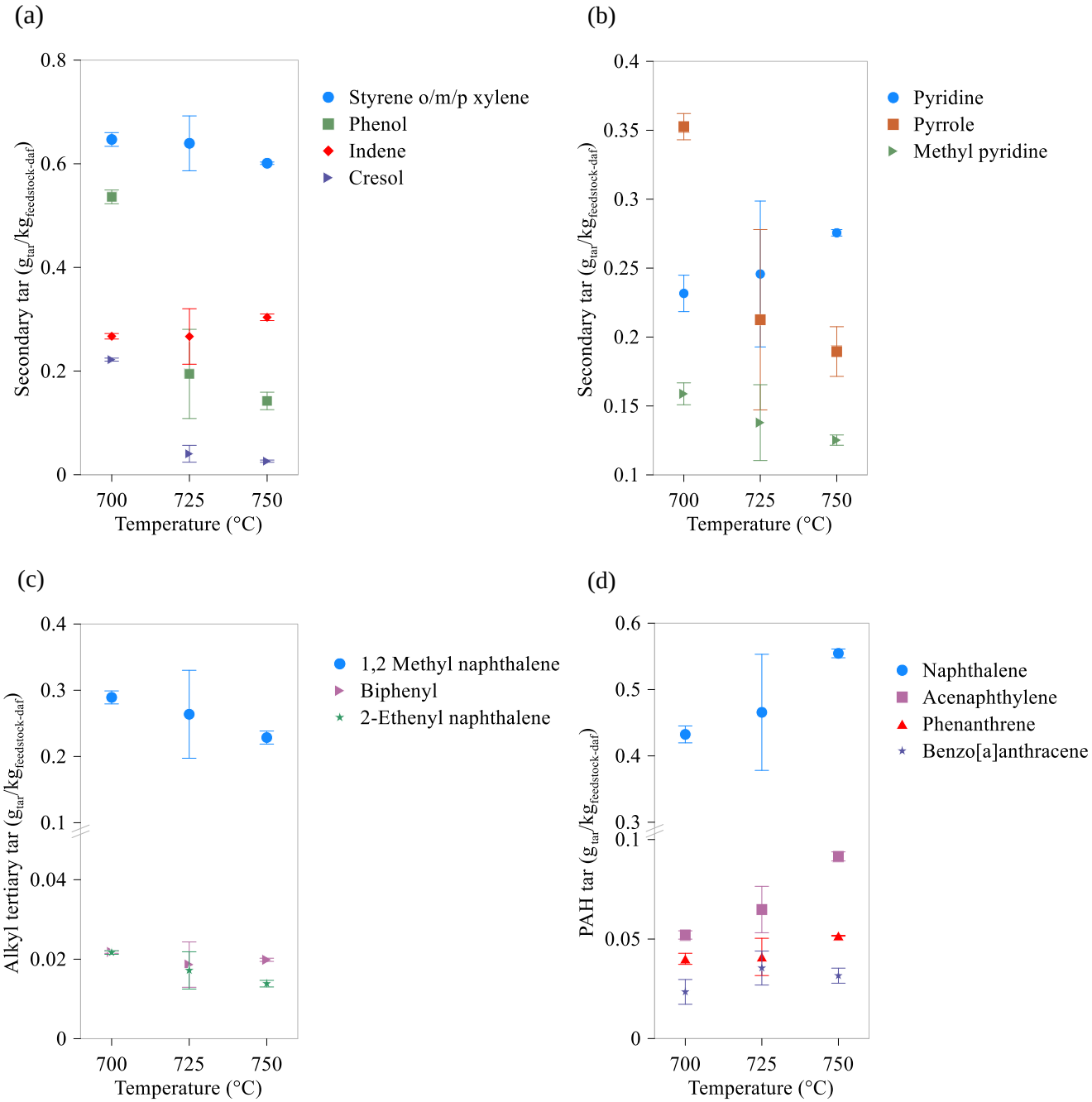

Figure 4.5: Effect of temperature on the evolution of the most abundant individual tar compounds at an ER of 0.21

Methyl naphthalene is the most abundant of the alkyl tertiary tar compounds, indicating decreased yields in the tested temperature range. Biphenyl yield remains constant, while 2-ethenyl naphthalene reduces slightly. Dufour et al. [125] reported that reforming of methyl naphthalenes into naphthalene and acenaphthylene occurs at 800-900 °C. Horvat et al. [126] observed a peak in

the yield at 800 °C for alkylated naphthalene. Steady increase of biphenyl yield was observed at the temperature range 660-850 °C using torrefied feedstock. Biphenyl may act as an intermediate in the polymerisation pathway promoted by higher temperatures [135].

Tertiary PAH tar evolution shows an upward trend with rising temperature. The findings are in line with other researchers who observed that the production of PAH is driven by increased temperature [126,135]. Yu et al. [130] argued that at 850 °C the composition of tar consists mainly of PAHs. Naphthalene is the most abundant PAH compound ranging between 0.43-0.55 $g_{tar}/kg_{feedstock\text{-}daf}$. The low reforming rate of naphthalene is explained by its thermal stability. Naphthalene formation initiates either from the decomposition of heavier PAHs or by polymerisation reactions [136,137]. In this study the relatively low operating temperature resulted in low production of PAHs and the dominance of secondary tar.

4.6.4. Agglomeration

Agglomeration is a crucial phenomenon as regards the operational stability of fluidised bed gasifiers. The occurrence of bed agglomeration results in de-fluidisation conditions leading to local temperature and pressure deviations and consequent shutdown of the gasifier. The reason behind this phenomenon is the presence of inorganic compounds (P, K, Na, etc.) in the feedstock ash characterised by low melting temperatures. Agglomeration is exacerbated when silica sand is used as bed material as the reaction between silica and potassium may form low melting potassium silicate. Prevention or mitigation of such formation may be realised with the addition of calcium forming calcium phosphate, rather than with higher melting temperature [138]. Agglomeration in the first minutes of test 7 resulted in the interruption of the fluidisation conditions. After 10 minutes the feeding started again in order to investigate if the fluctuations appear again and although for 10 minutes (3-12 min in Fig 4.6) the gasifier seemed to operate smoothly, deviations of pressure and temperature occurred again leading to the termination of the experiment.

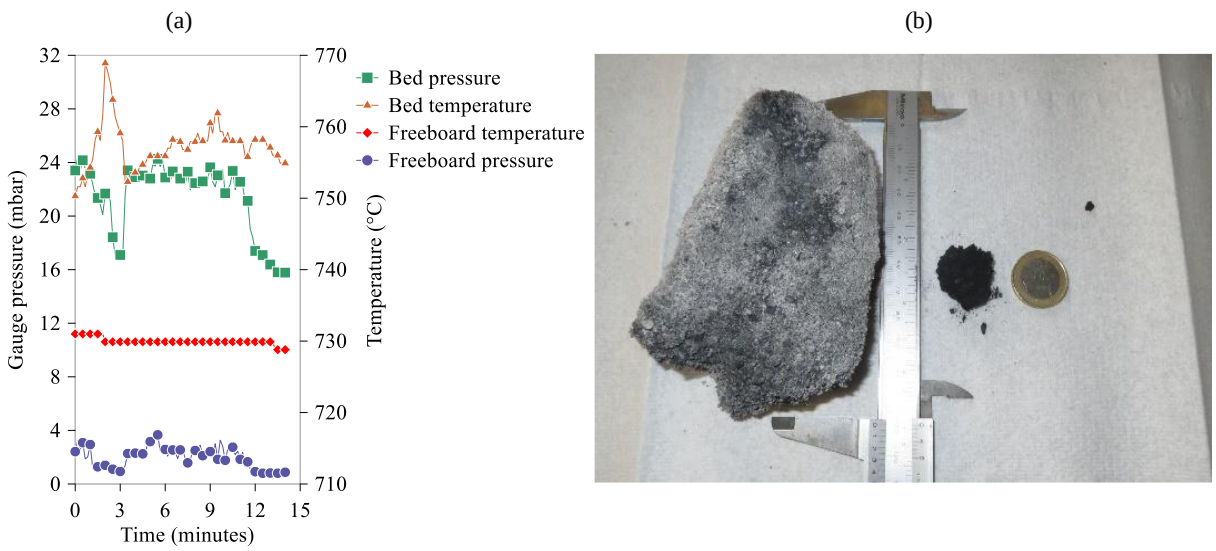

Figure 4.6: (a) Indication of agglomeration at ER 0.25 and temperature 750 °C, (b) Agglomerate removed after the shutdown of the gasifier

4.7. Effect of equivalence ratio (ER) on gasification performance and tar evolution-Results and discussion

Based on the findings regarding the maximum possible operating temperature without the presence of agglomeration, further experiments were conducted in order to investigate the effect of equivalence ratio under constant temperature conditions. Apart from fuel poultry litter, blend of poultry litter with beech wood (50:50 mass ratio) and beech wood alone were also tested in the lab-scale bubbling fluidised bed reactor. A summary of the experimental tests is presented in Table 4.4. Only two tests regarding PL gasification are reported (tests 1 and 2) since agglomeration occurred at the highest ER of 0.25 (see section 4.6.4.). Tests 3, 4 and 5 refer to PL/BW gasification. An attempt was made to gasify the PL/BW at the temperature of 800 °C but the bed agglomerated and the experiment was terminated. BW alone was gasified at 750 ℃ (tests 6, 7, 8) and the results are considered as the reference point. It can be observed from Table 4.5 that the feeding rate was consistent throughout the experimental campaign.

Table 4.5: Summary of operating conditions of experimental tests

Type of feedstock	**PL**		**PL/BW**			**BW**		
Test number	1	2	3	4	5	6	7	8
Fuel flow rate (kg/hour, a.r.)	0.548	0.548	0.559	0.559	0.559	0.546	0.546	0.546
ER (-)	0.17	0.21	0.17	0.21	0.25	0.18	0.225	0.27
Air flow rate (litres/min)	6.05	7.6	6.5	8.2	9.8	6.05	7.6	9.08
Nitrogen flow rate (litres/min)	5.95	4.4	5.5	3.8	2.2	5.95	4.4	2.92
Minimum fluid. Velocity (m/sec)	0.033	0.033	0.033	0.033	0.033	0.033	0.033	0.033
Superficial fluid. Velocity (m/sec)	0.138	0.138	0.138	0.138	0.138	0.138	0.138	0.138
Gasifier T (°C)	750	750	750	750	750	750	750	750
Fluidization medium T (°C)	160	160	160	160	160	160	160	160

"Fluid" stands for fluidisation

4.7.1. Composition of the product gas

Figure 4.7 presents the gas composition of the main species as a function of ER. An increase in CO_2 content with ERs can be observed for all the tested fuels. This is attributed to the higher availability of oxygen in the reactions with volatiles and char combustion. The results related to CO_2 concentration are in line with the findings of previous research reported in [29,139,140]. In general, the presence of oxygen in the reactor decreases the concentration of CO due to its oxidation and formation of a more stable compound CO_2. However, the concentration of CO in this study shows different behaviour with respect to the fuels. Particularly, for PL and BW it increases while the blend of PL and BW showed an opposite trend. A possible explanation could be decomposition of higher hydrocarbons resulting in an increase of the CO concentration. The tar analysis presented in Figure 5, confirmed this by analysing the GC-detectable tar conversion over the tested range of ER. Noticeable decrease in the concentrations of C_6H_6 and C_7H_8 (see Table 4)

can be seen in BW explaining the observed increase in CO concentration. A similar conclusion was drawn by Kwapinska et al. [141] from gasification of Miscanthus x giganteous at ER ranging between 0.18 - 0.32. Additionally, an increase in ER can affect the optimal mixing conditions and could be the possible reason for higher concentrations of CO, since local spots may be created with very low air concentrations. As a consequence of imperfect mixing, higher amounts of unconverted fuel are expected. The concentration of H_2, although expected to decrease with increasing ERs due to oxidation, in the cases of BW and blend it fluctuates, while in the two test runs of PL remains approximately stable. Similarly, the fluctuations in H_2 concentration could also be attributed to the decomposition of higher hydrocarbons. Methane concentration shows a relatively stable trend for all fuels which is mainly produced in the pyrolysis zone. The steam reforming of CH_4 is kinetically limited and unlikely to occur at temperatures below 1000 ºC [139,142]. Furthermore, an increase in ER promotes the decomposition of tar compounds into lighter hydrocarbons, a fact that could explain the observed decrease in C_7H_8 concentration in this study. Finally, the compositions of minor species (C_2H_2, C_2H_4, and C_2H_6, H_2S, COS) are not affected by changes in ER. C_2H_4 is the most abundant between the minor hydrocarbons, and his concentration falls between 1.17-1.25 vol. %, on a dry basis.

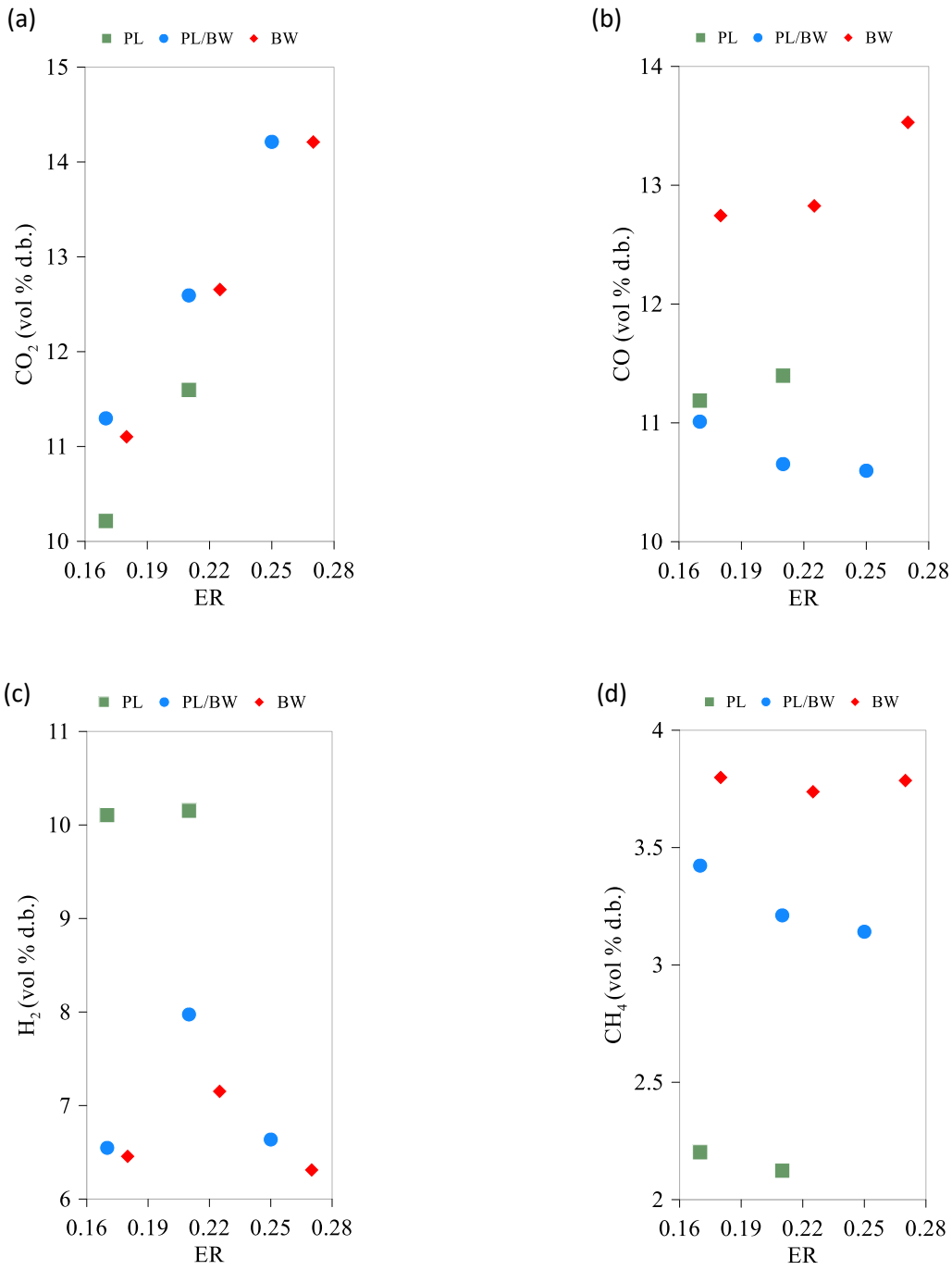

Figure 4.7: Evolution of the major gas species as a function of ER.

4.7.2. Gas yield and carbon conversion efficiency (CCE)

The effect of ER on the total gas yield is shown in Figure 4.8(a) and it is reported on a nitrogen and dry ash free basis ascertaining the actual gas production without any dilution effects. As observed, PL results in the highest amount of total gas yield of 1.25 m^3/kg_{daf} N_{2free} at an ER of 0.21.

Moreover, with an increase in ER, the gas yield from poultry litter and BW showed an upward trend, probably due to higher char conversion and release of volatiles since more oxygen is consumed in the reactor. On the other hand, the gas yield resulted from gasification of PL/BW blend remains fairly constant at the tested ER range. The possible explanation for the inconsistency in the gas yield during the co-gasification of blended PL/BW could be either due to high attrition and char entrainment or due to increased N_2 concentration in the dry gas. Indicatively, the measured carbon content in cyclone fine and bed ash collected from PL/BW was reported to be higher (18 g/hour) compared to the BW alone (8.9 g/hour). CCE shown in Figure 4.8(b), is increasing with ER, implying that higher amounts of char are converted due to increased amounts of oxygen available in the reactor. It should be noted that during test 2, a small fraction of bed material was extracted due to high ash accumulation in the bed which might have affected the CCE calculation resulting in the drop of CCE.

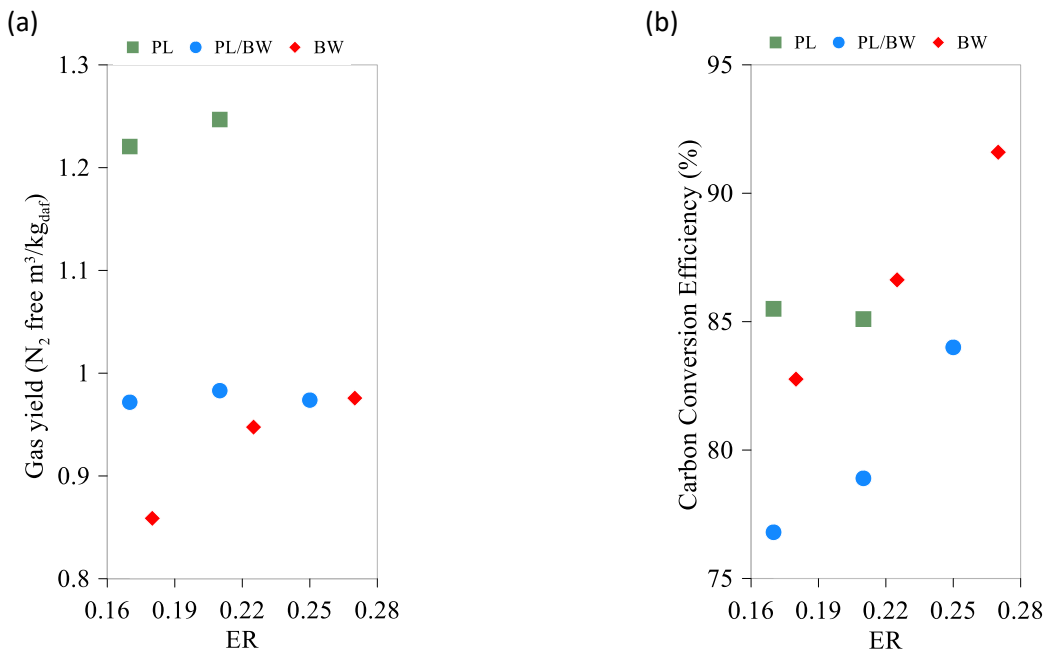

Figure 4.8: Effect of ER on a) Gas yield and b) CCE.

4.7.3. Lower calorific value (LCV) and cold gas efficiency (CGE)

Figure 4.9(a) displays the effect of ER on the LCV of all tested fuels. In line with [29,124,128,139,143,144], the LCV of the product gas decreased with an increase in ER. The explanation stems from the fact that at higher ERs there is a higher amount of oxygen available to react with volatiles evolving in the pyrolysis zone and further extension afterwards of oxidation

reactions. In all cases the decrease in LCV is small (<5%). This can be explained from the fluctuations in the composition of H_2, CO and higher hydrocarbons. Especially higher hydrocarbons (C_6H_6, C_7H_8), although present in small quantities, they have much higher LCV compared to H_2 and CO and therefore even a small change can have a significant effect on LCV. BW acquires the highest LCV accounting for 4.96 MJ/Nm^3, followed by PL/BW and PL respectively. The effect of ER on CGE is presented in Figure 4.9(b) and shows a declining trend with ERs. At higher ER, the higher amount of air injected in the gasifier promotes carbon and hydrogen oxidation, resulting in the decrease of the chemical energy contained in the product gas. The obtained values of CGE are within the limits (50 - 80%) which are in line with findings given by Arena [145] for gasification of municipal solid waste with air and oxygen enriched air. Among the fuels tested in this study, BW has the highest CGE (63%).

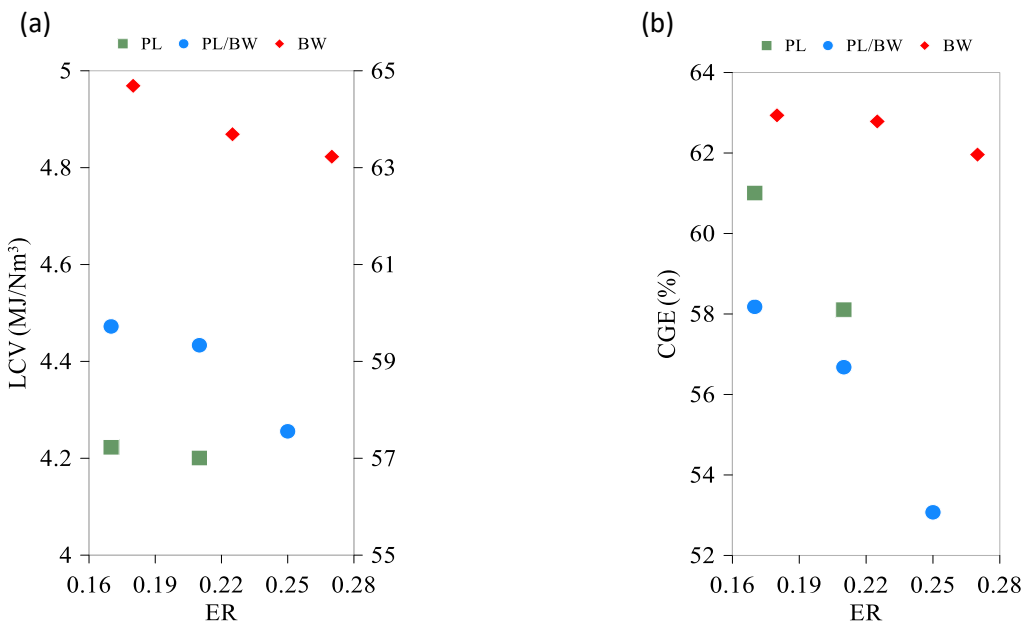

Figure 4.9: Effect of ER on a) LCV and b) CGE.

4.7.4. Tar evolution and composition

Table 4.6 presents the identified tar compounds in the order they were eluted. The tar compounds derived from the blend of PL/BW are not shown because they are the same with the respective ones eluted for PL alone. As can be observed, the main difference between PL and BW are the nitrogen-containing tar compounds reflecting the high nitrogen content of PL compared to BW.

Ten nitrogen-containing tar compounds were identified and reported in Table 4.6 (designated by *). In addition to that sulphur-containing tar compound, thiophene was identified in PL derived tar.

Table 4.6: Identified tar compounds with the chromatographic retention times

	Poultry litter (PL)		**Beech wood (BW)**	
	Tar compound	Retention time (min)	Tar compound	Retention time (min)
1	Thiophene	2.96	//	
2	Pyridine*	4.54	//	
3	Pyrrole*	5.12	//	
4	Methyl pyridine*	7.24	//	
5	Methyl pyrazine *	7.54	//	
6	Ethylbenzene	8.69	Ethylbenzene	8.70
7	o/m/p Xylene	8.95	o/m/p Xylene	8.97
8	Phenylethyne	9.37	Phenylethyne	9.43
9	Styrene	9.74	Styrene	9.78
10	Iso-dimethyl pyridine*	10.97	//	
11	Ethenyl pyridine*	11.11	//	
12	Benzonitrile*	13.15	//	
13	Phenol	13.95	Phenol	13.52
14	o/m/p Methyl styrene	14.66	o/m/p Methyl styrene	14.59
15	Indene	15.06	Indene	15.07
16	o/m/p Cresol	16.34	o/m/p Cresol	15.98
	Naphthalene, 1,2 dihydro	18.43	Naphthalene, 1,2 dihydro	18.38
17	Naphthalene	19.35	Naphthalene	19.37
18	Quinoline*	21.11	//	
19	Isoquinoline*	21.36	//	
20	Indole*	22.79	//	
21	2-Methyl naphthalene	22.97	2-Methyl naphthalene	22.50
22	Biphenyl	24.86	Biphenyl	24.83
23	//		Ethenyl naphthalene	26.07
	Acenaphthylene	26.49	Acenaphthylene	26.46
24	Acenaphthene	27.40	Acenaphthene	27.37
25	Dibenzofuran	28.28	Dibenzofuran	28.24
26	Fluorene	29.77	Fluorene	29.69
27	Phenanthrene	34.04	Phenanthrene	33.97
28	Anthracene	34.36	Anthracene	34.27
29	4H-Cyclopenta(def)phenanthrene	36.67	4H-Cyclopenta(def)phenanthrene	36.59
30	2-Phenyl naphthalene	37.71	//	
31	Fluoranthrene	38.96	Fluoranthrene	38.86
32	Pyrene	39.64	Pyrene	39.54
	//		Benzo[a/b]fluorene	40.89
33	Benzo[a]anthracene	43.91	Benzo[a]anthracene	43.90
34	//		Benzo(k)fluorathrene	47.56

Figure 4.10 depicts the effect of ER on the amount of total GC-detectable tar. It is evident that there is a decrease in total GC-detectable tar for all fuels at rising ERs. The most significant decrease relates to the total GC-detectable tar of PL (21.8 %) while the other two fuels present a similar decreasing rate (10.1% for PL/BW and 10.7% for BW). A possible explanation for the decrease in tar yield may be the oxidation of tar compounds due to the higher presence of oxygen within the reactor. The results are in line with previous work of Hanping et al. [146]. The authors gasified three different biomass samples at an ER ranging between 0.15-0.35 and temperature at 800 °C, reporting a considerable reduction of tar when ER was increased. On the contrary, a more recent study carried out by Horvat et al. [126] found that at constant temperature, the ER has relatively little impact on the yield or composition of tar from a grassy biomass. Campoy et al. [139], performed gasification experiments of different feedstocks and found that the maximum decrease in the gravimetric tar content was 40% for orujillo (exhausted olive cake) when increasing the ER from 0.23 to 0.43. However, the experiments took place in a pilot scale reactor where temperature was ER dependent, thus tar evolution could not be investigated separately.

Low tar yields of PL can be attributed to its high ash content along with the low organic fraction (low lignin content) compared to BW. PL ash contains significant amounts of inorganics that act as tar cracking catalysts causing a reduction in the total amount of tar [147]. Lignin was reported to be a tar precursor producing higher total GC-detectable tar and PAH compared to cellulose and hemicellulose [148–150]. Although the chemical content of all tested fuels was not investigated, in the study of Font Palma [148] the chemical analysis of several types of woody biomass (not including beech wood) along with the one of PL are given, showing that the lignin content of all woody biomass is superior to PL. Tar yield of PL/BW falls between the two fuels. Due to the moderate operating temperature of 750 °C, secondary tar is predominant group in all cases, whereas alkyl tertiary tar displays the lowest yields. Generally, it is expected that the yield of PAH tertiary tar would increase at temperatures higher than 750 °C, through decomposition of secondary tar compounds and subsequent recombination into PAH tertiary tar compounds. On the other hand, alkyl tertiary tars develop at temperatures 750 - 850 °C, acting as intermediates between secondary and PAH tertiary tar groups, while at temperatures higher than 850 °C, reform into unsubstituted PAHs [78]. However due to the limitation of operating temperature range, it was not possible to study in detail the evolution profiles of PAH and alkyl tertiary tar groups.

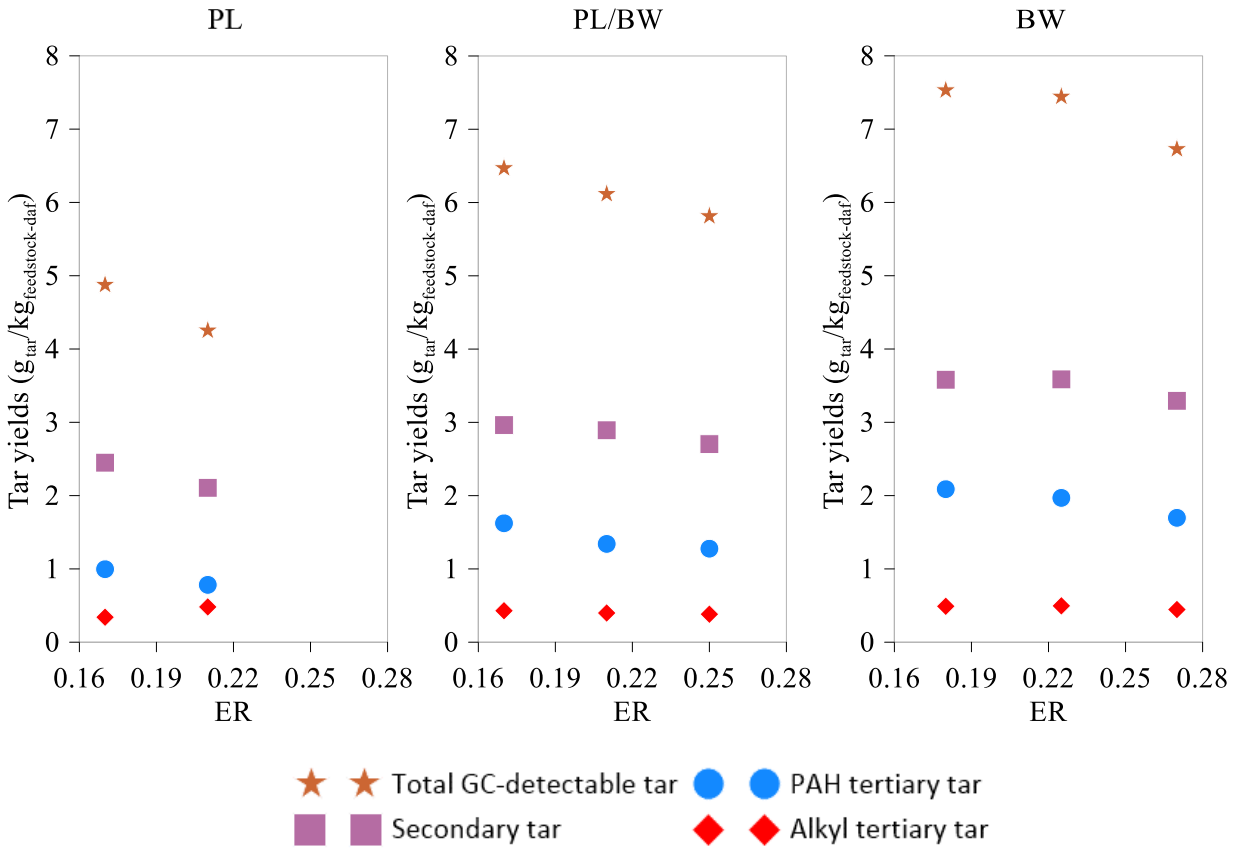

Figure 4.10: Tar groups classified according to Milne et al., 1998 and total GC- detectable tar as a function of ER.

The amount of detected but not identified tar is in the range 20 -25% for all fuels and was calculated by subtracting the identified tar compounds from total GC-detectable tar. Figure 4.11 shows twelve tar compounds present in all fuels and with quantity ≥0.05 gtar/kg $_{feedstock-daf}$ at the lowest ER. Naphthalene is the most abundant compound in the PAH tertiary tar group followed by phenol, indene, and styrene which belong to the secondary tar group. Overall, naphthalene is considered as a very stable compound remaining present at temperatures of 900 °C even after catalytic tar cracking [151,152]. It is formed by either the breakdown of heavy tar (GC-undetectable and heavy PAH), or by polymerisation reactions from smaller building blocks.

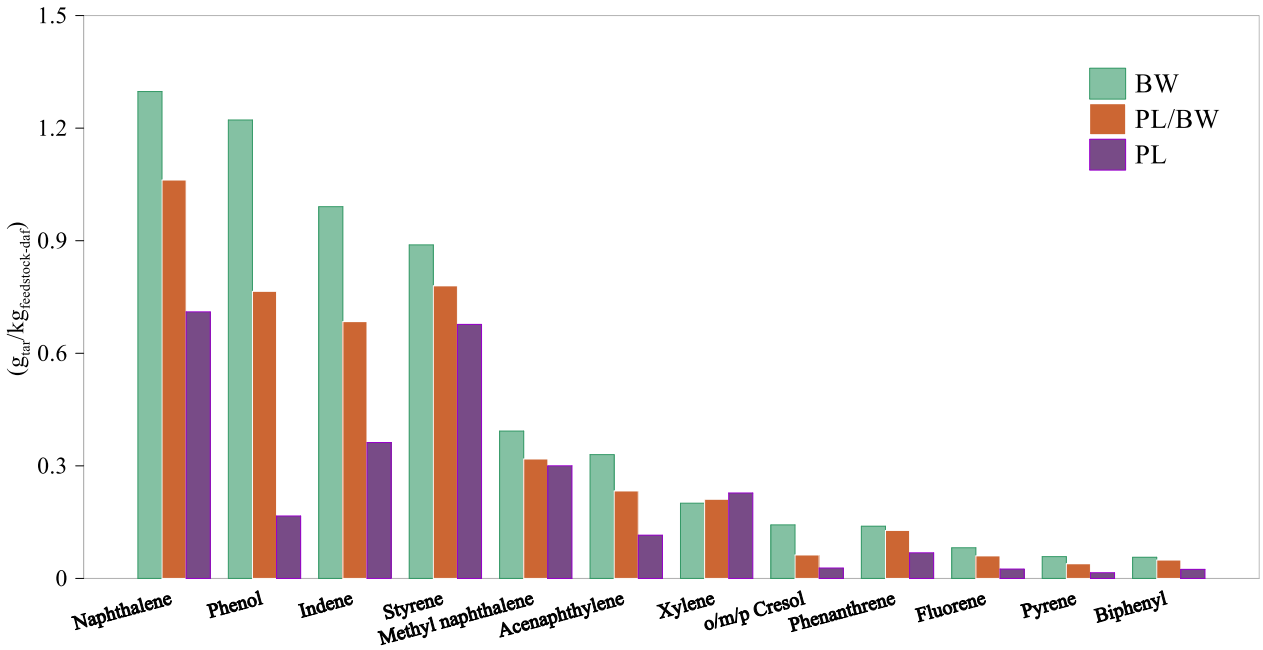

Figure 4.11: Yield of individual tar compounds as a function of fuel at the lowest ER.

4.7.5: Mass balance

Table 4.7 presents mass balance calculations pertaining to the PL/BW and BW at 750 °C and different ERs, in order to ascertain the accuracy of the experimental measurements. The mass balance for the PL refers to a temperature of 700 °C and the different ERs, since the respective mass balance at 750 °C was not performed due to the fact that the material from the cyclone was not collected for one of the tests. The input streams comprise of solid feedstock, air, nitrogen and moisture content whilst the output consists of dry gas, unconverted material collected from the bed and cyclone (char and ash), along with the moisture present in the gas. An impinger bottle containing 100 ml of sodium pentoxide was placed in bath at 4ºC after the hot filter for the sampling of moisture. The moisture content was determined by the mass difference of the impinger bottle before and after the sampling. It should be noted that accumulation of char and ash in the bed were estimated as average over the day of the experiments, whereas material from the cyclone was collected at the end of each experimental test. Furthermore, deviations in hydrogen balance can be attributed to lack of information regarding elements such as ammonia but also due to errors in moisture determination and no-inclusion of heavy hydrocarbon compounds in the tar.

Table 4.7: Mass balance for all tested fuels

	PL (ER=0.17)			**PL** (ER=0.21)			**PL** (ER=0.25)		
Elements	Input	Output	Relative error (%)	Input	Output	Relative error (%)	Input	Output	Relative error (%)
C (kg/h)	0.21	0.15	28.57	0.21	0.16	23.8	0.21	0.17	19
H (kg/h)	0.033	0.027	18.2	0.033	0.027	18.2	0.033	0.028	15.1
N (kg/h)	0.854	0.863	-1.05	0.831	0.850	-2.3	0.81	0.83	-2.47
	PL/BW (ER=0.17)			**PL/BW** (ER=0.21)			**PL/BW** (ER=0.25)		
Elements	Input	Output	Relative error (%)	Input	Output	Relative error (%)	Input	Output	Relative error (%)
C (kg/h)	0.228	0.197	13.6	0.228	0.197	13.6	0.228	0.199	12.7
H (kg/h)	0.033	0.03	9.1	0.033	0.031	6	0.033	0.043	-30.3
N (kg/h)	0.84	0.868	-3.3	0.81	0.826	-1.97	0.79	0.8	-1.26
	BW (ER=0.18)			**BW** (ER=0.225)			**BW** (ER=0.27)		
Elements	Input	Output	Relative error (%)	Input	Output	Relative error (%)	Input	Output	Relative error (%)
C (kg/h)	0.232	0.201	13.36	0.232	0.210	9.5	0.232	0.222	4.3
H (kg/h)	0.036	0.029	19.5	0.036	0.032	11.1	0.036	0.034	5.55
N (kg/h)	0.824	0.832	-0.97	0.800	0.818	-2.25	0.776	0.795	-2.44

*Relative error: [(Input-Output)/Input] *100%*

4.8. Summary

The effect of temperature and ER on the gasification behaviour of PL was experimentally studied in a lab-scale fluidised bed reactor. Gas yield, lower calorific value (LCV) and cold gas efficiency (CGE) showed an upward trend with increasing temperature from 700 ºC to 750 ºC. Although the LCV of 4.2 MJ/m^3 is low, if the presence of tar in the gas stream is considered, represented as naphthalene, the value rises to 5.8 MJ/Nm^3, a fact that is useful if the product gas is destined directly for combustion without prior cleaning. Due to the high ash content of PL comprising of inorganic components characterised by low melting temperatures, agglomeration occurred at a temperature as low as 750 °C and ER 0.25. However, it was demonstrated that blending poultry litter with beech wood can prevent agglomeration occurring at 750 °C. Nevertheless, when the temperature increased at 800 °C, again agglomeration interrupted the smooth operation of the gasifier. Total GC-detectable tar yield decreased with temperature (from 5.6 $g_{tar}/kg_{feedstock\text{-}daf}$ at 700 ºC to 4.25 $g_{tar}/kg_{feedstock\text{-}daf}$ at 750 ºC). For the temperature range tested, secondary tar was the dominant category among the tar groups consisting of oxygen-containing phenolic compounds, substituted one-ring aromatics and nitrogen-containing hydrocarbons.

ER had a negative effect on LCV, whereas it enhanced CCE. The highest LCV (4.96 MJ/Nm^3) and CCE (91.6%) were reported during BW gasification. Tar yields are affected by the fuel type and decreased with ER. In the cases of PL and PL/BW, significant amounts of nitrogen-containing tar compounds were identified due to higher nitrogen content in PL compared to BW.

As expected, total GC-detectable tar yield of PL was lower compared to BW, due to both the low content of lignin in PL and the presence of inorganic compounds which act as tar reduction catalysts.

5. Modelling and techno-economic analysis of a combined heat and power (CHP) plant running on poultry litter

In the context of energy valorisation via thermochemical conversion of animal waste, this chapter includes the theoretical analysis of a combined heat and power (CHP) system based on combustion of poultry litter (PL). As discussed in the previous chapters, combustion is the most commercial technology with a number of large-scale plants running on poultry litter installed during the last decades. On the contrary, to the best of the author's knowledge, there aren't any gasification plants running on poultry litter so far. Combustion systems but on a smaller scale (farm level) are also gaining momentum nowadays, aiming to help the farm owners achieve energy security, whilst avoiding the costs associated to PL disposal.

The study builds partly on real data retrieved from a poultry farm that installed a combustion boiler in one of its facilities, while the rest of the data and assumptions have been obtained from the open literature. Two different prime movers have been investigated; a screw expander currently installed in the farm and an Organic Rankine Cycle (ORC) system. Currently, ORC commercial applications have grown substantially over the last decades, reaching a total installed capacity of 2600 MW, whilst 750 MW were under construction, in July 2016 [153]. On the contrary, other technologies that could act as competitors to ORC (Kalina cycle, trilateral flash cycle, etc.), have still very limited market share. In particular, there are very few systems installed worldwide, based on Kalina technology. Some important reasons explaining the few existing applications are the complex layout of plants including mixers and separators, the larger heat surface areas needed, as well as the high pressures in the evaporator (e.g. 100 bar), which necessitates the use of high pressure resistant materials [154,155]. In regard to the trilateral flash cycle (TFC), currently, there are no reported installations of TFC reported in the open literature. The system is in the early development stage and the research is concentrated on the design of an efficient expander, which will handle efficiently the two phase operating fluid [156].

For convenience, the steam boiler coupled to a screw expander will be referred as system 1, while the thermal oil boiler coupled to ORC as system 2. The CHP models have been developed in Aspen Plus ™ simulator and a detailed description is provided in the following sections.

The poultry farm is located in Oxfordshire, England, and it consists of eleven sheds with a total capacity of 462,000 broilers. Day old broilers are introduced in pre-warmed poultry sheds (34 °C), and they are raised there for six weeks. Afterwards, they are transported to processing plants where

they are converted into meet products. The accumulated poultry manure is removed from the sheds and stored under negative pressure to avoid the release of odours and greenhouse gases to the atmosphere [157]. The sheds are being washed and disinfected for a period of 5-7 days before the next batch of broilers is introduced, resulting in approximately 7.5 production cycles/year. In the past, boilers running on propane were utilised in order to cover the heating demand, while electricity was bought from the grid. However, due to increased fuel costs and environmental concerns regarding poultry litter disposal, the farm owners decided to switch to boilers running on poultry litter which is available in abundance in the farm.

5.1. Description of steam boiler coupled with screw expander

Figure 5.1 provides a schematic description of the CHP system based on steam boiler and screw expander technologies. Poultry litter is inserted in a grate fired biomass boiler where it is combusted, resulting in the production of heat. The heat from combustion converts water circulating within the boiler tubes into saturated steam, which is supplied downstream to an expansion machine (screw expander) connected to a generator for the production of electricity. Exiting the screw expander, steam is introduced in a condenser where it turns into water, by rejecting heat to a water stream which circulates in a closed loop, transferring the required energy to heat-up the poultry sheds. Water liquid exiting the condenser is further pumped to the required high pressure before entering the boiler, and the cycle is repeated. Exhaust gases exiting the boiler are further cooled producing extra energy to be utilised onsite. Furthermore, a fraction of the cooled exhaust gases is recirculated back to the boiler in order to maintain the operating temperature at the desired level.

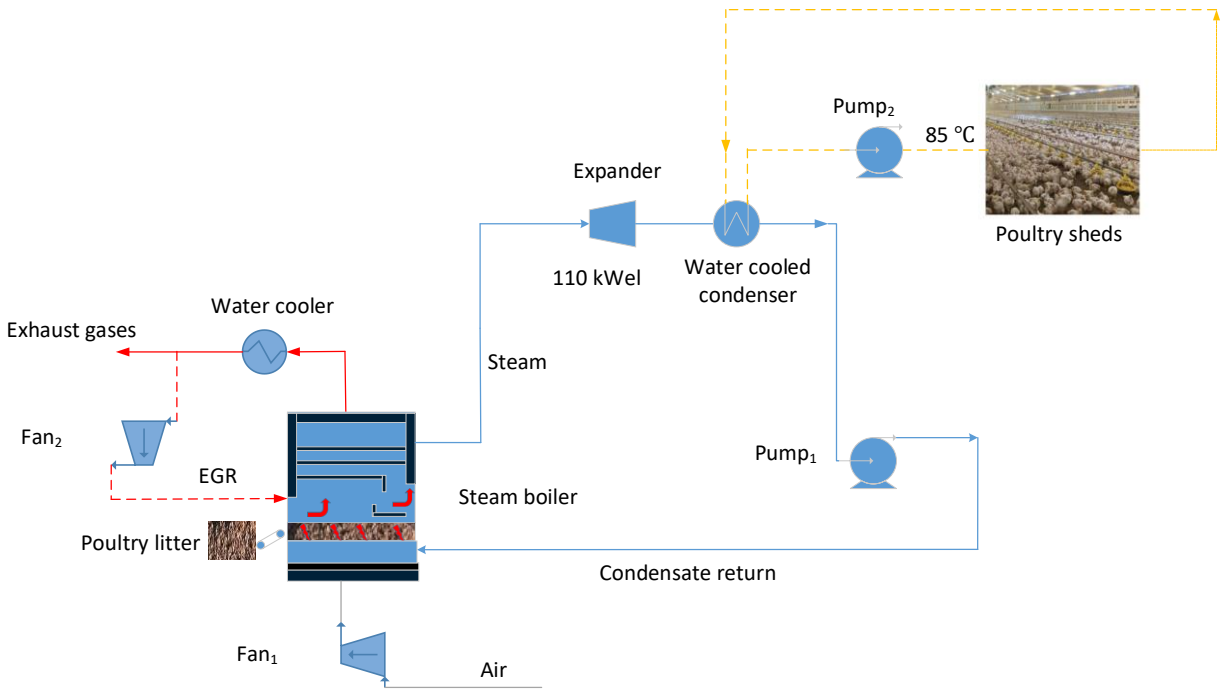

Figure 5.1: Schematic overview of the CHP plant based on steam boiler and screw expander

5.2. Modelling of steam boiler coupled with screw expander in Aspen plus

Aspen Plus has been widely used in the modelling of complex steady state processes in the fields of chemical engineering and in the oil industry respectively. It consists of several building models such as fans, heat exchangers and reactors where most industry processes can be simulated. Furthermore, it has a large property databank containing information about thermophysical properties of different chemical substances and mixtures.

In the current study, PL fuel and ash are considered as unconventional components since they are not included in the database of Aspen plus. Therefore, property models HCOALGEN and DCOALLIGT are being selected for the determination of enthalpy, specific heat capacity, and density of the unconventional components based on their ultimate and proximate analysis.

In Figure 5.2 the model development of system 1 (Steam boiler coupled with screw expander is presented. Fuel PL (stream PL) is introduced in RYIELD reactor (Block: DECOMPO) which converts PL into a conventional component based on its ultimate and proximate analysis. Afterwards PL enters the furnace of the steam boiler simulated by an RGIBBS reactor (Block: COMBUST), where it is combusted producing heat at the specified operating temperature (1273 Kelvin). The operating principle of RGIBBS reactor is based on the minimisation of the Gibbs free

energy which gives the composition of the produced gas free of ash content (stream: EXGASES1). Air needed for the combustion process is supplied by a compressor (Block: AIRCC). Exhaust gases pass through two heat exchangers, the economiser (Block: ECON) and the evaporator (Block: EVAP) respectively, where heat is transferred to liquid water in order to be converted into saturated steam. Exhaust gases (stream: TOCOOL) are further cooled at 150 °C in another heat exchanger (Block: COOL) producing hot water at 50 °C to be used onsite. Part of the exhaust gases are circulated back to the furnace, to control the operating temperature at the desired level (stream: EGROUT). Saturated steam (Stream: TOEXPAND) enters the expander (Block: Expander) where it is expanded producing 110 kW gross electrical output. Exiting the expander, it is condensed (Block: COND) and recirculated back to the boiler (stream CONDOUT), while the heat rejected produces water at 85 °C supplied to cover the heating demand in the poultry sheds (Stream: TOSHEDS).

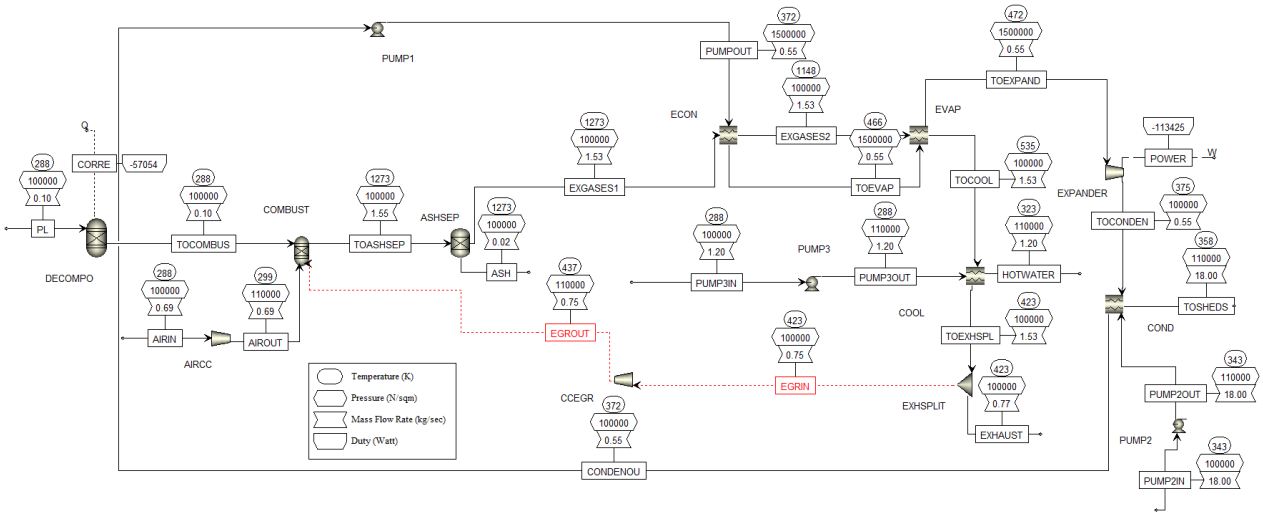

Figure 5.2: Schematic overview of system 1 model developed in Aspen plus

The input model parameters, along with the needed assumptions are presented in Table 5.1. The steam boiler's capacity of 1765 kW_{th} and its efficiency have been derived from the actual poultry farm's specifications [157,158]. Based on the boiler capacity and the LCV of PL (taken from Chapter 3), the mass flow of PL equals 0.1 kg/sec and is used as input to the model (see equation 5.1). Similarly, the mass flow of steam is determined in order to meet the design gross electrical output of 110 kW. Thermal output of the boiler is calculated as shown in equation 5.2, taking into account the mass flow of steam and the energy content of saturated steam at 15 bars exiting the

boiler. Combining the results of equations 5.1 and 5.2, the efficiency of the boiler can be calculated (see equation 5.3).

$$Thermal\ input\ (kW) = \dot{m}_{PL} * LCV_{PL} \tag{5.1}$$

$$Thermal\ output\ (kW) = \dot{m}_{steam} * specific\ enthalpy_{Steam} \tag{5.2}$$

$$n_{Boiler} = \frac{Thermal\ output}{Thermal\ input} \tag{5.3}$$

The operating temperature of grate combustion systems typically range between 850-1200 °C [32]. In the present study, the operating temperature of 1000 °C is chosen, derived from two real biomass combustion plants equipped with grate furnaces, located in Germany and Poland respectively [159,160]. Exhaust gas recirculation (EGR) is applied in order to control the operating temperature at the desired level of 1000 °C. Apart from controlling the temperature, exhaust gas recirculation (EGR) is known to be as one of the oldest and effective primary measures regarding NO_x emissions reduction, by reducing flame temperatures and overall excess air [161,162]. The percentage of oxygen in the exhaust gas stream is set to 7%, in order to comply with the European regulations demanding at least 6% oxygen concentration in the exhaust gases [163]. Exhaust gases are cooled down to a temperature of 150 °C in order to avoid condensation of any of the gaseous compounds that may lead to corrosion on the pipes [154]. The design specifications of the expander have been taken from the actual machine being installed in the poultry farm, with an expansion ratio of 15 bar and a gross electrical output of 110 kW [158]. Typical values regarding the isentropic efficiencies of the fans and pumps have been taken from [164,165]. The generator efficiency calculated as the ratio of the produced electrical output to the mechanical input supplied to the generator is taken from Prando et al. [164]. The required temperature of hot water transferring the heat to the poultry sheds, is set to 85 °C [166].

Table 5.1: Input parameters and assumptions of system 1

Boiler capacity (kW_{th})	1765
LCV of PL on a dry basis (kJ/kg)	17210
Mass flow of PL (kg/sec)	0.1
Combustion temperature (°C)	1000
FGR ratio (-)	0.49
Residual oxygen in the exhaust gases (vol. %)	7
Cooling temperature of exhaust gases (°C)	150
Steam mass flow (kg/sec)	0.55
Steam inlet temperature to the expander (°C)	198.5
Steam inlet pressure to the expander (bar)	15
Expansion ratio	15
Minimum DT in the heat exchangers (°C)	5
Generator efficiency	0.97
Gross electrical output (kW)	110
Pump efficiency	0.7
Fan efficiency	0.75
Desired water temperature in the poultry sheds (°C)	85

The calculation steps for the electrical efficiency and the total efficiency of the CHP system are given in equations 5.4-5.6, respectively.

$$n_{el} = \frac{\dot{W}_{Net}}{\dot{m}_{PL} * LCV_{PL}} \tag{5.4}$$

$$\dot{W}_{net} = \dot{W}_{Gross} - \dot{W}_{Fans} - \dot{W}_{Pumps} \tag{5.5}$$

$$n_{CHP} = \frac{\dot{W}_{net} + \dot{Q}_{condenser} + \dot{Q}_{exhaust}}{\dot{m}_{PL} * LCV_{PL}} \tag{5.6}$$

Where,

- $\dot{W}_{Gross}$ is the gross electrical output of the screw expander (kW)
- $\dot{W}_{Fans}$ is the work required for the operation of the fans (kW)
- $\dot{W}_{Pumps}$ stands for the work required for the operation of the pumps (kW)
- $\dot{Q}_{condenser}$ refers to the heat duty of the condenser (kW)
- $\dot{Q}_{exhaust}$ is the heat duty from cooling the exhaust gases at 150 °C
- $\dot{m}_{PL}$ represents the mass flow of the fuel poultry litter entering the boiler (kg/sec)
- LCV_{PL} represents the LCV of PL on a dry basis (kJ/kg)

5.3. Simulation results of steam boiler coupled with screw expander

Table 5.2 summarises the results derived from the simulation of the CHP system in Aspen plus™ software. As can be observed, net electrical power output amounts to 89 kW, by deducting from gross electrical output the electrical consumption required for the operation of the fans and pumps. Pumps require a very small electrical input (<2 kW), therefore electrical consumption is mainly attributed to the operation of the fans required for the introduction of combustion air in the biomass boiler and the exhaust gases recirculation. The electrical efficiency of the screw expander has a low value of 5%, due to the limited electrical output compared to the thermal input in the plant. A comparable electrical efficiency of 6.7% has been reported for a similar system installed in a distillery [167]. The heat duty in the condenser is quite significant, reaching the value of ~1.2 MW. In poultry farms, where there is a substantial heating demand, any system to be installed will be sized accordingly to meet the heating demand rather than the electrical needs, which can be either covered from the grid or from a similar system discussed in the current analysis. Cooling the exhaust gases from a temperature of 300 °C when exiting the boiler, to a temperature of 150 °C, can provide additional energy to cover the farm's energy needs. In particular, the heat duty of 187.5 kW can either be utilised onsite to satisfy hot water and/or space heating needs, or as an addition to the energy provided by the condenser to heat-up the poultry sheds. In the former case,

hot water needs to reach a temperature of 50-60 °C, typically required in hot water/space heating applications, whereas in the latter case the water temperature should reach the specified design temperature of 85 °C. The CHP efficiency calculated based on equation 5.6 described above, reaches ~87%, revealing the significant benefits that arise when the installation of CHP systems is a preferable option compared to plants with only one output (electricity or heat).

Table 5.2: Performance indicators of the CHP system based on steam boiler -screw expander

Efficiency of steam boiler (n_{Boiler}%)	77.5
Gross electrical output (kW)	110
Net Electrical output (kW)	89
Isentropic efficiency of the expander (-)	~ 50%
Heat duty in the condenser (kW)	1253
Heat duty from cooling the exhaust gases (kW)	187.5
Electrical efficiency of CHP system (n_{el} %)	5
CHP system efficiency (%)	87

5.4. Description of thermal oil boiler coupled with ORC

In Figure 5.3 the schematic overview of system 2 is illustrated. The operating conditions of the combustion section are identical with system 1 and thus they will not be repeated. In regard to the ORC cycle, the principle of operation and the components are similar to the traditional Rankine cycle, which is utilized in large scale stationary power generation. More specifically, in the evaporator, the heat source transfers the necessary energy in order the high-pressure operating fluid to turn into saturated vapour. The heat transfer takes place either direct, or through a secondary loop, which usually consists of thermal oil. The latter case is applied when ORC uses high temperature heat sources (>350 °C) in order to allow better process control and to prevent overheating in the evaporator. Afterwards, the saturated vapour enters an expansion machine connected to a generator, producing electrical power. Exiting the turbine, the low-pressure saturated gas passes through a condenser, where it is transformed into saturated liquid which then enters the pump in order the cycle to be repeated. Heat rejected during the condensation process, is utilised to produce water for heating up the poultry sheds.

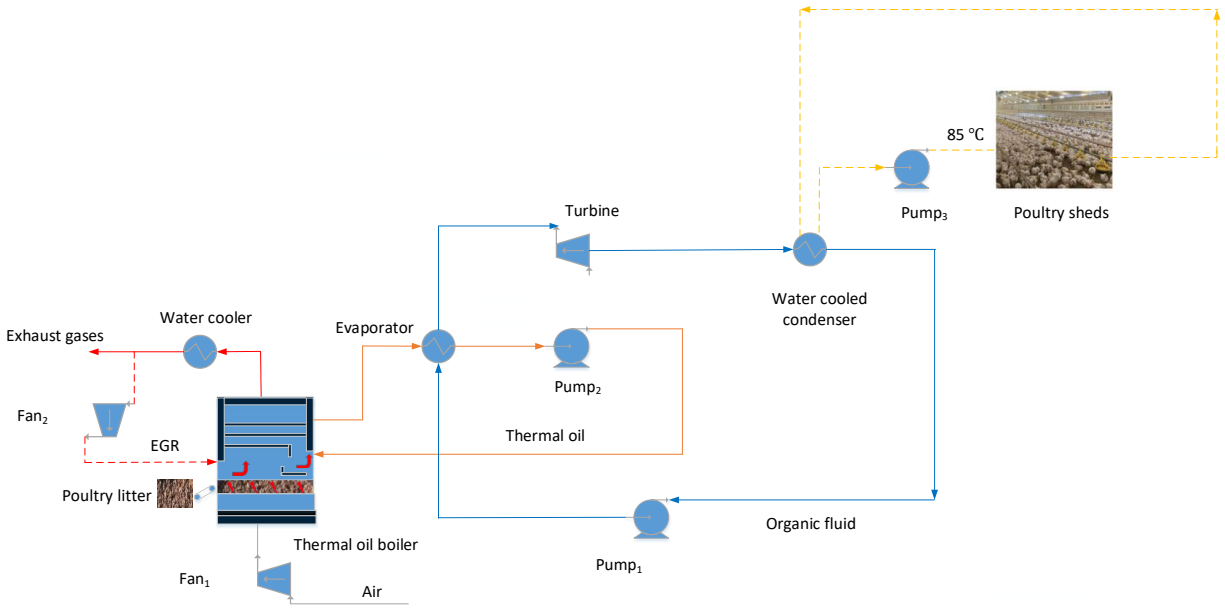

Figure 5.3: Schematic overview of the CHP plant based on biomass boiler and ORC

5.5. Modelling of thermal oil boiler coupled with ORC in Aspen plus

Fig 5.4 presents the model of system 2 (thermal oil boiler coupled with ORC) developed in Aspen plus. The combustion section is similar to system 1, except that the produced exhaust gases (Stream: EXGASES1) warm up the thermal oil re-circulating inside the boiler from 513 K to 563 K. The heat transfer process is modelled by a heat exchanger (Block: OIL). Thereafter, thermal oil is introduced in the evaporator of the ORC cycle (Block: EVAP), where the liquid organic fluid MDM (Stream: PUMP1OUT) is converted into gas which is further expanded in the ORC turbine, producing electrical power. Water needed for the heating of poultry sheds (Stream: TOSHEDS) is produced by the heat rejected during the condensation of MDM (Block: COND), which is then recycled back to the evaporator (Stream: CONDOUT). Additionally, hot water is produced via cooling the exhaust gases at 150 °C (Stream: HOTWATER).

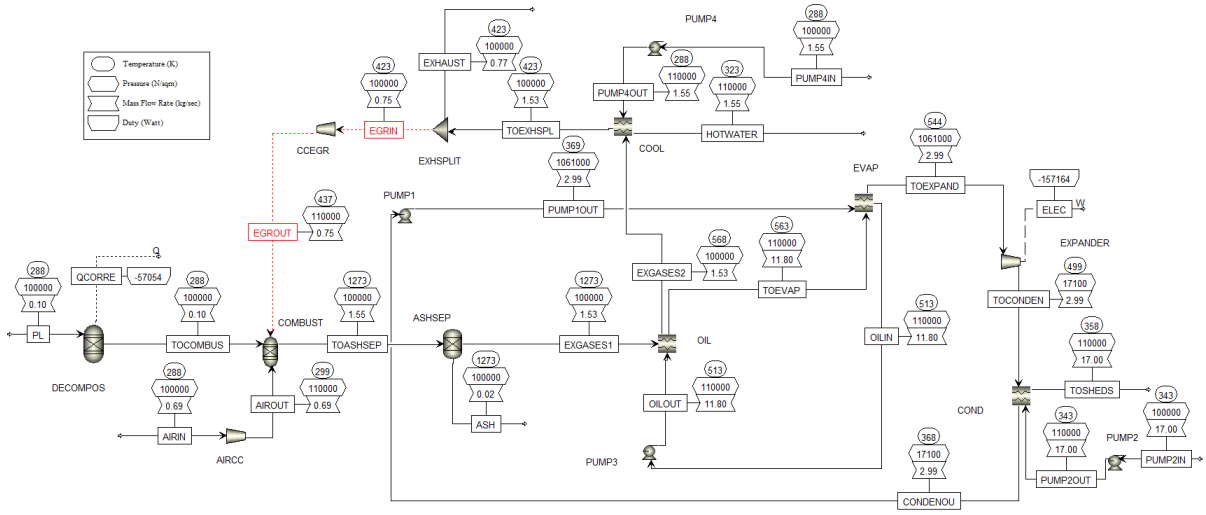

Figure 5.4: Schematic overview of system 2 model developed in Aspen plus

Table 5.3 presents the input parameters and assumptions needed to build the ORC model in Aspen plus simulator. The selection of the appropriate organic fluid plays a vital role in the ORC performance and the respective electrical output. Although a lot of research has been devoted to the comparison of various organic fluids in order to optimize the operation of ORC, it is generally admitted that there is no optimal organic fluid satisfying all the different operating conditions of ORC [154]. In the present work fluid MDM (octamethyltrisiloxane) was chosen since it has been used in real biomass combustion plants coupled with ORC technology [164,168]. The particular organic fluid belongs to the family of siloxanes, characterised by low toxicity and flammability, good material compatibility, and thermal stability as well. Furthermore, its critical pressure and temperature are 14.1 bars and 291°C respectively, making it suitable for high temperature applications. Therminol-55 was used as heat transfer medium [169], whereas the inlet and outlet conditions of the thermal oil from the boiler have been retrieved from two biomass plants coupled with ORC, located in Germany and Poland respectively [159]. The pressure levels of the ORC cycle and the isentropic efficiency of the turbine have been adopted from a biomass plant coupled with ORC using MDM as organic fluid, which is located in south Italy [164]. The efficiencies of the different components (pumps, fans, generators) and the desired water temperature supplied to the poultry sheds, are set equal to system 1 for comparison purposes.

Table 5.3: Input parameters and assumptions of system 2

Inlet temperature of thermal oil (°C)	240
Outlet temperature of thermal oil (°C)	290
High pressure of ORC (bar)	10.6
Low pressure of ORC (bar)	0.17
Turbine isentropic efficiency	0.8
Fan efficiency	0.75
Pump efficiency	0.7
Electrical generator efficiency	0.97
Minimum DT in the heat exchangers (°C)	5
Desired water temperature in the poultry sheds (°C)	85

5.6. Simulation results of thermal oil boiler coupled with ORC

Table 5.4 summarises the performance indicators resulting from the simulation of system 2. The mass flows of thermal oil and MDM have been calculated based on the energy balances performed in the boiler and the evaporator of the ORC respectively. Net electrical output has been calculated based on eq. 5.5 considering the electrical consumption needed for the operation of fans and pumps. The electrical efficiency of the ORC is calculated as the ratio between the net electrical output and the thermal input to the evaporator transferred via the thermal oil loop. Generally, the efficiency of the ORC alone ranges between 6-17%, with the upper limit referring to a plant with electrical output of 1 MW [164]. The efficiency of the overall CHP system reaches 87%, including the heat rejected in the condenser and the heat derived from cooling the exhausts at 150 °C (see eq. 5.6).

Table 5.4: Performance indicators of the CHP system based on thermal oil boiler-ORC

Thermal oil boiler efficiency (%)	74.3
Mass flow of organic fluid MDM (kg/sec)	3
Mass flow of thermal oil (kg/sec)	12
Gross electrical output (kW)	157.4
Net Electrical output of ORC (kW)	126.5
Net electrical efficiency of ORC (%)	9.65
Heat duty in the condenser (kW)	1157
Heat from cooling the exhausts (kW)	243
CHP system efficiency (%)	87

5.7. Economic evaluation

A comprehensive analysis of an energy system, apart from the thermal design, should include also the economic aspects in order to realise the potential benefits that arise from the installation. However, the cost engineering techniques applied from the research community to estimate total capital investments (TCI) of energy systems, often display limited accuracy. The most common are the cost capacity ratio and the factorial estimation techniques. In the former, the cost of a plant is calculated based on known cost and capacity of a similar existing plant by applying an exponential factor, which is typically close to 0.6 for the chemical industry. This method requires low amount of data and its accuracy is considered rather low. In the latter method, purchased cost of the major plant components are multiplied by a bare module factor in order to obtain the TCI. This factor considers construction material, operating pressures, as well as direct and indirect project expenses. It should be mentioned that many of the cost correlations are based on data that are at least 10 years old and thus may be considered outdated. Accuracies ranging between -20% and +30% should be excepted when applying the factorial method [153].

In the present study, in order to eliminate the uncertainty in cost estimation as much as possible, the assessment was performed on the basis of personal communications or by using cost figures of real installations available in the open literature. In particular, the installation and the annual operation and maintenance costs of system 1 have been retrieved from a similar system installed in a nursery. The reference system consists of 1765 kW_{th} steam output producing 130 kW_{el} gross output in a screw expander. Although this system displays slightly higher boiler thermal output and

gross electrical output compared to system 1 investigated in the current study, it is assumed that the economic figures can be representative, and thus they are adopted in the cost analysis of the system 1 [170]. Regarding system 2, the economic figures have been considered separately. In particular, the cost of the ORC system has been determined via personal communication with an experienced European manufacturer of such systems on 2nd of June, 2020.The suggested purchased cost considered was 2500 euros/kWel multiplied by a factor of 1.5 to account also for the installation costs. Additionally, the cost of the biomass boiler alone was derived from a report produced on behalf of Netherlands Environmental Assessment Agency. The aim of the report was to address the different subsidies required depending on the renewable energy source being utilised in Netherlands. The figure of 400 euros/kW$_{th}$ was recommended including installation, for a grate boiler with thermal output less than 5 MW$_{th}$ equipped with exhaust gas cleaning [171].

Typical economic factors and indices needed in order to perform the economic evaluation of the two systems are given in Table 5.5. The projected lifetime of the systems is set to 20 years. The prices for electricity and gas refer to the ones purchased from medium size industrial consumers in the UK based on statistical data from the department for Business, Energy, and Industrial Strategy (BEIS) of the UK [172]. Inflation rate is the percentage increase in the level of prices over a time period, and the value of 1.8% was chosen for the economic analysis [173] Discount rate of 8% has been assumed [174], whereas the financial depreciation is considered to be linear over the plant's lifetime. Operation and maintenance (O&M) costs are usually taken as a percentage of the TCI. However, since the O&M costs of system 1, have been set equal to the ones of the real plant (nursery), the same amount was considered for system 2. Furthermore, it is assumed that there are constant electricity and heating demands throughout the year.

Table 5.5: Economic factors and indices for the economic evaluation

Construction time (years)	1
Plant lifetime (years)	20
Price of electricity (£/kWh)	0.127
Price of natural gas (£/kWh)	0.026
Inflation (%)	1.8
Discount rate (%)	8
Financial depreciation (-)	Linear
Operational & maintenance costs (£/year)	40000
Electricity demand (operating hours)	8760
Heating demand (operating hours)	8760

Table 5.6 presents the economic feasibility of the project by considering two financial tools widely employed to assess the profitability of a project, the Net Present Value (NPV) and the Payback Period (PBP). The former index takes the time value of money into account, whereas the latter indicates the time required to recover the cost of an investment. Electricity and heating generated from both systems are calculated based on the net electrical output and the heat recovered from both systems multiplied by the hours where there is a demand for electricity and heating respectively. The associated cost savings result from the produced energy (electricity and heating) and the market price for medium size industrial sites as described above. Payback period and NPV results reveal the economic feasibility of both systems. The earnings from energy savings are quite high according to NPV for a lifetime of 20 years, whereas the PBP is less than 5 years, which is regarded as satisfactory for return of investment. It should be highlighted that incentives such as the Renewable Heating Incentive (RHI) the feed-in tariffs widely employed the last decade, are currently or have already been phased out, and thus incentives are not included in the cost calculations [175].

Table 5.6: Economic feasibility of the system

Outputs/Systems	**Steam boiler-screw expander**	**Thermal oil boiler-ORC**
Electricity generated (kWh/year)	773500	1112520
Heating generated (kWh/year)	12719520	11201500
Electricity cost savings (£/year)	98622	141846
Heating cost savings (£/year)	287461	253154
Total installation costs (£)	1300000	968625
Operation & Maintenance (£/year)	40000	40000
Depreciation costs (£/year)	65000	48431
NPV (£)	1900484	2515685
PBP (years)	4.4	3.1

5.8. Summary

In this chapter, the theoretical analysis of combined heat and power (CHP) systems based on combustion of poultry litter (PL) has been performed. Two different systems have been investigated, a steam boiler coupled with a screw expander (system 1) and a thermal oil boiler coupled to an Organic Rankine Cycle (ORC), referred as system 2. The simulation results revealed that for the same thermal capacity of the boilers (1750 kW_{th}), system 1 and 2 demonstrated electrical outputs of 110 kW and 157 kW respectively. Additionally, the heating load in the condenser acquired similar values for both systems, around 1.2 MW. Furthermore, the CHP efficiency (n_{CHP}) amounted 87%, taking into account also the heat load resulting from cooling the exhaust gases at 150 °C. An assessment regarding the economic feasibility of both systems has also been performed, by applying two widely used financial tools, namely Net Present Value (NPV) and Payback Period (PBP). System 1 illustrated a NPV equal to £1900484 with a PBP of 4.4 years, whereas the respective values for system 2 were £2515685 and 3.1 years.

6. Conclusions and recommendations for further work

The continuous increase in the amount of poultry litter (PL) generated as a by-product from animal farming activities, necessitates the development of a sustainable solution regarding its disposal. In this context, producing energy from animal waste can be a viable solution with significant environmental and economic benefits. In particular, utilisation of poultry litter as a fuel for energy generation onsite, should contribute to the coverage of the energy demand of the farm without the need for fossil fuels, decreasing in this way the carbon footprint during the operation of the farm. Landfilling considered as the least preferred option in terms of a sustainable waste management is also avoided. Regarding the economic benefits, farm owners can avoid the disposal costs, while at the same time they are able to decrease or even eliminate their dependence on energy market prices.

Two different pathways can be exploited in regard to the conversion of PL into energy, namely biochemical and thermochemical routes. The present thesis focused on the thermochemical conversion of PL, by investigating two technologies with different level of matureness, that being combustion and gasification. Both experimental and modelling studies were conducted, in order to assess the potential of poultry litter as a fuel for energy production. The experimental work was performed in two different locations within the framework of BRISK2 (Biofuels Research Infrastructure). Experiments on combustion of poultry litter were conducted in BEST (Bioenergy and Sustainable Technologies) located in Graz, Austria. Gasification experiments were performed at the Energy Research Centre of the Netherlands (ECN part of TNO). Building of thermodynamic models was realised in Aspen Plus software, using as inputs data from a poultry farm in the UK and from the open literature. The details of each study are summarised below.

- Experiments on combustion technology: A lab scale batch reactor designed to simulate thermal decomposition of biomass under fixed-bed conditions was employed. PL was tested along with a mixture of poultry litter with woodchips (PL/WC) and softwood pellets (SP) on its own, for comparison purposes. Test results included thermal decomposition of fuels over time, evolution of N gaseous species, release of ash forming elements and subsequent estimation of aerosol emissions, for the three different fuels.

- Experiments on gasification technology: A lab scale bubbling fluidised bed reactor was employed for the gasification experiments. Three different fuels were tested, namely PL, blend of PL with beechwood (PL/BW) and BW on its own, for comparison purposes. The

obtained results provided useful insights pertaining to the effect of process parameters (air equivalence ratio and temperature) on the gasification performance, the tar evolution and the presence of agglomeration phenomenon.

- Modelling in Aspen Plus software: Combined heat and power (CHP) models were developed based on combustion of PL. Two different prime movers were employed, namely a steam screw expander and an Organic Rankine Cycle (ORC). The obtained results provided details on the energetic performance of the two CHP systems in terms of electrical and heating outputs. An economic analysis was also conducted to investigate the feasibility of both systems.

6.1. Conclusions

In this particular section, the major findings and conclusions of the present thesis are provided.

In chapter two, a thorough literature review was conducted on the different technologies related to treatment and energy recovery from PL, regarding the positive characteristics and limitations of each technology. Firstly, a number of research findings relevant to biochemical conversion of PL via anaerobic digestion revealed the growing interest in the particular technology and the use of PL as potential input. However, this technology is mostly suitable for high degradable biomass characterised by increased levels of moisture as well. PL is a feedstock containing high amounts of solids, while it also presents variable moisture content, factors implying that it might not be suitable for anaerobic digestion process. Additionally, most of the research work found in the literature highlighted the need for an additional fuel input in the digester that will be mixed with PL in order to balance the C/N (carbon/nitrogen) ratio, which is a crucial factor in terms of biogas yield. On the contrary, the research findings suggested that thermochemical conversion might be a more suitable option for PL treatment and energy recovery. Three different technologies exist within the thermochemical conversion framework, that being combustion, gasification, and pyrolysis. Combustion is the most commercialised among the technologies, with a number of existing large-scale plants running on PL installed in the last decades. Regarding gasification and pyrolysis, the limited research work found in literature, focused on experimental tests aiming to assess the suitability of PL as a fuel input to those technologies.

In chapter three, the combustion behaviour of PL, blend of PL/WC (woodchips) and softwood pellets (SP), was experimentally studied in a discontinuous lab-scale fixed bed reactor. After the completion of the test runs data was gathered related to the thermal decomposition behaviour of the three fuels, the release of N gaseous species and aerosol forming elements, as well as the potential of aerosol emissions and ash melting behaviour. Ammonia (NH_3) showed the highest concentration among the N (nitrogen) gaseous species in cases of PL and blend combustion. On the contrary, hydrogen cyanide (HCN) was the most abundant compound during SP combustion. N initially bound with the SP showed an almost complete conversion into N gaseous species, whereas the corresponding conversion for PL and the blend amounted around 50% and 40% respectively. High release rates of chlorine (Cl) and sulphur (S) were observed. The release rates of alkali metals K (potassium) and Na (sodium) for all tested fuels ranged between 15-50%. Overall, during combustion, easily volatile elements such as Cl show the highest release rates (>80%), while K and Na are considered semi-volatile elements showing usually moderate release rates as in the present thesis. The most significant factor affecting the release rate of K is the fuel bed temperature. In terms of estimated aerosol emissions, the maximum quantity was calculated during PL combustion reaching the value of 2806 mg/Nm^3 (dry flue gas, 13 vol% O_2), followed by 2584 mg/Nm^3 (dry flue gas, 13 vol% O_2) in the case of blend (PL/BW). Negligible quantities of aerosol emissions were estimated from SP combustion. Finally, based on the fuel index 2S/Cl related to corrosion, PL and the blend show higher risk compared to SP.

In conclusion, the performed evaluation of the tested fuels revealed the associated challenges of PL during combustion. Initially, presence of nitrogen in high concentrations in the PL composition, implies that primary measures may not be sufficient, and therefore secondary measures (Selective Non-Catalytic Reduction) will be needed for effective control of NO_x emissions. Moreover, increased concentration of aerosol emissions is closely related to ash deposition and corrosion in the heat exchangers, and thus proper dust cleaning equipment will be essential, as well as a careful selection of materials resilient to corrosion. Ash melting is another decisive factor regarding the efficient operation of a plant running on PL. In this particular study ash melting temperatures of PL and blend are estimated to be high and thus it wouldn’t be expected to create any significant problem associated to ash melting. However, given the fact that composition of PL varies considerably, a pre-evaluation of the ash melting temperature is recommended prior to utilisation. Possible low ash melting temperatures will lead to lower operating temperatures in the combustion chamber, a fact that could affect considerably the efficiency of the combustion process.

In chapter four, the effect of temperature and equivalence ratio (ER) on the gasification behaviour of PL was experimentally studied in a lab-scale fluidised bed reactor. Gas yield, lower calorific value (LCV), and cold gas efficiency (CGE) showed an upward trend with increasing temperature from 700 ºC to 750 ºC. Although the LCV of 4.2 MJ/m^3 is low, if the presence of tar in the gas stream is taken into consideration, represented as naphthalene, the value rises to 5.8 MJ/Nm^3, a fact that is useful if the product gas is destined directly for combustion without prior cleaning. Due to the high ash content of PL comprising of inorganic components characterised by low melting temperatures, agglomeration occurred at a temperature of around 750 °C and ER 0.25. Total GC-detectable (gas chromatography) tar yield was found to be lower compared to lignocellulosic biomass, due to the low content of lignin in PL and the presence of inorganic compounds which act as tar reduction catalysts. Total GC-detectable tar yield decreased with increasing temperature (from 5.6 $gtar/kg_{feedstock\text{-}daf}$ at 700 ºC to 4.25 $gtar/kg_{feedstock\text{-}daf}$ at 750 ºC). For the temperature range tested, secondary tar was the dominant category among the tar groups consisting of oxygen-containing phenolic compounds, substituted one-ring aromatics and nitrogen-containing hydrocarbons. The effect of ER on the gasification performance when keeping the temperature fixed at 750 ºC was also investigated. Apart from poultry litter, a blend of poultry with beech wood (PL/BW) and beech wood (BW) on its own were also studied for comparison purposes. ER had a negative effect on LCV, whereas it enhanced CCE. The highest LCV (4.96 MJ/Nm^3) and CCE (91.6%) were reported while gasifying the BW. Tar yields are affected by the fuel type and decreased with ER. As expected, due to the higher lignin content compared to the other two fuels, BW displayed the highest amount of GC-detectable tar at the lowest tested ER (7.52 $gtar/kg_{feedstock\text{-}daf}$). In the cases of PL and PL/BW, significant amounts of nitrogen-containing tar compounds were identified due to higher nitrogen content in PL compared to BW. Finally, it was demonstrated that blending poultry litter with beech wood prevented agglomeration occurring at 750 °C, but when the temperature increased to 800 °C, again agglomeration interrupted the smooth operation of the gasifier.

It can be concluded that despite the fact that the PL is considered a low-quality fuel, its energy content shows a potential as alternative resource for onsite (farm) energy generation. Additionally, the fact that the amount of generated tar is lower compared to traditional biomass, implies that gas cleaning requirements will be smaller, resulting in smaller sizes of equipment and improved economics. Nevertheless, increasing the operating temperature to improve the gasification performance while avoiding agglomeration conditions are the two crucial aspects that need to be further addressed, prior to the further utilisation of PL as a fuel in gasification processes.

In chapter five, two theoretical CHP models have been developed based on poultry litter combustion. The first one consists of a biomass boiler coupled with steam expander (system 1). Some input parameters regarding the modelling of system 1 have been retrieved by a real identical system installed in a farm, located in the UK. The second one (system 2) comprises of a thermal oil boiler coupled with an Organic Rankine Cycle (ORC). The thermal input to the systems was the same (0.1 kg/sec of PL) for comparison purposes. The design gross electrical output of system 1 was 110 kW_{el} resulting in electrical efficiency of 5%. Moreover, the heating generated in the condenser amounted ~1.25 MW_{th}. System 2 produced 157 kW_{th} gross electrical output, and the ORC efficiency was 9.7%. The heating generated in the condenser was ~1.15 MW_{th} for system 2. Both systems displayed CHP efficiency of 87%, considering also the useful heat derived from cooling the exhaust gases at 150 °C. A conducted economic analysis revealed the profitability of both systems in terms of Net present Value (NPV) and payback period (PBP). The former index was positive in a time framework of 20 years, acquiring the values of ~ £1.9 million for system 1 and ~ £2.5 million for system 2. The time periods for recovering the investments, were less than five years for both systems.

6.2. Recommendations for further work

The present thesis investigated the thermochemical conversion of PL by performing experiments on combustion and gasification technologies. The findings revealed the advantages but also the associated challenges that need to be addressed prior to the further utilisation of PL as a fuel for distributed energy generation (on farm), for both technologies. Apart from the experimental work, a theoretical modelling study was conducted based on combustion technology coupled with two different prime movers (steam expander and ORC). The simulation results provided useful insights in terms of energy performance, while an economic analysis revealed the feasibility of both systems. However, there is still significant work that needs to be done for the optimal design of both technologies running on PL and some recommendations for future work are presented below.

- Combustion tests on the lab-scale fixed bed reactor, presented data regarding the flue gas composition above the fuel bed of a grate reactor including N gaseous species. An estimation of the aerosol emissions was also provided based on the release rate of volatile compounds contained in the fuel. However, in order to acquire the actual concentration of the flue gases exiting the boiler including NO_x and aerosol formation, experiments in a pilot-scale reactor are proposed. In this way, first a comparison can be performed between

the lab-scale and pilot scale as regards the flue gas composition above the fuel beds. Afterwards, the actual flue gas composition exiting the boiler can be determined from the pilot scale tests including the influence of secondary air injection.

- Contrary to the lab-scale reactors that operate under allothermal conditions, industrial scale gasifiers mostly operate in auto-thermal mode and the reactor temperature is mainly regulated by the ER. Therefore, modelling of the gasification process is proposed for future work in order to investigate if any of the conducted tests are close to auto-thermal conditions, which will provide the possibility to scale-up the experimental findings to an industrial gasifier level.

- Agglomeration is a major issue during gasification of fuels rich in alkali metals such as poultry PL. In this study, mixing PL with beechwood (BW) at a 50:50 mass ratio prevented agglomeration at 750 °C at all tested ERs. However, an attempt to increase the temperature to 800 °C failed due to instabilities of the reactor caused by agglomeration. Testing different mixing ratios of poultry litter with woody biomass in order to decrease the ash content in the fuel intake, or the addition of additives (e.g., dolomite) are two potential measures to counteract agglomeration, that need to be further investigated.

- A theoretical modelling study of two CHP systems running on poultry litter showed the potential benefits from installing such systems, compared to being dependent on fossil fuels. However, it is crucial to have knowledge of the actual energy demand of a real farm in order to ascertain the real energy and economic savings, and to what extent the installation of such systems can contribute to farm's energy independency. This, together with performance data from actual plant are necessary for further development of the CHP technologies.

APPENDIX

Table A1: Tar compounds in PL at 700°C/ER 0.21.

	(gtar/Nm^{3}a.r.)	(gtar/kgfeedstock-daf)	(gtar/Nm^{3}a.r.)	(gtar/kgfeedstock-daf)	(gtar/Nm^{3}a.r.)	(gtar/kgfeedstock-daf)
Total tar	4.22	10.55	4.23	10.58	4.34	10.85
Benzene	1.165	2.915	1.162	2.907	1.193	2.984
Thiophene	0.027	0.068	0.027	0.068	0.026	0.065
Pyridine	0.087	0.218	0.093	0.232	0.098	0.245
Pyrrole	0.137	0.342	0.143	0.359	0.143	0.358
Toluene	0.842	2.105	0.835	2.088	0.864	2.160
2/3/4 Methyl pyridine	0.051	0.128	0.053	0.132	0.055	0.138
Pyrazine-methyl	0.025	0.062	0.025	0.063	0.027	0.067
2/3/4 Methyl pyridine	0.010	0.026	0.012	0.029	0.009	0.024
Ethylbenzene	0.056	0.141	0.055	0.137	0.055	0.137
o/m/p Xylene	0.097	0.242	0.097	0.243	0.100	0.249
Phenylethyne	0.006	0.016	0.007	0.017	0.006	0.016
Styrene/o/m/p Xylene	0.257	0.643	0.255	0.637	0.264	0.660
Iso-dimethyl pyridine	0.004	0.010	0.004	0.011	0.005	0.012
2/3/4 Ethenyl pyridine	0.017	0.043	0.016	0.041	0.017	0.043
Benzonitrile	0.005	0.012	0.005	0.011	0.005	0.012
Phenol	0.217	0.544	0.208	0.521	0.217	0.544
o/m/p Methyl Styrene	0.010	0.024	0.010	0.026	0.010	0.025
o/m/p Methyl Styrene	0.004	0.010	0.005	0.012	0.005	0.013
Indene	0.105	0.263	0.106	0.266	0.109	0.273
o/m/p Cresol	0.046	0.115	0.045	0.113	0.047	0.118
o/m/p Cresol	0.041	0.103	0.043	0.107	0.044	0.110
Naphthalene-1,2 diydro	0.025	0.063	0.025	0.063	0.026	0.064
Naphthalene	0.143	0.358	0.147	0.368	0.152	0.381
Quinoline	0.005	0.012	0.005	0.013	0.005	0.012
Isoquiolilne	0.015	0.037	0.014	0.036	0.015	0.038
2-Methyl naphthalene	0.051	0.129	0.055	0.139	0.056	0.141
Indole	0.030	0.076	0.031	0.078	0.033	0.082
1-Methyl naphthalene	0.060	0.151	0.061	0.152	0.063	0.157
Biphenyl	0.009	0.022	0.009	0.022	0.009	0.022
2-Ethenyl naphthalene	0.009	0.021	0.009	0.022	0.009	0.022
Acenaphthylene	0.021	0.052	0.022	0.054	0.020	0.050
Acenaphthene	0.004	0.009	0.003	0.009	0.004	0.010
Dibenzofuran	0.006	0.015	0.006	0.016	0.007	0.018
Fluorene	0.011	0.027	0.011	0.027	0.011	0.028
Phenanthrene	0.015	0.038	0.016	0.039	0.017	0.043
Anthracene	0.004	0.011	0.005	0.013	0.005	0.013
4h-cyclopenta(def)phenanthrene	0.002	0.006	0.002	0.006	0.003	0.007
Fluoranthrene	0.002	0.004	0.002	0.004	0.002	0.004
Pyrene	0.004	0.010	0.004	0.010	0.004	0.010
Benzo[a]anthracene	0.008	0.020	0.012	0.031	0.008	0.020

Table A2: Tar compounds in PL at 725°C/ER 0.21.

	(gtar/Nm^{3}a.r.)	(gtar/kgfeedstock-daf)	(gtar/Nm^{3}a.r.)	(gtar/kgfeedstock-daf)	(gtar/Nm^{3}a.r.)	(gtar/kgfeedstock-daf)
Total tar	3.51	9.42	3.20	8.57	4.40	11.78
Benzene	1.217	3.262	1.122	3.006	1.377	3.692
Thiophene	0.021	0.057	0.017	0.045	0.021	0.057
Pyridine	0.083	0.222	0.078	0.209	0.114	0.306
Pyrrole	0.065	0.175	0.065	0.175	0.107	0.288
Toluene	0.711	1.907	0.652	1.749	0.911	2.443
2/3/4 Methyl pyridine	0.044	0.119	0.043	0.115	0.062	0.166
Pyrazine-methyl	0.019	0.052	0.017	0.046	0.026	0.069
2/3/4 Methyl pyridine	0.002	0.005	0.002	0.005	0.001	0.004
Ethylbenzene	0.021	0.056	0.020	0.053	0.030	0.080
o/m/p Xylene	0.080	0.215	0.073	0.197	0.099	0.266
Phenylethyne	0.003	0.008	0.003	0.009	0.007	0.018
Styrene/o/m/p Xylene	0.229	0.613	0.208	0.558	0.279	0.748
Iso-dimethyl pyridine	0.001	0.004	0.001	0.004	0.003	0.007
2/3/4 Ethenyl pyridine	0.009	0.025	0.008	0.022	0.013	0.035
Benzonitrile	0.003	0.008	0.003	0.007	0.005	0.013
Phenol	0.061	0.165	0.048	0.127	0.109	0.291
o/m/p Methyl Styrene or B	0.008	0.023	0.007	0.020	0.012	0.031
o/m/p Mehyl Styrene or Be	0.004	0.011	0.004	0.011	0.006	0.015
Indene	0.092	0.247	0.084	0.226	0.122	0.327
o/m/p Cresol	0.007	0.019	0.005	0.014	0.014	0.037
o/m/p Cresol	0.006	0.016	0.005	0.014	0.008	0.022
Naphthalene-1,2 diydro	0.014	0.036	0.013	0.034	0.018	0.048
Naphthalene	0.149	0.398	0.137	0.366	0.192	0.515
Quinoline	0.004	0.009	0.004	0.011	0.003	0.009
Isoquiololilne	0.009	0.023	0.009	0.024	0.014	0.037
2-Methyl naphthalene	0.038	0.101	0.035	0.094	0.050	0.135
Indole	0.001	0.004	0.001	0.004	0.002	0.004
1-Methyl naphthalene	0.051	0.137	0.045	0.119	0.076	0.204
Biphenyl	0.006	0.016	0.005	0.014	0.009	0.025
2-Ethenyl naphthalene	0.006	0.016	0.005	0.013	0.008	0.022
Acenaphthylene	0.022	0.060	0.021	0.056	0.029	0.078
Acenaphthene	0.003	0.007	0.002	0.006	0.004	0.012
Dibenzofuran	0.004	0.010	0.004	0.009	0.005	0.014
Fluorene	0.006	0.017	0.006	0.016	0.008	0.022
Phenanthrene	0.014	0.038	0.013	0.034	0.019	0.052
Anthracene	0.003	0.008	0.002	0.006	0.004	0.012
4h-cyclopenta(def)phenant	0.002	0.006	0.002	0.006	0.003	0.008
Fluoranthrene	0.002	0.005	0.002	0.004	0.003	0.007
Pyrene	0.003	0.009	0.003	0.008	0.005	0.013
Benzo[a]anthracene	0.014	0.037	0.010	0.026	0.016	0.043

Table A3: Tar compounds in PL at 750 °C/ER-0.17

	(gtar/Nm^{3}a.r.)	(gtar/kgfeedstock-daf)	(gtar/Nm^{3}a.r.)	(gtar/kgfeedstock-daf)	(gtar/Nm^{3}a.r.)	(gtar/kgfeedstock-daf)
Total tar	4.52	11.16	4.95	12.23	4.49	11.08
Benzene	1.307	3.228	1.407	3.476	1.325	3.271
Thiophene	0.025	0.062	0.026	0.063	0.033	0.082
Pyridine	0.107	0.264	0.119	0.293	0.107	0.265
Pyrrole	0.098	0.243	0.124	0.307	0.088	0.218
Toluene	0.872	2.153	0.945	2.333	0.876	2.163
2/3/4 Methyl pyridine	0.062	0.154	0.067	0.166	0.057	0.142
Pyrazine-methyl	0.023	0.058	0.027	0.066	0.025	0.063
2/3/4 Methyl pyridine	0.002	0.004	0.001	0.003	0.001	0.003
Ethylbenzene	0.042	0.103	0.049	0.120	0.041	0.102
o/m/p Xylene	0.096	0.238	0.103	0.254	0.098	0.242
Phenylethyne	0.006	0.015	0.006	0.015	0.006	0.016
Styrene/o/m/p Xylene	0.268	0.663	0.292	0.720	0.270	0.666
Iso-dimethyl pyridine	0.004	0.011	0.005	0.012	0.005	0.011
2/3/4 Ethenyl pyridine	0.016	0.039	0.018	0.044	0.016	0.040
Benzonitrile	0.005	0.012	0.005	0.013	0.005	0.013
Phenol	0.228	0.564	0.251	0.620	0.220	0.543
o/m/p Methyl Styrene or Bezene 1/2 propenyl	0.009	0.022	0.010	0.024	0.008	0.021
o/m/p Mehyl Styrene or Benzene 1/2 propenyl	0.003	0.008	0.004	0.011	0.003	0.008
Indene	0.115	0.285	0.128	0.315	0.117	0.289
o/m/p Cresol	0.042	0.104	0.049	0.120	0.045	0.112
o/m/p Cresol	0.052	0.129	0.063	0.155	0.051	0.126
Naphthalene-1,2 diydro	0.024	0.058	0.026	0.065	0.024	0.059
Naphthalene	0.181	0.448	0.199	0.492	0.181	0.446
Quinoline	0.005	0.011	0.005	0.013	0.004	0.010
Isoquiolilne	0.017	0.043	0.019	0.047	0.017	0.043
2-Methyl naphthalene	0.065	0.160	0.070	0.173	0.062	0.152
Indole	0.037	0.092	0.043	0.105	0.036	0.090
1-Methyl naphthalene	0.065	0.162	0.072	0.179	0.067	0.165
Biphenyl	0.010	0.025	0.011	0.027	0.010	0.025
2-Ethenyl naphthalene	0.011	0.026	0.011	0.028	0.010	0.026
Acenaphthylene	0.030	0.073	0.032	0.079	0.029	0.072
Acenaphthene	0.004	0.011	0.005	0.011	0.005	0.012
Dibenzofuran	0.008	0.021	0.008	0.019	0.008	0.019
Fluorene	0.012	0.031	0.014	0.034	0.012	0.030
Phenanthrene	0.021	0.052	0.023	0.056	0.021	0.052
Anthracene	0.007	0.017	0.007	0.018	0.007	0.016
4h-cyclopenta(def)phenanthrene	0.003	0.007	0.003	0.008	0.004	0.009
Fluoranthrene	0.002	0.006	0.003	0.006	0.002	0.006
Pyrene	0.005	0.013	0.005	0.013	0.005	0.013
Benzo[a]anthracene	0.007	0.018	0.008	0.019	0.011	0.027

Table A4: Tar compounds in PL at 750°C/ER 0.21.

	(gtar/Nm^{3}a.r.)	(gtar/kgfeedstock-daf)	(gtar/Nm^{3}a.r.)	(gtar/kgfeedstock-daf)	(gtar/Nm^{3}a.r.)	(gtar/kgfeedstock-daf)
Total tar	3.67	10.29	3.64	10.20	3.65	10.23
Benzene	1.407	3.947	1.382	3.878	1.419	3.982
Thiophene	0.018	0.050	0.017	0.047	0.019	0.054
Pyridine	0.098	0.276	0.099	0.278	0.097	0.273
Pyrrole	0.062	0.173	0.074	0.209	0.067	0.187
Toluene	0.723	2.030	0.729	2.045	0.747	2.095
2/3/4 Methyl pyridine	0.043	0.119	0.045	0.127	0.044	0.123
Pyrazine-methyl	0.016	0.044	0.015	0.041	0.015	0.043
2/3/4 Methyl pyridine	0.001	0.003	0.001	0.002	0.001	0.002
Ethylbenzene	0.007	0.019	0.007	0.019	0.007	0.021
o/m/p Xylene	0.073	0.205	0.071	0.199	0.071	0.198
Phenylethyne	0.002	0.006	0.002	0.007	0.002	0.006
Styrene/o/m/p Xylene	0.219	0.613	0.211	0.591	0.213	0.599
Iso-dimethyl pyridine	0.001	0.002	0.001	0.002	0.001	0.002
2/3/4 Ethenyl pyridine	0.007	0.019	0.007	0.019	0.007	0.019
Benzonitrile	0.002	0.007	0.002	0.006	0.002	0.006
Phenol	0.056	0.157	0.052	0.146	0.044	0.124
o/m/p Methyl Styrene or Bezene 1/2 propenyl	0.007	0.019	0.006	0.018	0.005	0.015
o/m/p Mehyl Styrene or Benzene 1/2 propenyl	0.005	0.014	0.007	0.019	0.006	0.016
Indene	0.110	0.308	0.109	0.307	0.106	0.296
o/m/p Cresol	0.005	0.015	0.005	0.014	0.004	0.012
o/m/p Cresol	0.005	0.013	0.004	0.012	0.004	0.011
Naphthalene-1,2 diydro	0.007	0.021	0.007	0.020	0.007	0.020
Naphthalene	0.193	0.540	0.188	0.529	0.190	0.534
Quinoline	0.002	0.006	0.001	0.004	0.001	0.004
Isoquiolilne	0.012	0.035	0.013	0.036	0.013	0.036
2-Methyl naphthalene	0.039	0.111	0.039	0.109	0.039	0.109
Indole	0.001	0.003	0.001	0.003	0.001	0.001
1-Methyl naphthalene	0.042	0.117	0.041	0.114	0.045	0.126
Biphenyl	0.007	0.020	0.007	0.019	0.007	0.020
2-Ethenyl naphthalene	0.005	0.015	0.005	0.013	0.005	0.013
Acenaphthylene	0.032	0.089	0.033	0.092	0.033	0.093
Acenaphthene	0.003	0.008	0.003	0.007	0.002	0.007
Dibenzofuran	0.004	0.011	0.004	0.012	0.004	0.011
Fluorene	0.007	0.021	0.007	0.020	0.007	0.020
Phenanthrene	0.018	0.052	0.018	0.051	0.018	0.052
Anthracene	0.003	0.009	0.003	0.008	0.003	0.008
4h-cyclopenta(def)phenanthrene	0.002	0.007	0.003	0.007	0.003	0.007
Fluoranthrene	0.002	0.006	0.002	0.006	0.002	0.006
Pyrene	0.004	0.011	0.004	0.011	0.004	0.012
Benzo[a]anthracene	0.010	0.027	0.012	0.033	0.012	0.035

Table A5: Tar compounds in PL/BW at 750 °C/ER-0.17

	(gtar/Nm^{3}a.r.)	(gtar/kgfeedstock-daf)	(gtar/Nm^{3}a.r.)	(gtar/kgfeedstock-daf)	(gtar/Nm^{3}a.r.)	(gtar/kgfeedstock-daf)
Total tar	5.64	13.76	5.66	13.80	5.89	14.36
Benzene	2.106	5.135	2.152	5.248	2.233	5.443
Thiophene	0.016	0.038	0.018	0.044	0.016	0.040
Pyridine	0.065	0.158	0.063	0.153	0.070	0.170
Toluene	0.887	2.162	0.916	2.233	0.939	2.288
2/3/4 Methyl pyridine	0.018	0.045	0.017	0.040	0.019	0.047
Pyrazine-methyl	0.011	0.026	0.008	0.019	0.009	0.022
Ethylbenzene	0.007	0.016	0.006	0.015	0.006	0.014
o/m/p Xylene	0.089	0.217	0.084	0.206	0.086	0.210
Phenylethyne	0.006	0.015	0.008	0.019	0.007	0.017
Styrene/o/m/p Xylene	0.315	0.769	0.317	0.773	0.327	0.797
2/3/4 Ethenyl pyridine	0.006	0.015	0.005	0.012	0.005	0.013
Benzonitrile	0.003	0.007	0.003	0.008	0.003	0.008
Phenol	0.314	0.766	0.308	0.750	0.319	0.779
o/m/p Methyl Styrene or Bezene 1/2 propenyl	0.011	0.027	0.011	0.027	0.012	0.029
o/m/p Mehyl Styrene or Benzene 1/2 propenyl	0.009	0.022	0.010	0.025	0.010	0.024
Indene	0.274	0.667	0.279	0.680	0.290	0.706
o/m/p Cresol	0.009	0.022	0.007	0.017	0.008	0.019
o/m/p Cresol	0.020	0.048	0.015	0.037	0.018	0.044
Naphthalene-1,2 diydro	0.013	0.033	0.013	0.031	0.013	0.032
Naphthalene	0.420	1.023	0.421	1.027	0.426	1.039
Quinoline	0.003	0.008	0.003	0.008	0.003	0.008
Isoquiolilne	0.011	0.028	0.011	0.028	0.012	0.030
2-Methyl naphthalene	0.076	0.186	0.076	0.184	0.079	0.192
Indole	0.005	0.013	0.004	0.009	0.006	0.014
1-Methyl naphthalene	0.054	0.132	0.052	0.128	0.055	0.133
Biphenyl	0.020	0.048	0.020	0.050	0.020	0.050
2-Ethenyl naphthalene	0.014	0.035	0.014	0.034	0.015	0.036
Acenaphthylene	0.094	0.229	0.094	0.230	0.098	0.240
Acenaphthene	0.006	0.015	0.006	0.015	0.006	0.015
Dibenzofuran	0.010	0.024	0.008	0.019	0.008	0.019
Fluorene	0.025	0.061	0.024	0.059	0.025	0.061
Phenanthrene	0.052	0.126	0.051	0.125	0.055	0.133
Anthracene	0.014	0.034	0.015	0.036	0.015	0.036
4h-cyclopenta(def)phenanthrene	0.008	0.019	0.008	0.019	0.009	0.022
Fluoranthrene	0.008	0.020	0.008	0.021	0.009	0.022
Pyrene	0.016	0.039	0.016	0.039	0.016	0.040
Benzo[a/b]fluorene/1-Methl pyrene	0.006	0.015	0.006	0.014	0.006	0.016
Benzo(a/b)fluorene/1-Methyl pyrene	0.005	0.012	0.005	0.012	0.005	0.013
Benzo[a]anthracene	0.013	0.033	0.008	0.020	0.014	0.035
Benzo(k)fluorathrene	0.003	0.007	0.003	0.006	0.004	0.009

Table A6: Tar compounds in PL/BW at 750 °C/ER-0.21

	(gtar/Nm^{3}a.r.)	(gtar/kgfeedstock-daf)	(gtar/Nm^{3}a.r.)	(gtar/kgfeedstock-daf)	(gtar/Nm^{3}a.r.)	(gtar/kgfeedstock-daf)
Total tar	5.30	12.62	5.30	12.62	5.44	12.95
Benzene	1.912	4.553	1.913	4.555	1.952	4.649
Thiophene	0.013	0.031	0.014	0.033	0.016	0.037
Pyridine	0.052	0.125	0.056	0.134	0.061	0.145
Toluene	0.859	2.045	0.839	1.998	0.861	2.051
2/3/4 Methyl pyridine	0.014	0.034	0.016	0.037	0.019	0.044
Pyrazine-methyl	0.008	0.019	0.009	0.022	0.011	0.027
Ethylbenzene	0.010	0.023	0.010	0.023	0.010	0.024
o/m/p Xylene	0.078	0.186	0.082	0.195	0.084	0.201
Phenylethyne	0.007	0.016	0.007	0.016	0.006	0.015
Styrene/o/m/p Xylene	0.310	0.737	0.309	0.735	0.318	0.758
2/3/4 Ethenyl pyridine	0.006	0.015	0.006	0.014	0.007	0.016
Benzonitrile	0.004	0.008	0.004	0.010	0.004	0.010
Phenol	0.344	0.818	0.339	0.808	0.351	0.837
o/m/p Methyl Styrene or Bezene 1/2 propenyl	0.012	0.028	0.013	0.030	0.012	0.029
o/m/p Mehyl Styrene or Benzene 1/2 propenyl	0.009	0.021	0.009	0.022	0.010	0.023
Indene	0.247	0.589	0.246	0.586	0.252	0.601
o/m/p Cresol	0.019	0.045	0.019	0.044	0.020	0.048
o/m/p Cresol	0.034	0.082	0.032	0.076	0.035	0.083
Naphthalene-1,2 diydro	0.017	0.040	0.017	0.040	0.017	0.041
Naphthalene	0.356	0.848	0.357	0.849	0.363	0.863
Quinoline	0.004	0.009	0.003	0.008	0.004	0.009
Isoquiolilne	0.006	0.015	0.006	0.015	0.007	0.016
2-Methyl naphthalene	0.073	0.175	0.074	0.176	0.076	0.180
Indole	0.004	0.010	0.005	0.012	0.007	0.016
1-Methyl naphthalene	0.052	0.125	0.052	0.125	0.054	0.129
Biphenyl	0.017	0.039	0.018	0.042	0.017	0.041
2-Ethenyl naphthalene	0.013	0.032	0.013	0.032	0.014	0.034
Acenaphthylene	0.078	0.187	0.078	0.187	0.080	0.191
Acenaphthene	0.006	0.014	0.006	0.014	0.006	0.015
Dibenzofuran	0.009	0.020	0.009	0.021	0.009	0.021
Fluorene	0.022	0.052	0.022	0.053	0.023	0.054
Phenanthrene	0.040	0.096	0.041	0.098	0.042	0.099
Anthracene	0.011	0.026	0.012	0.028	0.012	0.029
4h-cyclopenta(def)phenanthrene	0.006	0.014	0.006	0.015	0.007	0.016
Fluoranthrene	0.007	0.016	0.007	0.016	0.007	0.016
Pyrene	0.013	0.031	0.013	0.031	0.013	0.031
Benzo[a/b]fluorene/1-Methl pyrene	0.005	0.012	0.005	0.012	0.005	0.013
Benzo(a/b)fluorene/1-Methyl pyrene	0.004	0.009	0.004	0.010	0.004	0.010
Benzo[a]anthracene	0.009	0.021	0.007	0.018	0.007	0.018
Benzo(k)fluorathrene	0.002	0.005	0.002	0.005	0.002	0.005

Table A7: Tar compounds in PL/BW at 750 °C/ER-0.25

	(gtar/Nm^{3}a.r.)	(gtar/kgfeedstock-daf)	(gtar/Nm^{3}a.r.)	(gtar/kgfeedstock-daf)	(gtar/Nm^{3}a.r.)	(gtar/kgfeedstock-daf)
Total tar	6.19	14.74	5.46	12.99	5.44	12.94
Benzene	2.301	5.479	2.010	4.785	2.038	4.852
Thiophene	0.019	0.045	0.014	0.034	0.017	0.040
Pyridine	0.064	0.152	0.050	0.119	0.049	0.116
Toluene	1.138	2.709	1.001	2.382	0.987	2.350
2/3/4 Methyl pyridine	0.017	0.040	0.015	0.036	0.015	0.036
Pyrazine-methyl	0.013	0.032	0.010	0.024	0.009	0.022
Ethylbenzene	0.025	0.059	0.022	0.052	0.023	0.056
o/m/p Xylene	0.121	0.288	0.107	0.256	0.108	0.258
Phenylethyne	0.007	0.016	0.006	0.015	0.006	0.015
Styrene/o/m/p Xylene	0.411	0.978	0.358	0.851	0.360	0.858
2/3/4 Ethenyl pyridine	0.008	0.020	0.006	0.014	0.007	0.017
Benzonitrile	0.007	0.016	0.006	0.013	0.005	0.012
Phenol	0.318	0.757	0.282	0.671	0.292	0.696
o/m/p Methyl Styrene or Bezene 1/2 propenyl	0.019	0.046	0.018	0.043	0.017	0.040
o/m/p Mehyl Styrene or Benzene 1/2 propenyl	0.016	0.037	0.015	0.036	0.014	0.033
Indene	0.220	0.524	0.194	0.462	0.193	0.459
o/m/p Cresol	0.018	0.042	0.012	0.029	0.017	0.041
o/m/p Cresol	0.015	0.036	0.014	0.032	0.009	0.022
Naphthalene-1,2 diydro	0.020	0.047	0.018	0.042	0.018	0.043
Naphthalene	0.378	0.899	0.331	0.787	0.322	0.766
Quinoline	0.007	0.016	0.006	0.014	0.006	0.014
Isoquiolilne	0.010	0.023	0.009	0.022	0.009	0.021
2-Methyl naphthalene	0.082	0.194	0.069	0.165	0.069	0.164
Indole	0.001	0.003	0.001	0.003	0.001	0.002
1-Methyl naphthalene	0.085	0.203	0.073	0.174	0.064	0.153
Biphenyl	0.018	0.042	0.015	0.035	0.015	0.035
2-Ethenyl naphthalene	0.012	0.029	0.009	0.021	0.009	0.022
Acenaphthylene	0.077	0.184	0.065	0.155	0.064	0.152
Acenaphthene	0.006	0.013	0.004	0.010	0.004	0.011
Dibenzofuran	0.009	0.022	0.009	0.022	0.009	0.021
Fluorene	0.012	0.029	0.010	0.024	0.010	0.024
Phenanthrene	0.037	0.088	0.030	0.071	0.029	0.068
Anthracene	0.009	0.021	0.007	0.017	0.007	0.017
4h-cyclopenta(def)phenanthrene	0.003	0.006	0.002	0.004	0.002	0.005
Fluoranthrene	0.006	0.015	0.005	0.011	0.004	0.011
Pyrene	0.012	0.029	0.009	0.022	0.009	0.021
Benzo[a/b]fluorene/1-Methl pyrene	0.003	0.007	0.002	0.005	0.003	0.007
Benzo(a/b)fluorene/1-Methyl pyrene	0.003	0.007	0.002	0.005	0.003	0.006
Benzo[a]anthracene	0.016	0.038	0.014	0.032	0.012	0.029
Benzo(k)fluorathrene	0.003	0.007	0.003	0.006	0.002	0.005

Table A8: Tar compounds in BW at 750 °C/ER-0.18

	(gtar/Nm^{3}a.r.)	(gtar/kgfeedstock-daf)	(gtar/Nm^{3}a.r.)	(gtar/kgfeedstock-daf)	(gtar/Nm^{3}a.r.)	(gtar/kgfeedstock-daf)
Total tar	7.02	14.98	6.77	14.45	7.69	16.40
Benzene	2.603	5.552	2.506	5.346	2.648	5.649
Toluene	1.017	2.170	0.997	2.126	1.128	2.406
Ethylbenzene	0.009	0.019	0.008	0.017	0.008	0.018
o/m/p Xylene	0.093	0.199	0.085	0.182	0.103	0.221
Phenylethyne	0.013	0.028	0.013	0.027	0.015	0.032
Styrene/o/m/p Xylene	0.405	0.863	0.390	0.833	0.455	0.971
Phenol	0.549	1.170	0.527	1.123	0.643	1.372
o/m/p Methyl Styrene or Bezene 1/2 propenyl	0.009	0.020	0.009	0.019	0.010	0.021
o/m/p Mehyl Styrene or Benzene 1/2 propenyl	0.007	0.015	0.007	0.015	0.008	0.017
Indene	0.456	0.972	0.427	0.910	0.511	1.090
o/m/p Cresol	0.032	0.069	0.030	0.065	0.039	0.083
o/m/p Cresol	0.028	0.061	0.028	0.061	0.042	0.090
Naphthalene-1,2 diydro	0.023	0.049	0.022	0.047	0.026	0.055
Naphthalene	0.569	1.214	0.536	1.144	0.648	1.383
2-Methyl naphthalene	0.103	0.219	0.100	0.212	0.122	0.260
1-Methyl naphthalene	0.073	0.155	0.070	0.150	0.086	0.183
Biphenyl	0.025	0.053	0.025	0.053	0.030	0.064
2-Ethenyl naphthalene	0.017	0.037	0.018	0.037	0.022	0.048
Acenaphthylene	0.148	0.316	0.144	0.307	0.172	0.367
Acenaphthene	0.009	0.019	0.008	0.016	0.009	0.019
Dibenzofuran	0.012	0.025	0.012	0.025	0.014	0.030
Fluorene	0.037	0.079	0.036	0.077	0.042	0.089
Phenanthrene	0.062	0.133	0.061	0.130	0.072	0.154
Anthracene	0.019	0.040	0.019	0.041	0.023	0.048
4h-cyclopenta(def)phenanthrene	0.011	0.023	0.012	0.025	0.016	0.033
Fluoranthrene	0.015	0.033	0.016	0.033	0.018	0.039
Pyrene	0.026	0.055	0.025	0.054	0.031	0.066
11H-Benzo[a/b]fluorene/1-Methl pyrene	0.010	0.022	0.010	0.021	0.012	0.026
11H-Benzo[a/b]fluorene/1-Methl pyrene	0.009	0.019	0.009	0.018	0.010	0.022
Benzo[a]anthracene	0.016	0.034	0.012	0.027	0.019	0.041
Benzo(k)fluorathrene	0.004	0.009	0.004	0.008	0.005	0.010

Table A9: Tar compounds in BW at 750 °C/ER-0.225

	(gtar/Nm^{3}a.r.)	(gtar/kgfeedstock-daf)	(gtar/Nm^{3}a.r.)	(gtar/kgfeedstock-daf)
Total tar	6.71	15.46	6.60	15.20
Benzene	2.476	5.704	2.398	5.524
Toluene	1.020	2.349	0.986	2.270
Ethylbenzene	0.010	0.024	0.010	0.023
o/m/p Xylene	0.102	0.234	0.101	0.232
Phenylethyne	0.011	0.026	0.011	0.026
Styrene/o/m/p Xylene	0.386	0.890	0.372	0.857
Phenol	0.532	1.226	0.521	1.201
o/m/p Methyl Styrene or Bezene 1/2 propenyl	0.009	0.021	0.009	0.020
o/m/p Mehyl Styrene or Benzene 1/2 propenyl	0.007	0.016	0.007	0.016
Indene	0.432	0.994	0.421	0.969
o/m/p Cresol	0.032	0.074	0.034	0.078
o/m/p Cresol	0.032	0.073	0.034	0.079
Naphthalene-1,2 diydro	0.024	0.055	0.024	0.055
Naphthalene	0.527	1.215	0.518	1.194
2-Methyl naphthalene	0.095	0.218	0.095	0.219
1-Methyl naphthalene	0.067	0.154	0.067	0.155
Biphenyl	0.022	0.051	0.022	0.052
2-Ethenyl naphthalene	0.015	0.034	0.016	0.036
Acenaphthylene	0.126	0.291	0.128	0.295
Acenaphthene	0.008	0.017	0.008	0.018
Dibenzofuran	0.010	0.024	0.011	0.026
Fluorene	0.031	0.072	0.033	0.075
Phenanthrene	0.052	0.119	0.054	0.124
Anthracene	0.016	0.036	0.016	0.037
4h-cyclopenta(def)phenanthrene	0.009	0.022	0.010	0.024
Fluoranthrene	0.013	0.029	0.013	0.031
Pyrene	0.023	0.052	0.025	0.058
11H-Benzo[a/b]fluorene/1-Methl pyrene	0.008	0.019	0.009	0.020
11H-Benzo[a/b]fluorene/1-Methl pyrene	0.007	0.016	0.008	0.018
Benzo[a]anthracene	0.014	0.033	0.017	0.040
Benzo(k)fluorathrene	0.003	0.008	0.004	0.008

Table A10: Tar compounds in BW at 750 °C/ER-0.27

	(gtar/Nm^{3}a.r.)	(gtar/kgfeedstock-daf)	(gtar/Nm^{3}a.r.)	(gtar/kgfeedstock-daf)
Total tar	6.20	14.06	6.07	13.76
Benzene	2.273	5.157	2.207	5.007
Toluene	0.948	2.150	0.936	2.124
Ethylbenzene	0.012	0.028	0.013	0.030
o/m/p Xylene	0.098	0.221	0.097	0.221
Phenylethyne	0.010	0.023	0.010	0.023
Styrene/o/m/p Xylene	0.361	0.818	0.354	0.804
Phenol	0.493	1.119	0.495	1.122
o/m/p Methyl Styrene or Bezene 1/2 propenyl	0.009	0.020	0.009	0.020
o/m/p Mehyl Styrene or Benzene 1/2 propenyl	0.006	0.015	0.007	0.015
Indene	0.387	0.877	0.374	0.849
o/m/p Cresol	0.033	0.075	0.036	0.081
o/m/p Cresol	0.031	0.070	0.033	0.075
Naphthalene-1,2 diydro	0.025	0.057	0.025	0.058
Naphthalene	0.469	1.063	0.450	1.021
2-Methyl naphthalene	0.088	0.199	0.086	0.195
1-Methyl naphthalene	0.063	0.142	0.062	0.141
Biphenyl	0.020	0.045	0.020	0.045
2-Ethenyl naphthalene	0.014	0.032	0.014	0.032
Acenaphthylene	0.110	0.250	0.107	0.242
Acenaphthene	0.008	0.017	0.008	0.017
Dibenzofuran	0.010	0.023	0.011	0.024
Fluorene	0.027	0.062	0.026	0.060
Phenanthrene	0.046	0.104	0.045	0.101
Anthracene	0.013	0.031	0.013	0.030
4h-cyclopenta(def)phenanthrene	0.007	0.017	0.008	0.017
Fluoranthrene	0.011	0.024	0.011	0.024
Pyrene	0.020	0.046	0.021	0.048
11H-Benzo[a/b]fluorene/1-Methl pyrene	0.007	0.016	0.007	0.016
11H-Benzo[a/b]fluorene/1-Methl pyrene	0.006	0.015	0.006	0.014
Benzo[a]anthracene	0.012	0.027	0.016	0.037
Benzo(k)fluorathrene	0.003	0.006	0.003	0.007

REFERENCES

[1] Yu Z, Bidarmaghz A, Narsilio G, Aye L. Heating and Cooling Loads of a Poultry Shed in Central Coast , NSW , Australia. World Sustain Built Environ Conf 2017 Hong Kong 2017:2127-2133 (6).

[2] European Commission. Paris Agreement Key elements Mitigation : reducing emissions Transparency and global socktake 2019.

[3] Bioenergy Europe. Bioenergy Europe Statistical Report. 2018.

[4] Intelligent Energy. Energy from field energy crops-a handbook for energy producers. 2009.

[5] Ong Z, Cheng Y, Maneerung T, Yao Z, Tong YW, Wang CH, et al. Co-gasification of woody biomass and sewage sludge in a fixed-bed downdraft gasifier. AIChE J 2015. https://doi.org/10.1002/aic.14836.

[6] Abelha P, Franco C, Pinto F, Lopes H, Gulyurtlu I, Gominho J, et al. Thermal conversion of Cynara cardunculus l. and mixtures with Eucalyptus globulus by fluidized-bed combustion and gasification. Energy and Fuels 2013;27:6725–37. https://doi.org/10.1021/ef401246p.

[7] Pandey DS. Experimental and mathematical modelling of biowaste gasification in a bubbling fluidised bed reactor. University of Limerick, Ireland, 2016.

[8] Bioenergy Europe. Solid Bioenergy in Questions 1. An asset to EU forests? 2018.

[9] Indufor. Outlook of Wood Biomass for Energy in the EU-28. 2017.

[10] statistic_id237632_global-production-of-meat-2016-2020-by-type 2019.

[11] Eurostat. Poultry meat production in EU at new high in 2018. Eur Comm Eurostat 2019. https://ec.europa.eu/eurostat/web/products-eurostat-news/-/DDN-20190325-1 (accessed June 26, 2019).

[12] Ramírez CA, Patel M, Blok K. How much energy to process one pound of meat? A comparison of energy use and specific energy consumption in the meat industry of four European countries. Energy 2006;31:1711–27. https://doi.org/10.1016/j.energy.2005.08.007.

[13] Barbut S. Global Perspective. Sci. Poult. Meat Process., 2015, p. 1–21.

[14] Magdelaine P, Spiess MP, Valceschini E. Poultry meat consumption trends in Europe. Worlds Poult Sci J 2008;64:10–4. https://doi.org/10.1017/S0043933907001717.

[15] Bolan NS, Szogi AA, Chuasavathi T, Seshadri B, Rothrock MJ, Pannerselvam P. Uses and management of poultry litter. Worlds Poult Sci J 2010;66:673–98. https://doi.org/10.1017/s0043933910000656.

[16] Bradley S. Turning Chesapeake Bay Watershed Poultry Manure and Litter into Energy : Power 2008.

[17] Rumsey Julie. E&W Poultry Slaughterhouse Survey, DARD and RESAS 2016.

[18] Kelleher BP, Leahy JJ, Henihan AM, O'Dwyer TF, Sutton D, Leahy MJ. Advances in poultry litter disposal technology - A review. Bioresour Technol 2002;83:27–36. https://doi.org/10.1016/S0960-8524(01)00133-X.

[19] Pilar BM. Evaluation of manure management systems in Europe. 2015.

[20] Kawata K, Nissato K, Shiota N, Hori T, Asada T, Oikawa K. Variation in Pesticide Concentrations During Composting of Food Waste and Fowl Droppings. Corresp to K Kawata Bull Environ Contam Toxicol 2006;77:391–8. https://doi.org/10.1007/s00128-006-1078-8.

[21] Billen P, Costa J, Van Der Aa L, Van Caneghem J, Vandecasteele C. Electricity from poultry manure: A cleaner alternative to direct land application. J Clean Prod 2015;96:467–75. https://doi.org/10.1016/j.jclepro.2014.04.016.

[22] Joseph P, Tretsiakova-McNally S, McKenna S. Characterization of cellulosic wastes and gasification products from chicken farms. Waste Manag 2012;32:701–9. https://doi.org/10.1016/j.wasman.2011.09.024.

[23] Lynch D, Henihan AM, Bowen B, Lynch D, McDonnell K, Kwapinski W, et al. Utilisation of poultry litter as an energy feedstock. Biomass and Bioenergy 2013;49:197–204. https://doi.org/10.1016/j.biombioe.2012.12.009.

[24] Taupe NC, Lynch D, Wnetrzak R, Kwapinska M, Kwapinski W, Leahy JJ. Updraft gasification of poultry litter at farm-scale: A case study. Waste Manag 2016;50:324–33. https://doi.org/10.1016/j.wasman.2016.02.036.

[25] European Commission. The EU Nitrates Directive The background to the Directive. 2010.

[26] Lynch D, Henihan AM, Bowen B, Lynch D, McDonnell K, Kwapinski W, et al. Utilisation of poultry litter as an energy feedstock. Biomass and Bioenergy 2013;49:197–204. https://doi.org/10.1016/j.biombioe.2012.12.009.

[27] SEAI. Energy Use in Agriculture. 2011.

[28] Key Factors for Poultry House Ventilation | The Poultry Site n.d. https://www.thepoultrysite.com/articles/key-factors-for-poultry-house-ventilation (accessed December 18, 2020).

[29] Pandey DS, Kwapinska M, Gómez-Barea A, Horvat A, Fryda LE, Rabou LPLM, et al. Poultry Litter Gasification in a Fluidized Bed Reactor: Effects of Gasifying Agent and Limestone Addition. Energy and Fuels 2016. https://doi.org/10.1021/acs.energyfuels.6b00058.

[30] Burra KG, Hussein MS, Amano RS, Gupta AK. Syngas evolutionary behavior during chicken manure pyrolysis and air gasification. Appl Energy 2016;181:408–15. https://doi.org/10.1016/j.apenergy.2016.08.095.

[31] Joseph P, Tretsiakova-Mcnally S, Mckenna S. Characterization of cellulosic wastes and gasification products from chicken farms. Waste Manag 2012;32:701–9. https://doi.org/10.1016/j.wasman.2011.09.024.

[32] Arena U. Process and technological aspects of municipal solid waste gasification. A review. Waste Manag 2012;32:625–39. https://doi.org/10.1016/j.wasman.2011.09.025.

[33] Eksi G, Karaosmanoglu F. Combined bioheat and biopower: A technology review and an assessment for Turkey. Renew Sustain Energy Rev 2017;73:1313–32. https://doi.org/10.1016/j.rser.2017.01.093.

[34] Raj NT, Iniyan S, Goic R. A review of renewable energy based cogeneration technologies. Renew Sustain Energy Rev 2011;15:3640–8. https://doi.org/10.1016/j.rser.2011.06.003.

[35] European Parliament Council. EUR-Lex - 32008L0098 - EN - EUR-Lex. 2008.

[36] European Commission. Being wise with waste : the EU ' s approach to waste management. 2010. https://doi.org/10.2779/93543.

[37] Holm-Nielsen JB, Seadi T Al, Oleskowicz-Popiel P. The future of anaerobic digestion and biogas utilization. Bioresour Technol J 2009;100:5478–84. https://doi.org/10.1016/j.biortech.2008.12.046.

[38] Weiland P. Biogas production: current state and perspectives. Appl Microbiol Biotechnol 2010;85:849–60. https://doi.org/10.1007/s00253-009-2246-7.

[39] Pöschl M, Ward S, Owende P. Evaluation of energy efficiency of various biogas production and utilization pathways. Appl Energy 2010;87:3305–21. https://doi.org/10.1016/j.apenergy.2010.05.011.

[40] No RP. Conversion of Waste to Energy in the Chicken Meat Industry. 2013.

[41] Parawira W, Read JS, Mattiasson B, Björnsson L. Energy production from agricultural residues: High methane yields in pilot-scale two-stage anaerobic digestion. Biomass and Bioenergy 2008;32:44–50. https://doi.org/10.1016/j.biombioe.2007.06.003.

[42] Gowreesunker BL, Tassou SA. Energy generation potential of anaerobic digestion from the food and farming wastes of the UK food chain. Renew Bioresurces 2014;2:7.

[43] Kapdi SS, Vijay VK, Rajesh SK, Prasad R. Biogas scrubbing, compression and storage: Perspective and prospectus in Indian context. Renew Energy 2005;30:1195–202. https://doi.org/10.1016/j.renene.2004.09.012.

[44] Rahman MA, Møller HB, Saha CK, Alam MM, Wahid R, Feng L. Optimal ratio for anaerobic co-digestion of poultry droppings and lignocellulosic-rich substrates for enhanced biogas production. Energy Sustain Dev 2017;39:59–66. https://doi.org/10.1016/j.esd.2017.04.004.

[45] Li Y, Zhang R, Chen C, Liu G, He Y, Liu X. Biogas production from co-digestion of corn stover and chicken manure under anaerobic wet, hemi-solid, and solid state conditions. Bioresour Technol 2013;149:406–12. https://doi.org/10.1016/j.biortech.2013.09.091.

[46] Wang X, Yang G, Feng Y, Ren G, Han X. Optimizing feeding composition and carbon-nitrogen ratios for improved methane yield during anaerobic co-digestion of dairy, chicken manure and wheat straw. Bioresour Technol 2012;120:78–83. https://doi.org/10.1016/j.biortech.2012.06.058.

[47] Zhang T, Yang Y, Liu L, Han Y, Ren G, Yang G. Improved biogas production from chicken manure anaerobic digestion using cereal residues as co-substrates. Energy and Fuels 2014;28:2490–5. https://doi.org/10.1021/ef500262m.

[48] Werther J, Saenger M, Hartge EU, Ogada T, Siagi Z. Combustion of agricultural residues. Prog Energy Combust Sci 2000;26:1–27. https://doi.org/10.1016/S0360-1285(99)00005-2.

[49] Anca-Couce A, Sommersacher P, Evic N, Mehrabian R, Scharler R. Experiments and modelling of NOx precursors release (NH3 and HCN) in fixed-bed biomass combustion conditions. Fuel 2018;222:529–37. https://doi.org/10.1016/j.fuel.2018.03.003.

[50] Deirdre Lynch. Fluidised bed combustion of poultry litter with investigation into its ash chemistry. 2013.

[51] Lynch D, Henihan AM, Kwapinski W, Zhang L, Leahy JJ. Ash agglomeration and deposition during combustion of poultry litter in a bubbling fluidized-bed combustor. Energy and Fuels, vol. 27, 2013, p. 4684–94. https://doi.org/10.1021/ef400744u.

[52] Billen P, Costa J, Van Der Aa L, Caneghem J Van, Vandecasteele C. Electricity from poultry manure: a cleaner alternative to direct land application. J Clean Prod 2015;96:467–75. https://doi.org/10.1016/j.jclepro.2014.04.016.

[53] Wargadalam VJ, Löffler G, Winter F, Hofbauer H. Homogeneous formation of NO and N2O from the oxidation of HCN and NH3 at 600-1000°C. Combust Flame 2000;120:465–78. https://doi.org/10.1016/S0010-2180(99)00107-8.

[54] Stubenberger G, Scharler R, Obernberger I. Nitrogen Release Behavior of Different Biomass Fuels Under Lab-Scale and Pilot-Scale Conditions. 15th Eur Biomass Conf Exhib 2007:1412–20.

[55] Stubenberger G, Scharler R, Zahirović S, Obernberger I. Experimental investigation of nitrogen species release from different solid biomass fuels as a basis for release models. Fuel 2008;87:793–806. https://doi.org/10.1016/j.fuel.2007.05.034.

[56] EC. Commission regulation (EU) No 592/2014 of 3 June 2014 amending Regulation (EU) No 142/2011 as regards the use of animal by-products and derived products as a fuel in combustion plants. Off J Eur Union 2014;L:33–40.

[57] Ma Q, Paudel KP, Bhandari D, Theegala C, Cisneros M. Implications of poultry litter usage for electricity production. Waste Manag 2019;95:493–503. https://doi.org/10.1016/j.wasman.2019.06.022.

[58] Santos Dalólio F, da Silva JN, Carneiro de Oliveira AC, Ferreira Tinôco I de F, Christiam Barbosa R, Resende M de O, et al. Poultry litter as biomass energy: A review and future perspectives. Renew Sustain Energy Rev 2017;76:941–9. https://doi.org/10.1016/j.rser.2017.03.104.

[59] Savoie P, Villeneuve J, Fournel S, Godbout S, Palacios JH, Heitz M, et al. Influence of biomass properties on technical and environmental performance of a multi-fuel boiler during on-farm combustion of energy crops. Appl Energy 2015;141:247–59. https://doi.org/10.1016/j.apenergy.2014.12.022.

[60] Klason T. Modelling of Biomass Combustion in Furnaces. 2006.

[61] Nussbaumer T. Combustion and Co-combustion of Biomass: Fundamentals, Technologies, and Primary Measures for Emission Reduction. Energy and Fuels 2003;17:1510–21. https://doi.org/10.1021/ef030031q.

[62] Yin C, Rosendahl LA, Kær SK. Grate-firing of biomass for heat and power production. Prog Energy Combust Sci 2008;34:725–54. https://doi.org/10.1016/j.pecs.2008.05.002.

[63] Basu P. Combustion and gasification of fluidised beds. vol. 33. 2006.

[64] Anicic B, Lin W, Dam-Johansen K, Wu H. Agglomeration mechanism in biomass fluidized bed combustion – Reaction between potassium carbonate and silica sand. Fuel Process Technol 2018;173:182–90. https://doi.org/10.1016/j.fuproc.2017.10.005.

[65] Qian X, Lee S, Chandrasekaran R, Yang Y, Caballes M, Alamu O, et al. Electricity evaluation and emission characteristics of poultry litter co-combustion process. Appl Sci 2019;9:1–15. https://doi.org/10.3390/app9194116.

[66] Abelha P, Gulyurtlu I, Boavida D, Barros JS, Cabrita I, Leahy J, et al. Combustion of poultry litter in a fluidised bed combustor. Fuel 2003;82:687–92. https://doi.org/10.1016/S0016-2361(02)00317-4.

[67] Topal H, Taner T, Altıncı Y, Amirabedin E. Application of trigeneration with direct co-combustion of poultry waste and coal: A case study in the poultry industry from Turkey. Therm Sci 2018;22:3073–82.

[68] Zhu S, Lee SW. Co-combustion performance of poultry wastes and natural gas in the advanced Swirling Fluidized Bed Combustor (SFBC). Waste Manag 2005;25:511–8. https://doi.org/10.1016/j.wasman.2004.09.003.

[69] Eye Power Station 2020. https://www.kem.dk/cases/eye-power-station-uk/ (accessed August 8, 2020).

[70] Alcorn -Eprl J. Norfolk Farming Conference Overview of Energy Power Resources Limited and Fuel Sourcing. 2012.

[71] EPR 2020. https://www.aet-biomass.com/en-gb/home/references/biomass-fired-plants/epr-glanford-scunthorpe.aspx (accessed August 8, 2020).

[72] Arena U. Process and technological aspects of municipal solid waste gasification. A review. Waste Manag 2012;32:625–39. https://doi.org/10.1016/j.wasman.2011.09.025.

[73] Arena U, Di Gregorio F, Santonastasi M. A techno-economic comparison between two design configurations for a small scale, biomass-to-energy gasification based system. Chem Eng J 2010;162:580–90. https://doi.org/10.1016/j.cej.2010.05.067.

[74] Lombardi L, Carnevale E, Corti A. A review of technologies and performances of thermal treatment systems for energy recovery from waste. Waste Manag 2015;37:26–44. https://doi.org/10.1016/j.wasman.2014.11.010.

[75] Gómez-Barea A, Leckner B. Modeling of biomass gasification in fluidized bed. Prog

Energy Combust Sci 2010;36:444–509. https://doi.org/10.1016/j.pecs.2009.12.002.

[76] Basu P. Biomass gasification and pyrolysis. vol. 5. 2012. https://doi.org/10.1016/B978-0-08-087872-0.00514-X.

[77] Milne TA, Evans RJ, Abatzoglou N. Biomass Gasifier " Tars " : Their Nature, Formation, and Conversion 1998:570–25357.

[78] Van Paasen SVB, Kiel JH a. Tar formation in a fluidised-bed gasifier: Impact of fuel properties and operating conditions. Kardiol Pol 2004;67:58. https://doi.org/ECN-C--04-013.

[79] Horvat A, Kwapinska M, Xue G, Rabou LPLM, Pandey DS, Kwapinski W, et al. Tars from Fluidized Bed Gasification of Raw and Torrefied Miscanthus x giganteus. Energy and Fuels 2016;30:5693–704.

[80] Valderrama Rios ML, González AM, Lora EES, Almazán del Olmo OA. Reduction of tar generated during biomass gasification: A review. Biomass and Bioenergy 2018;108:345–70. https://doi.org/10.1016/j.biombioe.2017.12.002.

[81] Paasen S Van, Kiel J. Tar formation in a fluidised bed gasifier. 2004.

[82] Molino A, Chianese S, Musmarra D. Biomass gasification technology: The state of the art overview. J Energy Chem 2016;25:10–25. https://doi.org/10.1111/luts.12156.

[83] Horvat A. A study of the uncertainty associated with tar measurement and an investigation of tar evolution and composition during the air-blown fluidised bed gasification of torrefied and non-torrefied grassy biomass. 2016.

[84] Sansaniwal SK, Pal K, Rosen MA, Tyagi SK. Recent advances in the development of biomass gasification technology: A comprehensive review. Renew Sustain Energy Rev 2017;72:363–84. https://doi.org/10.1016/j.rser.2017.01.038.

[85] Cummer KR, Brown RC. Ancillary equipment for biomass gasification. Biomass and Bioenergy 2002;23:113–28. https://doi.org/10.1016/S0961-9534(02)00038-7.

[86] Nagel F-P. Electricity from wood through the combination of gasification and solid oxide fuel cells systems analysis and Proof-of-concept ETH Library. 2008. https://doi.org/10.3929/ethz-a-005773119.

[87] Belgiorno V, De Feo G, Della Rocca C, Napoli RMA. Energy from gasification of solid wastes. Waste Manag 2002;23:1–15.

[88] Entrained Flow Gasifier | Biofuels Academy n.d. http://biofuelsacademy.org/index.html%3Fp=204.html (accessed August 17, 2020).

[89] Di Gregorio F, Santoro D, Arena U. The effect of ash composition on gasification of poultry wastes in a fluidized bed reactor. Waste Manag Res 2014. https://doi.org/10.1177/0734242X14525821.

[90] Priyadarsan S, Annamalai K, Sweeten JM, Holtzapple MT, Mukhtar S. Co-gasification of blended coal with feedlot and chicken litter biomass. Proc Combust Inst 2005;30 II:2973–

80. https://doi.org/10.1016/j.proci.2004.08.137.

[91] Font Palma C, Martin AD. Inorganic constituents formed during small-scale gasification of poultry litter: A model based study 2013. https://doi.org/10.1016/j.fuproc.2013.07.018.

[92] Huang Y, Anderson M, McIlveen-Wright D, Lyons GA, McRoberts WC, Wang YD, et al. Biochar and renewable energy generation from poultry litter waste: A technical and economic analysis based on computational simulations. Appl Energy 2015;160:656–63. https://doi.org/10.1016/j.apenergy.2015.01.029.

[93] Cavalaglio G, Coccia V, Cotana F, Gelosia M, Nicolini A, Petrozzi A. Energy from poultry waste: An Aspen Plus-based approach to the thermo-chemical processes. Waste Manag 2018;73:496–503. https://doi.org/10.1016/j.wasman.2017.05.037.

[94] Sharma A, Pareek V, Zhang D. Biomass pyrolysis - A review of modelling, process parameters and catalytic studies. Renew Sustain Energy Rev 2015;50:1081–96. https://doi.org/10.1016/j.rser.2015.04.193.

[95] Jahirul MI, Rasul MG, Chowdhury AA, Ashwath N. Biofuels production through biomass pyrolysis- A technological review. Energies 2012;5:4952–5001. https://doi.org/10.3390/en5124952.

[96] Bridgwater A V. Review of fast pyrolysis of biomass and product upgrading. Biomass and Bioenergy 2012;38:68–94. https://doi.org/10.1016/j.biombioe.2011.01.048.

[97] Peters JF, Banks SW, Bridgwater A V, Dufour J. A kinetic reaction model for biomass pyrolysis processes in Aspen Plus. Appl Energy 2017;188:595–603. https://doi.org/10.1016/j.apenergy.2016.12.030.

[98] Czernik S, Bridgwater A V. Overview of applications of biomass fast pyrolysis oil. Energy and Fuels 2004;18:590–8. https://doi.org/10.1021/ef034067u.

[99] Baniasadi M, Tugnoli A, Conti R, Torri C, Fabbri D, Cozzani V. Waste to energy valorization of poultry litter by slow pyrolysis. Renew Energy 2016;90:458–68. https://doi.org/10.1016/j.renene.2016.01.018.

[100] Kim SS, Agblevor FA, Lim J. Fast pyrolysis of chicken litter and turkey litter in a fluidized bed reactor. J Ind Eng Chem 2009;15:247–52. https://doi.org/10.1016/j.jiec.2008.10.004.

[101] Azargohar R, Nanda S, Kozinski JA, Dalai AK, Sutarto R. Effects of temperature on the physicochemical characteristics of fast pyrolysis bio-chars derived from Canadian waste biomass. Fuel 2014;125:90–100. https://doi.org/10.1016/j.fuel.2014.01.083.

[102] Ro KS, Cantrell KB, Hunt PG. High-temperature pyrolysis of blended animal manures for producing renewable energy and value-added biochar. Ind Eng Chem Res 2010;49:10125–31. https://doi.org/10.1021/ie101155m.

[103] Simbolon LM, Pandey DS, Horvat A, Kwapinska M, Leahy JJ, Tassou SA. Investigation of chicken litter conversion into useful energy resources by using low temperature pyrolysis. Energy Procedia, vol. 161, Elsevier Ltd; 2019, p. 47–56. https://doi.org/10.1016/j.egypro.2019.02.057.

[104] Simbolon LM, Pandey DS, Tsekos C, Jong W, Tassou SA. Investigation of poultry litter conversion into useful energy resources using fast pyrolysis. Eur. Biomass Conf. Exhib. Proc., 2019, p. 1222–6.

[105] BRISK2 2020. https://brisk2.eu/ (accessed December 23, 2020).

[106] Brunner T, Biedermann F, Kanzian W, Evic N, Obernberger I. Advanced biomass fuel characterization based on tests with a specially designed lab-scale reactor. Energy and Fuels 2013;27:5691–8. https://doi.org/10.1021/ef400559j.

[107] Sommersacher P, Brunner T, Obernberger I, Kienzl N, Kanzian W. Application of novel and advanced fuel characterization tools for the combustion related characterization of different wood/kaolin and straw/kaolin mixtures. Energy and Fuels 2013;27:5192–206. https://doi.org/10.1021/ef400400n.

[108] Sommersacher P, Brunner T, Obernberger I. Fuel indexes: A novel method for the evaluation of relevant combustion properties of new biomass fuels. Energy and Fuels, vol. 26, 2012, p. 380–90. https://doi.org/10.1021/ef201282y.

[109] Giuntoli J, De Jong W, Verkooijen AHM, Piotrowska P, Zevenhoven M, Hupa M. Combustion characteristics of biomass residues and biowastes: Fate of fuel nitrogen. Energy and Fuels 2010;24:5309–19. https://doi.org/10.1021/ef100571n.

[110] Elled AL, Åmand LE, Steenari BM. Composition of agglomerates in fluidized bed reactors for thermochemical conversion of biomass and waste fuels: Experimental data in comparison with predictions by a thermodynamic equilibrium model. Fuel 2013;111:696–708. https://doi.org/10.1016/j.fuel.2013.03.018.

[111] Katsaros G, Pandey DS, Horvat A, Aranda Almansa G, Fryda LE, Leahy JJ, et al. Experimental investigation of poultry litter gasification and co-gasification with beech wood in a bubbling fluidised bed reactor – Effect of equivalence ratio on process performance and tar evolution. Fuel 2020;262. https://doi.org/10.1016/j.fuel.2019.116660.

[112] Sommersacher P, Brunner T, Obernberger I, Engineering P. Fuel indexes – A novel method for the evaluation of relevant combustion properties of new biomass fuels. Impacts Fuel Qual. Power Prod., 2020, p. 1–14.

[113] Zevenhoven-Onderwater MFJ. Ash forming matter in biomass fuels. 2001.

[114] Obernberger I. novel characterisation methods for biomass fuels and their application - Case study Straw. Impacts Fuel Qual. Power Prod. Environ., 2012.

[115] Wen CY, Yu YH. A Generalized Method for Preducting the Minimum Fluidization Velocity. AIChE J 1966;12:610–2.

[116] Micro gas chromatograph n.d. https://www.agilent.com/en/product/gas-chromatography/gc-systems/490-micro-gc-system (accessed December 29, 2020).

[117] Extractive Gas Analyzers | Supplier | Manufacturer - Analytical Measurement | Products | Instruments | Equipment | ABB n.d. https://new.abb.com/products/measurement-products/analytical/continuous-gas-analyzers/advance-optima-and-easyline-series (accessed December 29, 2020).

[118] Horvat A, Kwapinska M, Xue G, Dooley S, Kwapinski W, Leahy JJ. Detailed Measurement Uncertainty Analysis of Solid-Phase Adsorption-Total Gas Chromatography (GC)-Detectable Tar from Biomass Gasification. Energy and Fuels 2016;30:2187–97. https://doi.org/10.1021/acs.energyfuels.5b02579.

[119] Horvat A, Kwapinska M, Xue G, Kwapinski W, Dooley S, Leahy JJ. Study of post sampling treatment of solid phase adsorption method on tar yields and comparison of two methods for volatile tar compounds. Eur Biomass Conf Exhib Proc 2016;2016:6–9. https://doi.org/10.5071/24thEUBCE2016-2CV.3.53.

[120] Rabou LPLM, Zwart RWR, Vreugdenhil BJ, Bos L. Tar in biomass producer gas, the Energy research Centre of The Netherlands (ECN) experience: An enduring challenge. Energy and Fuels 2009;23:6189–98. https://doi.org/10.1021/ef9007032.

[121] Padban N, Wang W, Ye Z, Bjerle I, Odenbrand I. Tar Formation in Pressurized Fluidized Bed Air Gasification of Woody Biomass 2000. https://doi.org/10.1021/ef990185z.

[122] Agilent Technologies. Agilent 5975C TAD Series GC / MSD System Data Sheet. 2014.

[123] Devi L, Ptasinski KJ, Janssen FJJG, Van Paasen SVB, Bergman PCA, Kiel JHA. Catalytic decomposition of biomass tars: Use of dolomite and untreated olivine. Renew Energy 2005;30:565–87. https://doi.org/10.1016/j.renene.2004.07.014.

[124] Nilsson S, Gómez-Barea A, Fuentes-Cano D, Haro P, Pinna-Hernández G. Gasification of olive tree pruning in fluidized bed: Experiments in a laboratory-scale plant and scale-up to industrial operation. Energy and Fuels 2017;31:542–54. https://doi.org/10.1021/acs.energyfuels.6b02039.

[125] Dufour A, Masson E, Girods P, Rogaume Y, Zoulalian A. Evolution of aromatic tar composition in relation to methane and ethylene from biomass pyrolysis-gasification. Energy and Fuels 2011;25:4182–9. https://doi.org/10.1021/ef200846g.

[126] Horvat A, Kwapinska M, Xue G, Rabou LPLM, Pandey DS, Kwapinski W, et al. Tars from Fluidized Bed Gasification of Raw and Torrefied Miscanthus x giganteus. Energy and Fuels 2016;30:5693–704. https://doi.org/10.1021/acs.energyfuels.6b00532.

[127] Xue G, Kwapinska M, Horvat A, Kwapinski W, Rabou LPLM, Dooley S, et al. Gasification of torrefied Miscanthus×giganteus in an air-blown bubbling fluidized bed gasifier. Bioresour Technol 2014;159:397–403. https://doi.org/10.1016/j.biortech.2014.02.094.

[128] Kim YD, Yang CW, Kim BJ, Kim KS, Lee JW, Moon JH, et al. Air-blown gasification of woody biomass in a bubbling fluidized bed gasifier. Appl Energy 2013;112:414–20. https://doi.org/10.1016/j.apenergy.2013.03.072.

[129] Arena U, Di Gregorio F. Energy generation by air gasification of two industrial plastic wastes ina pilot scale fluidized bed reactor. Energy 2014;68:735–43. https://doi.org/10.1016/j.energy.2014.01.084.

[130] Yu H, Zhang Z, Li Z, Chen D. Characteristics of tar formation during cellulose, hemicellulose and lignin gasification. Fuel 2014;118:250–6. https://doi.org/10.1016/j.fuel.2013.10.080.

[131] Thersites: Tar dew point n.d. http://www.thersites.nl/tardewpoint.aspx (accessed November 21, 2018).

[132] Israelsson M, Seemann M, Thunman H. Assessment of the solid-phase adsorption method for sampling biomass-derived tar in industrial environments. Energy and Fuels 2013;27:7569–78. https://doi.org/10.1021/ef401893j.

[133] Neubert M, Reil S, Wolff M, Pöcher D, Stork H, Ultsch C, et al. Experimental comparison of solid phase adsorption (SPA), activated carbon test tubes and tar protocol (DIN CEN/TS 15439) for tar analysis of biomass derived syngas. Biomass and Bioenergy 2017;105:443–52. https://doi.org/10.1016/j.biombioe.2017.08.006.

[134] Xuebin Wang, Houzhang Tan, Jipeng Si, Yanqing Niu TX. Co-pyrolysis of Pyridine and Pyrrole as Nitrogenous Comounds Model of Coal. Asian J Chem 2010;22:6998–7004.

[135] Berrueco C, Montané D, Matas Güell B, del Alamo G. Effect of temperature and dolomite on tar formation during gasification of torrefied biomass in a pressurized fluidized bed. Energy 2014;66:849–59. https://doi.org/10.1016/j.energy.2013.12.035.

[136] Devi L, Ptasinski KJ, Janssen FJJG. Pretreated olivine as tar removal catalyst for biomass gasifiers: Investigation using naphthalene as model biomass tar. Fuel Process Technol 2005;86:707–30. https://doi.org/10.1016/j.fuproc.2004.07.001.

[137] Nilsson S, Gómez-Barea A, Fuentes-Cano D, Haro P, Pinna-Hernández G. Gasification of olive tree pruning in fluidized bed: Experiments in a laboratory-scale plant and scale-up to industrial operation. Energy and Fuels 2017;31:542–54. https://doi.org/10.1021/acs.energyfuels.6b02039.

[138] Pandey DS, Kwapinska M, Gómez-Barea A, Horvat A, Fryda LE, Rabou LPLM, et al. Poultry Litter Gasification in a Fluidized Bed Reactor: Effects of Gasifying Agent and Limestone Addition. Energy and Fuels 2016. https://doi.org/10.1021/acs.energyfuels.6b00058.

[139] Campoy M, Gómez-Barea A, Ollero P, Nilsson S. Gasification of wastes in a pilot fluidized bed gasifier. Fuel Process Technol 2014;121:63–9. https://doi.org/10.1016/j.fuproc.2013.12.019.

[140] Arena U, Di Gregorio F. Energy generation by air gasification of two industrial plastic wastes in a pilot scale fluidized bed reactor. Energy 2014;68:735–43. https://doi.org/10.1016/j.energy.2014.01.084.

[141] Kwapinska M, Xue G, Horvat A, Rabou LPLM, Dooley S, Kwapinski W, et al. Fluidized Bed Gasification of Torrefied and Raw Grassy Biomass (Miscanthus × gigantenus). the Effect of Operating Conditions on Process Performance. Energy and Fuels 2015;29:7290–300. https://doi.org/10.1021/acs.energyfuels.5b01144.

[142] Dupont C, Boissonnet G, Seiler J-M, Gauthier P, Schweich D. Study about the kinetic processes of biomass steam gasification. Fuel 2007;86:32–40. https://doi.org/10.1016/j.fuel.2006.06.011.

[143] Arena U, Di Gregorio F. Gasification of a solid recovered fuel in a pilot scale fluidized bed reactor. Fuel 2014;117:528–36. https://doi.org/10.1016/j.fuel.2013.09.044.

[144] Xue G, Kwapinska M, Horvat A, Kwapinski W, Rabou LPLM, Dooley S, et al. Gasification of torrefied Miscanthus×giganteus in an air-blown bubbling fluidized bed gasifier. Bioresour Technol 2014;159:397–403. https://doi.org/10.1016/j.biortech.2014.02.094.

[145] Arena U. Process and technological aspects of municipal solid waste gasification. A review. Waste Manag 2012;32:625–39. https://doi.org/10.1016/j.wasman.2011.09.025.

[146] Chen H, Li B, Yang H, Yang G, Zhang S. Experimental investigation of biomass gasification in a fluidized bed reactor. Energy and Fuels 2008;22:3493–8. https://doi.org/10.1021/ef800180e.

[147] Horvat A, Pandey DS, Kwapinska M, Mello BB, Gómez-Barea A, Fryda LE, et al. Tar yield and composition from poultry litter gasification in a fluidised bed reactor: Effects of equivalence ratio, temperature and limestone addition. RSC Adv 2019;9:13283–96. https://doi.org/10.1039/c9ra02548k.

[148] Font Palma C. Modelling of tar formation and evolution for biomass gasification: A review. Appl Energy 2013;111:129–41. https://doi.org/10.1016/j.apenergy.2013.04.082.

[149] Amen-Chen C, Pakdel H, Roy C. Production of monomeric phenols by thermochemical conversion of biomass: a review. Bioresour Technol 2001;79:277–99. https://doi.org/10.1016/S0960-8524(00)00180-2.

[150] Valderrama Rios ML, González AM, Lora EES, Almazán del Olmo OA. Reduction of tar generated during biomass gasification: A review. Biomass and Bioenergy 2018;108:345–70. https://doi.org/10.1016/j.biombioe.2017.12.002.

[151] Berrueco C, Montané D, Matas Güell B, Del Alamo G. Effect of temperature and dolomite on tar formation during gasification of torrefied biomass in a pressurized fluidized bed 2014. https://doi.org/10.1016/j.energy.2013.12.035.

[152] Devi L, Ptasinski KJ, Janssen FJJG. Pretreated olivine as tar removal catalyst for biomass gasifiers: investigation using naphthalene as model biomass tar. Fuel Process Technol 2005;86:707–30. https://doi.org/10.1016/j.fuproc.2004.07.001.

[153] Lemmens S. Technological innovation in the energy sector : case of the organic Rankine cycle Sanne Lemmens. 2017.

[154] Nguyen TQ, Slawnwhite JD, Boulama KG. Power generation from residual industrial heat. Energy Convers Manag 2010;51:2220–9. https://doi.org/10.1016/j.enconman.2010.03.016.

[155] Zhang X, He M, Zhang Y. A review of research on the Kalina cycle. Renew Sustain Energy Rev 2012;16:5309–18. https://doi.org/10.1016/j.rser.2012.05.040.

[156] Habeeb A. A Study of Trilateral Flash Cycles for Low Grade Waste Heat Recovery to Power Generation. 2014.

[157] Environment Agency. Notice of variation and consolidation with introductory note 2010:1–22.

[158] Heliex Power. GenSet Case Study : Poultry litter. n.d.

[159] Kalina J, Sachajdak A, Strzałka R, Swierzewski M, Cwięka J. Operational experience and modelling of biomass combustion process in cogeneration systems with ORC units. E3S Web Conf 2019;82. https://doi.org/10.1051/e3sconf/20198201008.

[160] Strzalka R, Erhart TG, Eicker U. Analysis and optimization of a cogeneration system based on biomass combustion. Appl. Therm. Eng., vol. 50, 2013, p. 1418–26. https://doi.org/10.1016/j.applthermaleng.2011.12.039.

[161] Houshfar E, Khalil RA, Løvås T, Skreiberg Ø. Enhanced NOxreduction by combined staged air and flue gas recirculation in biomass grate combustion. Energy and Fuels 2012;26:3003–11. https://doi.org/10.1021/ef300199g.

[162] Mladenović MR, Dakić D V, Nemoda S, Paprika MJ, Komatina MS, Repić BS, et al. The combustion of biomass – The impact of its types and combustion technologies on the emission of nitrogen oxide. Hem Ind 2016;70:287–98. https://doi.org/10.2298/HEMIND150409033M.

[163] Grieco E, Poggio A. Simulation of the influence of flue gas cleaning system on the energetic efficiency of a waste-to-energy plant. Appl Energy 2009;86:1517–23. https://doi.org/10.1016/j.apenergy.2008.12.035.

[164] Prando D, Renzi M, Gasparella A, Baratieri M. Monitoring of the energy performance of a district heating CHP plant based on biomass boiler and ORC generator. Appl Therm Eng 2015;79:98–107. https://doi.org/10.1016/j.applthermaleng.2014.12.063.

[165] How to Estimate Compressor Efficiency? 2011. http://www.jmcampbell.com/tip-of-the-month/2015/07/how-to-estimate-compressor-efficiency/ (accessed September 6, 2020).

[166] BHSL. Sustainable poultry production through environmental recycling. 2013.

[167] Myriad Heat and Power Products. Biomass CHP facilities. 2018.

[168] Erhart T, Eicker U, Infield D. Part-load characteristics of Organic-Rankine-Cycles 2011:1–11.

[169] Sheet SD. Therminol ® 66 Heat Transfer Fluid Therminol ® 66 Heat Transfer Fluid 2018:1–13.

[170] Energy W. Biomass Combined Heat & Power (CHP). 2016.

[171] PBL. Eindadvies basisbedragen SDE++2020 2020:64.

[172] Annut A. Gas and Electricity Prices 2020.

[173] Statista. United Kingdom Inflation Rate 2021.

[174] Huang Y, Wang YD, Rezvani S, McIlveen-Wright DR, Anderson M, Mondol J, et al. A techno-economic assessment of biomass fuelled trigeneration system integrated with organic Rankine cycle. Appl Therm Eng 2013;53:325–31. https://doi.org/10.1016/j.applthermaleng.2012.03.041.

[175] BEIS Department. Combined heat and power-Additional guidance for renewable CHP.2020.